JAIST Repository
https://dspace.jaist.ac.jp/

Title	カチオン性高分子のデザインと合成およびその抗がん活性
Author(s)	NISHANT, KUMAR
Citation	
Issue Date	2023-03
Type	Thesis or Dissertation
Text version	ETD
URL	http://hdl.handle.net/10119/18432
Rights	
Description	Supervisor: 松村 和明, 先端科学技術研究科, 博士

JAIST
JAPAN
ADVANCED INSTITUTE OF
SCIENCE AND TECHNOLOGY

Japan Advanced Institute of Science and Technology

Doctoral Dissertation

Design and synthesis of cationic polymers and evaluation of their *in vitro* anticancer activity

Nishant Kumar

Supervisor: Kazuaki Matsumura

Graduate School of Advanced Science and Technology

Japan Advanced Institute of Science and Technology

Materials Science

March 2023

Abstract

Design and synthesis of cationic polymers and evaluation of their in vitro anticancer activity

Nishant Kumar
Matsumura Laboratory, JAIST

Cancer is one of the leading causes of death worldwide. As the cancer burden continues to increase globally, it exerts tremendous physical, emotional, and financial strain on individuals, families, communities, and health care systems. Cancer can affect any part of the body and is characterized by its uncontrollable growth. Numerous treatments, such as radiation therapy and chemotherapy which utilize various drugs, are currently in use; however, their harmful side effects and the development of drug resistance have resulted in major roadblocks when treating cancer. With advancements in synthetic and polymer chemistry, the use of nanoparticle-based drug delivery systems and chemotherapeutic macromolecules have garnered increasing attention in the previous decade. Unfortunately, nanoparticle drug delivery systems are based on the activity of the drug itself and hence suffer from inherent limitations of the drug along with cellular barriers, burst release, significant off-target toxicity and resistance development. So, better therapeutic strategies are sought in clinics, which will help improve overall survival, reduce treatment side effects, increase patient compliance, and improve disease management and outcome. With the known limitations of small-molecule drugs and conventional drug delivery systems, the potential use of polymeric molecules as anticancer agents could be a game-changer in the field of polymer-based biopharmaceuticals. In this research I was focusing on these cationic polymers and evaluation of their biological activity against various cancer cell lines.

To resolve the issue related to the limitations of the small molecule drugs and the nanotechnology-based drug-delivery systems, the primary aim of this thesis is to develop anticancer cationic polymers. To this end I synthesized the cationic polymers containing the hydrophobic groups in them. We describe the design and synthesis of novel anticancer polymers containing hydrophobic groups. I established the fact that the cationic homopolymer of (3-acrylamidopropyl)trimethylammonium chloride does not show any anticancer activity on its own; however, the insertion of hydrophobic moieties (n-butyl methacrylate, n-hexyl methacrylate, n-octyl methacrylate) in copolymers enhances their anticancer activity with very low IC_{50} value. Also, I carried out the mechanistic investigation of the interaction between the cationic homopolymers and the copolymers with the cancer cell membrane and proved that the hydrophobicity enhanced the interaction along with enhanced cytotoxicity.

Further, I designed and developed systems comprising both a cationic charge and hydrophobic moieties with a focus on selectivity toward normal cells. A series of poly-L-lysine and nicotinic acid-based polymers with varying amount of dodecylsuccinic anhydride was synthesized. To obtain the selectivity, the cationic charge of polymers was concealed by coordination with the Zn^{2+} ions. The Zn-bound polymers were found to be highly selective and effective against the cancer cell lines use. Also, they exhibited potent anticancer activity against the drug resistance cell line (COR-L23/R). The obtained polymers were found to be effective when compared with the small molecule drug like doxorubicin and prevents the further tumour metastasis. Considering the easy synthetic route, availability and biodegradability of these polymers could proves to be a promising approach towards cancer treatment.

Next, I convert the bioactive anticancer compound methyl jasmonate a small molecule into the cationic polymer or to copolymerize it with the cationic monomers. For this purpose modified methyl jasmonate to the monomer and then further copolymerised it with (3-acrylamidopropyl)trimethylammonium chloride. The obtained copolymers showed the enhanced cytotoxicity towards the cancer cell lines when compared to the MJ alone. In order to obtained the selectivity the PEG-based copolymers of methyl jasmonate and the (3-acrylamidopropyl)trimethylammonium chloride were synthesised. The PEG-based copolymers showed enhanced selectivity and the better anticancer activity.

Lastly, I summarised the findings of each chapter. Also, I gave and outlook for each chapter for the further utilization of the research worked performed during this PhD.

Keywords: Anticancer agents, Cationic polymers, Membrane-polymer interaction, Hydrophobicity, Metal-coordinated polymers

Table of Contents

List of Tables and Figures

List of Abbreviations

Tricarboxylic acid (TCA), Intensity-modulated radiotherapy (IMRT), Image-guided radiotherapy (IGRT), 3D conformal radiotherapy (3DCRT), Stereotactic body radiation therapy (SBRT), Enhanced permeability and retention (EPR), Drug delivery systems (DDS), Tumor microenvironment (TME), Phosphatidylserine (PS), Anticancer cationic peptides (ACPs), Antimicrobial peptides (AMPs), (3-acrylamidopropyl)trimethylammonium chloride (AMPTMA), Poly(3-acrylamidopropyl)trimethylammonium chloride (PAMPTMA), Butyl methacrylate (BuMA), Hexyl methacrylate (HexMA), Octyl methacrylate (OctMA), *N*-(2-hydroxyethyl) acrylamide (HEAA), Lactate dehydrogenase (LDH), Diffusion ordered spectroscopy (DOSY), Egg phosphatidylcholine/L-α-phosphatidylcholine (EPC), Carboxyfluorescein (CF), Dynamic light scattering (DLS), Poly-L-lysine (PLL), Nicotinic acid (NA), Dodecylsuccinic anhydride (DDSA), 1-(3-dimethylaminopropyl)-3-ethylcarbodiimide Hydrochloride (EDC-HCl), X-ray photoelectron spectroscopy (XPS), Primary human dermal fibroblast (HDF), Human caucasian lung large cell carcinoma (COR-L23/R), Multidrug- resistance (MDR), 3-(4,5-dimethylthiazol-2-yl)-2,5-diphenyltetrazolium bromide (MTT), Doxorubicin (DOX), Methyl jasmonate (MJ), Jasmonic acid (JA), 4-dimethylaminopyridine (DMAP), Hexokinase-II enzyme (HK-II). Dipalmitoylphosphatidylcholine (DOPC), 1-palmitoyl-2-oleoyl-sn-glycero-3-phosphocholine (POPC).

Chapter 1

INTRODUCTION

Cancer is defined as a large group of heterogeneous diseases characterized by uncontrollable cellular growth. It can originate in any body part, like organs or tissues, and has the potential to invade and spread throughout the body. Genetic alterations, such as mutations in DNA repair genes, oncogenes, tumor suppressor genes, as well as other genes involved in cellular growth and differentiation, transform normal cells into malignant cancer cells. Cancer is one of the major causes of mortality and morbidity worldwide, ranking second after cardiovascular disease. According to WHO, in 2020 it accounted for one in six deaths resulting in an estimated 9.9 million deaths with 1.9 million new cases being recorded **(Figure 1.1)**. The most common cancer types are breast, lung, cervical, colorectal, and thyroid cancers; additionally, cancers of the mouth, liver, lung, stomach, prostate, and colon are more common in men. [1]

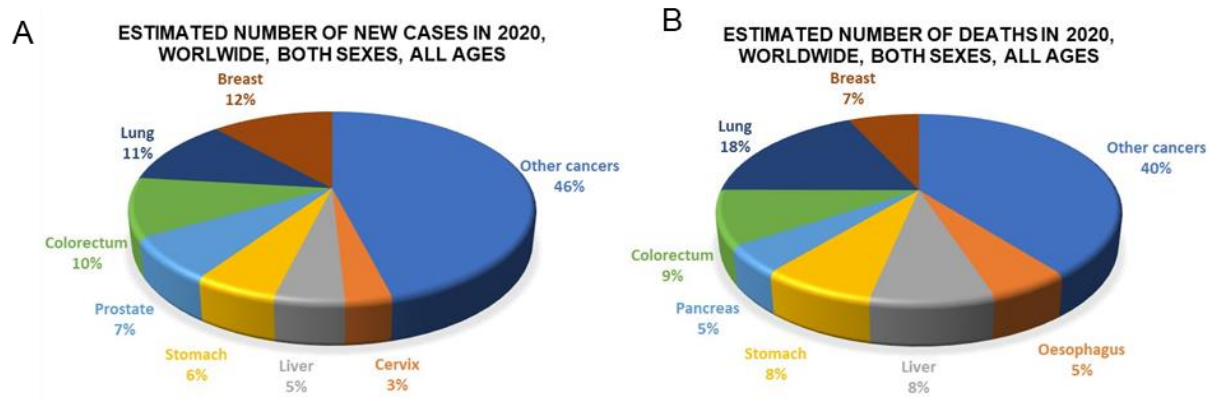

Figure 1.1: Global cancer burden in 2020. (A) Estimated new cases of cancer in 2020. (B) Estimated deaths due to cancer in 2020.[2]

1.1. Difference between cancer cells and normal cells

Cancer cells differ from normal cells in various aspects such as membrane composition, energy consumption, and rate of proliferation. Biomarkers are biological molecules present in cells, body tissues, or body fluids that indicate normal and abnormal processes.[3] They can be

detected in excretions (stool, urine), circulation (whole blood, plasma, or serum), or secretions (sputum or nipple discharge), and are thus a non-invasive, serial method that can be used to easily assess and evaluate health and diseases either through special imaging or biopsy. Hence, cancer biomarkers are vital for the screening, prognosis, detection, diagnosis, and monitoring of cancer.[3] In normal eukaryotic cells, phosphatidylethanolamine and phosphatidylserine are present in the inner leaflet of the cell membrane, whereas choline-containing phospholipids, sphingomyelin, and phosphatidylcholine are mainly present in the outer leaflet of the cell membrane. This array can be altered in response to a variety of internal and external stimuli that result in certain biological responses. Therefore, phosphatidylserine can be used as a biomarker that allows for the specific targeting of cancer cells without affecting normal cells. Many cancer cell types, such as glioblastoma (Gli36), breast cancer (MDA-MB-231-Luc-D3H2LN), and astrocytoma (U373) show overexpression of phosphatidylserine, whereas untransformed human Schwann cells possess the lowest surface expression of phosphatidylserine.[4] In addition to phosphatidylserine, O-glycosylated mucins,[5, 6] sialylated gangliosides,[7] and heparan sulfates[8] are also overexpressed in cancer cell membranes, whereas normal cell membranes are mainly composed of neutral zwitterionic phospholipids and sterols **(Figure 1.2A)**.[9] In tumor cells, a relatively higher number of microvilli are present in comparison to normal cells, thus increasing the surface area of the cancerous cells and allowing them to interact with more cationic anticancer peptides and polymers.[10] Otto Warburg proposed that the consumption of energy in cancer cells is different from that in normal cells.[11] Cancer cells do not preform the tricarboxylic acid (TCA) cycle for their energy production; they prefer the glycolytic pathway, even in the absence of oxygen, and thus have a higher lactate production, leading to acidification of the cell **(Figure 1.2B)**.[12]

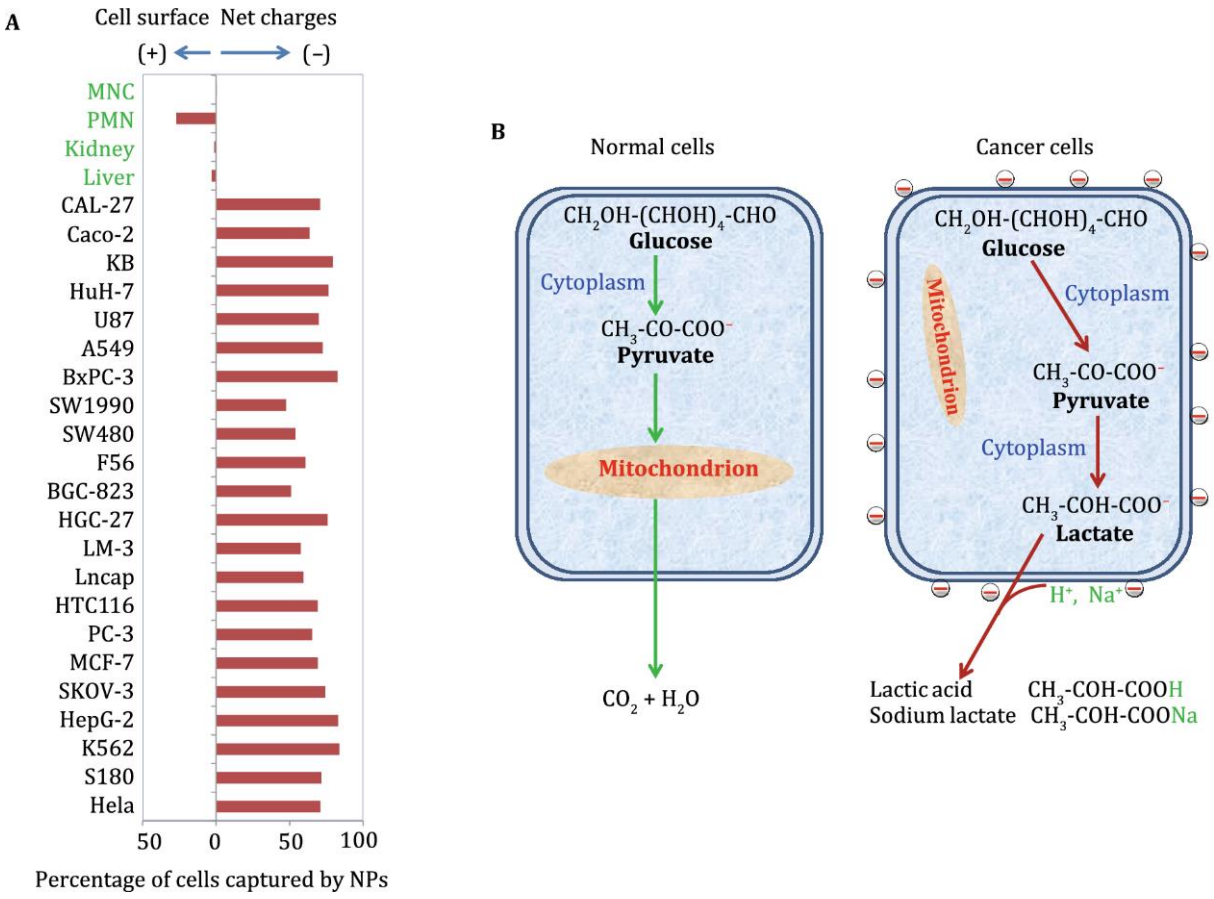

Figure 1.2: Difference in cancer and normal cell membrane. (A) The calculated net surface charges on the various cells lines. (B) Diagram showing the production of lactate ions, which result in a more acidic environment and the negative charge on cancer cells.[13]

1.2. Cancer treatment

1.2.1. A history of cancer treatment

The term cancer was derived from the Greek word "karkinos," which was first used to describe malignant tumors by the physician Hippocrates. Some of the earliest evidence of human bone cancer can be found in ancient Egyptian mummies and manuscripts (around 1600 BC). In medicine, the earliest written evidence of cancer, in the form of breast cancer, was found in an ancient Egyptian medical text (Edwin Smith Papyrus), which described it as a grave disease with no treatment.[14] Examples of treatments used by the Egyptians include cautery, surgery with knives, salts, and an arsenic paste that remained in use as "Egyptian ointment" until the

19th century.[15] In contrast, herbal remedies such as tea, figs, fruit juices, and boiled cabbage were used by the Sumerians, Indians, Chinese, and Persians, but in severe cases, they would use pastes of copper, iron, sulfur, and mercury. Some of these mixtures have been used on internal and external cancers for approximately 3000 years. Claudius Galen, a Greek medicine practitioner, wrote more than 100 notes on tumors and cancer, which were translated from Greek to Latin and other languages and were widely distributed in all known countries of his time.[16]

1.2.2. Surgical treatment of cancer

Aelius Galenus or Claudius Galenus, often anglicized as Galen, was a 2nd century doctor who was thought to be the highest medical authority in his time and his books were preserved for centuries. He studied cancer as much as Hippocrates did. Surgery has long since been the first-line treatment for malignant and solid tumors. After the discovery of anesthesia in 1846, surgeons such as Bilroth, Handley, and Halsted performed tumor removal operations by removing the entire tumor along with the lymph nodes. In the 1970s, less invasive techniques such as ultrasound (sonography), computed tomography (CT scans), magnetic resonance imaging (MRIs), and positron emission tomography (PET scans) were developed. Nowadays, surgeons can use miniature video cameras and endoscopy to remove esophageal, colon, and bladder tumors.

Different types of surgery are used for the treatment of cancer at different stages such as radical or curative surgery for removing the entire diagnosed tumor, surgery for symptomatic relief, conserving surgery, surgery for metastases, recurrent surgery, reconstructive surgery, etc. With advancements in technology, different ways of performing surgeries have been developed, eliminating the need to cut with a scalpel. These include cryosurgery, in which extremely cold liquid nitrogen or argon is used to destroy the abnormal cells or tissues; lasers, in which a

powerful beam of light is used to damage and cut the affected tissue; hyperthermia, a treatment in which the affected areas of the body are exposed to high temperatures; and photodynamic therapy, in which drugs are used that can react with certain types of light so that when the tumor is exposed to the light, the drugs are activated and kill the nearby cells.[17]

Since surgical methods involve pain and the possibility of infection and are very costly procedures that can lead to fatality, researchers have tried to develop alternative strategies to combat cancer that are less invasive, painful, and harmful to the patient.

1.2.3. Radiation therapy

Radiation therapy is a technique in which cancer cells are treated with a high dose of radiation. The radiation does not directly kill the cancer cells but damages the DNA beyond repair; as a result, the cells stop dividing, and die within weeks or months, and are finally removed from the body. Radiation treatment depends on the type of cancer, size of tumors, implications on the lymph nodes, and the type of radiation technique used.[18] Radiation therapy also affects nearby normal cells; therefore, tumor-specific targeting is required. Advancements in imaging techniques, powerful computers, software, and delivery methods have helped achieve this. Currently, the most advanced techniques developed are intensity-modulated radiotherapy (IMRT), image-guided radiotherapy (IGRT),[19] 3D conformal radiotherapy (3DCRT), and stereotactic body radiation therapy (SBRT).[20]

Radiation therapy has proven to be an important treatment method for cancer, and ongoing efforts towards new radiation treatments will improve the quality of life and survival of patients with cancer. Although improved imaging techniques and delivery methods have somewhat lowered the toxicity to nearby cells, further research is warranted to minimize the toxicity and side effects. Moreover, an understanding of the biological mechanisms is still required.

1.2.4. Chemotherapy

Chemotherapy involves the use of drugs to destroy cancer cells. This involves either stopping or slowing cancer cell growth, and its effects are systemic. Based on the mode of action, the following classes of anticancer drugs are available: a) DNA damaging alkylating agents; b) RNA and DNA building blocks replacing anti-metabolites; c) DNA replication interfering antibiotics; d) topoisomerase I or II inhibitors, enzymes involved in unwinding DNA replication and transcription; e) mitosis and cell division inhibitors; and f) corticosteroids.[21] Some well-known chemotherapeutic cytostatic drugs include capecitabine, irinotecan, docetaxel, ixabepilone, gemcitabine, and pemetrexed.

Although chemotherapy shows good results for cancer treatment, it alone fails to eradicate the disease in most patients. Moreover, chemotherapy is associated with severe side effects, including acute as well as chronic toxicity.[22] Immediate harmful effects on the hair, skin, blood, kidneys, and gastrointestinal tract can be observed. Neurotoxicity disorders can also induce paresthesia, somnolence, paralysis, spasms, ataxia, and coma. Additionally, the prolonged consequences of chemotherapy include drug resistance, carcinogenicity, and infertility.[23]

1.3. Material-based treatment

While the methods discussed in the preceding section have yielded impressive results, they also suffer from many drawbacks. As the prevalence of cancer is increasing each year, it is imperative that we develop new therapeutic materials to manage and treat it. Accordingly, over the years, many material-based cancer therapeutics have been developed. Material-based methods offer greater flexibility and potency when compared to conventional methods, and hence have gained widespread popularity in previous decades.

1.3.1. Nanoparticles as cancer therapy

Although surgical resection, radiation therapy, and chemotherapy have achieved success in the treatment of cancer, better therapeutic strategies that improve overall survival, reduce treatment side effects, increase patient compliance, and improve disease management and outcomes are sought-after in clinics. To achieve this, it is imperative that we develop a rational treatment strategy that combines and maximizes both efficacy and safety to not only treat the disease effectively but also maintain patient welfare. Nanotechnology-based treatment options, which allow for the combination of different treatment modalities, drugs, and materials in one single platform, have thus become extremely attractive. For instance, the loading of drugs into nanoparticles alters the pharmacokinetic properties of the drugs[24] (e.g., improved biodistribution, greater bioavailability, and lower clearance), prevents their degradation inside the body, and reduces drug toxicity and side effects[25]; the nanoparticles carrying the drugs interact primarily with the surrounding biological environment through their surface functional groups[26], which ultimately dictates the fate of the drug. In fact, the high surface-area-to-volume ratio of the nanoparticles is an advantage because of the subtle changes in surface functionality which can enable drastic changes in their properties inside the body. Additionally, the small size of nanoparticles (10–500 nm) provides unique advantages over the free drug molecules. This is because the enhanced permeability and retention (EPR) effects that are found in many tumors enable nanoparticle accumulation/retention at the tumor site, which is difficult to achieve when using small sized free drugs[27]. Moreover, the nanoparticle surface area can be appropriately modified to incorporate ligands targeting tumor sites without compromising the functional ability of the loaded drug. Importantly, the biggest advantage of nanoparticles in drug delivery is their ability to incorporate materials with different functionalities. “Multi-functional” nanoparticle systems can be designed via the loading of multiple drugs to increase the overall therapeutic efficacy; additionally, stimuli-responsive

materials for remote-controlled on-demand drug release, together with diagnostic and therapeutic components for image-guided drug delivery can also be incorporated.

1.3.1.1. Different nano-drug delivery systems

Broadly, nanoparticles for drug delivery applications can be classified based on the material used to synthesize them: polymer-based nanoparticles, lipid-based nanoparticles, non-polymeric nanoparticles, and nanoparticles derived from biological materials **(Figure 1.3)**.

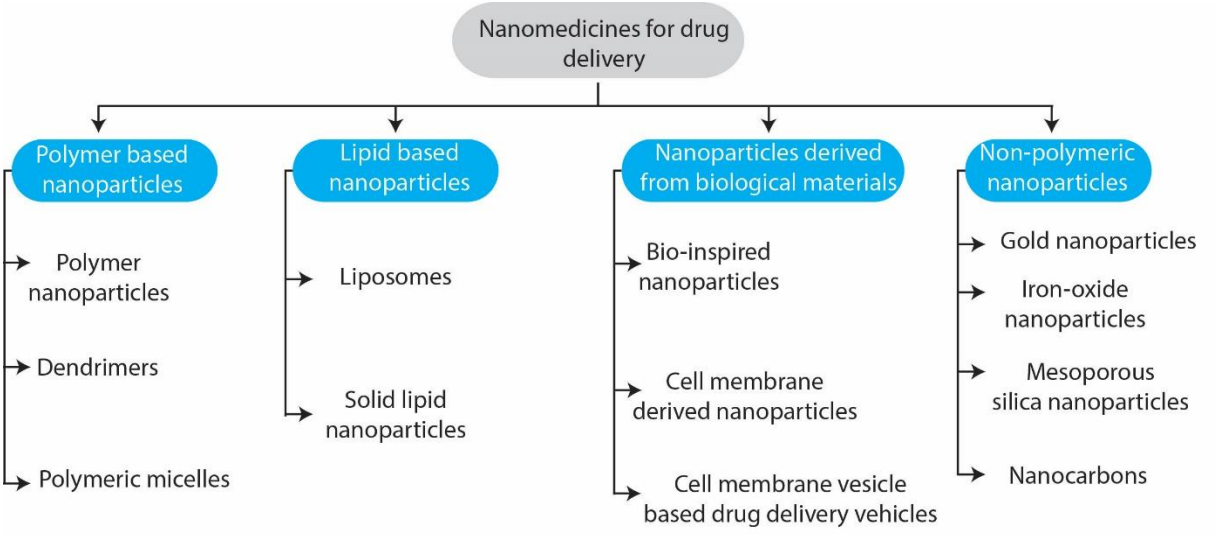

Figure 1.3: Classification of nanoparticles for drug delivery based on materials used for their synthesis.[2]

Nanoparticles made from polymeric materials are usually considered suitable for drug delivery applications because their physicochemical properties can be easily controlled (the chemical functionality of the polymer building blocks can be altered, as can be the reaction chemistry used for the synthesis of polymeric nanoparticles). Of note, for drug delivery applications, it is essential that nanoparticles can facilitate controlled drug release at the target site, without toxic effects. A few different types of artificial and natural polymers have been utilized for this purpose a little detail is explained below **(Table 1.1)**.

Table 1.1. Different types of polymer- and lipid-based nanoparticles.

	Loaded cargo	**Cancer type**	**Remarks**	**Reference**
Polymer NPs	siRNA	Prostate (*in vitro* – LnCaP, PC3, DU145)	The PRINT method enables a high encapsulation efficiency for cargo	[28]
	Paclitaxel	Brain (*in vivo* -C6 glioma; dose: 5 mg/Kg)		[29]
	Paclitaxel and IR780 dye	Ovarian (*in vivo* – ST30; dose: 7 mg/Kg)	Near-infrared (NIR) light-induced drug release	[30]
	KRAS-siRNA	Pancreas (*in vivo* – KPPC-1)	Successful KRAS knockdown was observed	[31]
	Doxorubicin	Brain (*in vivo* - glioblastoma 101/8; dose: 2.5 mg/Kg)		[32]
Dendrimers	mi-RNA and doxorubicin	Breast (*in vitro*- MDA-MB-231)		[33]
	AZD4320 (Bcl-2/Bcl-xL inhibitor)	Blood (*in vivo* – RS4 lymphoblastic leukemia)		[34]
	Doxorubicin	Breast (*in vivo* – Walker 256; dose: 2 mg/Kg)	Reduces non-specific uptake in major organs	[35]
	siRNA targeting Hsp27	Prostate (*in vivo* – PC-3; dose: 0.25 mg/Kg)	Targets amphiphilic dendrimers showing efficient gene silencing	[36]
Micelles	Doxorubicin	Breast (*in vivo* – 4 T1; dose: 10 mg/Kg)	Improves drug pharmacokinetics	[37]

	Loaded cargo	Cancer type	Remarks	Reference
			and tumor-specific accumulation	
	Curcumin	Cervical (*in vivo* – HeLa; dose: 10 mg/Kg)	Cross-linked micelles show enhanced tumor accumulation	[38]
	Doxorubicin	Breast (*in vivo* – 4 T1; dose: 20 mg/Kg)	Reversible cross-linked micelles used	[39]
	Docetaxel	Breast (*in vivo* – 4 T1; dose: 10 mg/Kg)	Therapeutic efficacy against breast cancer metastasis	[40]
Polymerosome	Docetaxel	Breast (*in vivo* −4T1, dose: 10 mg/Kg)	Folic acid conjugated NPs for tumor targeting	[41]
	Indocyanine green and doxorubicin	Breast (*in vivo* −4T1, dose: 10 mg/Kg)	Combined photothermal and drug delivery	[42]
	Iron oxide NPs and doxorubicin	Cervical (*in vitro* - HeLa)	Higher MR contrast obtained relative to IO NPs alone	[43]
	Doxorubicin	Cervical (*in vitro* - HeLa)	pH responsive drug release	[44]
Nanogels	Doxorubicin	Cervical (*in vitro* - HeLa)	Polymersome membrane cross-linked to form hollow-nanogels	[45]
	HSP-90 inhibitor (17-AAG), doxorubicin	Breast (*in vivo* - BT-474, dose: 6 mg/Kg)	Synergistic chemotherapy	[46]
	Nile red, Paclitaxel, Doxorubicin	Breast (*in vitro* - MCF-7)	Hydrophobic and hydrophilic drugs loaded	[47]

	Loaded cargo	Cancer type	Remarks	Reference
	Doxorubicin	Bone (*in vitro* - CAL-72)	Simple synthesis process using alginate biopolymer	[48]
Liposomes	Doxorubicin	Colon (*in vivo* - C26; dose: 10 mg/Kg)	Anti-angiogenesis therapy achieved by targeting with Arg-Gly-Asp (RGD) peptides	[49]
	5-Fluorouracil and doxorubicin	Breast (*in vivo* – 4 T1; dose: 3 mg/Kg doxorubicin and 0.62 mg/Kg 5-Fluorouracil)	Synergistic delivery of drugs achieves effective tumor therapy at low toxicity	[50]
Solid lipid NPs	Didoceylmethotrexate (ddMTX), a lipophilic prodrug form of methotrexate	Brain (*in vivo* – F98 glioma; dose: 1.6 mg/Kg)		[51]
	Paclitaxel	Lung (*in vivo* – M109; dose: 1 mg/Kg)	Effective tumor therapy achieved through the pulmonary route, reducing systemic toxicity	[52]
	Paclitaxel	Lung and breast (*in vivo* – H1975, H1650, H520, PC9, SK-BR-3; dose: 22 mg/Kg)		[53]

NPs, nanoparticles; PRINT, particle replication in non-wetting templates.

1.3.1.2. Summary of different nanomaterial systems.

Among the different nanomaterials used for drug delivery applications that have been discussed here, each has multiple advantages and disadvantages **(Figure 1.4)**. The use of a specific type of material for cancer therapy ultimately depends upon the net intended application which

could include drug delivery, active targeting, imaging, immunotherapy, and controlled long-term drug release. In the present research landscape, it is important to note that almost all nanomaterials investigated for drug delivery are engineered to possess multi-functionality, either though the addition of multiple functional chemical/biological groups (e.g., pH responsive polymers, enzyme cleavable linkers, antibody ligands, etc.)[54-56] or through the combination of different nanomaterials to form a hybrid/composite nanostructure. Two primary reasons could be considered for this shift in outlook: (a) the benefits of adding multiple functionalities (e.g., combined therapy and imaging, remote-controlled stimuli-responsive drug delivery) seem to show a multi-fold increase in therapeutic outcomes when compared to single-functional nanosystems; and (b) the improvement and increase in knowledge relating to the synthesis chemistries when combining multiple materials in one single platform. Even though these advantages have been highlighted in multiple studies for multi-functional/stimuli-responsive nano-materials, a corresponding increase in the clinical translation of such systems is suffering from multiple bottlenecks. One of the biggest disadvantages of utilizing multiple components to synthesize a specialized nanomedical system is the difficulty in determining the safety profile of every component encompassing the system. The other major disadvantage is the complexity related to the scale up of the synthetic chemistries of systems that tend to become more difficult with the addition of multiple components. Nevertheless, it is important to realize that these nanomedical systems show great promise in treating cancers which are difficult to treat using conventional treatment modalities but the transition from the bench to the bed-side requires more research and a clearer understanding of their cost-to-benefit ratios.

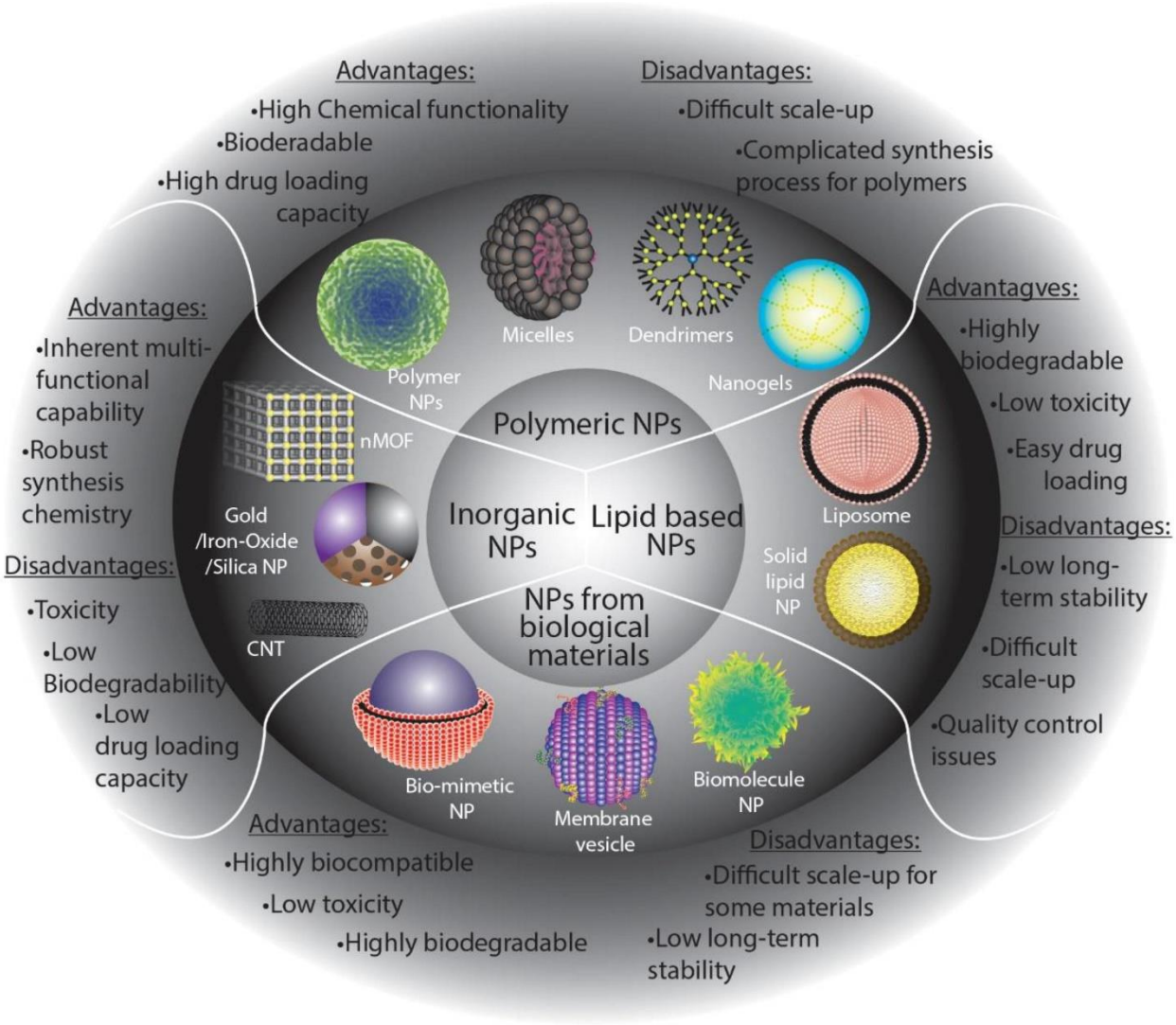

Figure 1.4: Summary of the advantages and disadvantages of the different nanomaterial systems used for cancer therapy.[2]

1.3.2. Material-based cancer immunotherapy

Cancer immunotherapy relies on the ability of the body's immune system to fight against cancer accurately and safely. In the previous two decades enormous progress has been made in relation to cancer immunotherapy and this has resulted in advances and positive outcomes.[57-59] Drugs are designed to incite healthy primary and secondary antitumor immune responses via the revamping/improvement of natural mechanisms that are altered in cancer foci, thus constraining tumor growth and metastasis.[60] Therefore, the development of cancer immunotherapy approaches depends on our understanding of the relationship between the

immune system and cancer, famously known as the cancer-immunity cycle.[61] The first cancer immunotherapeutic drug, the cytokine interferon-a (IFN-a) was approved by the FDA for the treatment of hairy cell leukemia.[62] However, there are several problems associated with immunotherapeutic drugs, such as the large dose requirement due to their short half-life which causes autoimmune side effects, their limited effectiveness (in few patients), and the restricted use of the treatments for hematological tumors, due to the complex tumor microenvironment (TME) of solid tumors.[63]

To overcome such side effects and improve the efficacy/accuracy of immunotherapy approaches, novel drug delivery systems (DDS) are required. In recent years, DDSs were designed for the prolonged release of immunotherapeutic drugs in vivo[64]; a variety of biomaterials-based systems have been developed including liposomes, hydrogels, polymers, and silica nanorods (Table 6) that have improved capacities for the specific and targeted delivery of drugs, low toxicity, high efficacy, and immune-stimulating effects.[64, 65] Recently, it was found that combined photothermal immunotherapy could enhance the antitumor immune response and overcome the problems associated with photothermal therapy (PTT).[66-71]

Although cancer immunotherapy is attracting increasing amounts of attention, there remains a huge gap between human patient treatments in vivo and in vitro laboratory models, as very few formulations are undergoing clinical trials. Indeed, resources for the development of biomaterials for DDSs are available; however, the economical large-scale production of such materials is still challenging. Therefore, there is an urgent need for new cost-effective materials and humanized models for the appropriate development of efficient and potent immunotherapy-based cancer treatment options.

1.3.3. Cationic polymeric molecules

Polymers which bear positive charges either intrinsically present in the polymer backbone or in the side chains or synthesized in the presence of novel cationic entities are known as cationic

polymers. Easy further modification and their unique physico-chemical properties made them appealing for biological application. Maximumly, these polymers possess any of the primary, secondary or tertiary amine functional groups which may further be protonated. Like the normal polymers, these polymers were also divided on the basis of their polymeric structure (linear, branched, hyperbranched and dendrimer-like) and can be further differentiated by the placement of the positive charges (backbone or side chains).

1.3.3.1. Types of cationic polymers

Also, they can further be divided on the source of their origin: natural, semi-synthetic and synthetic **(Figure 1.5)**. [72, 73]

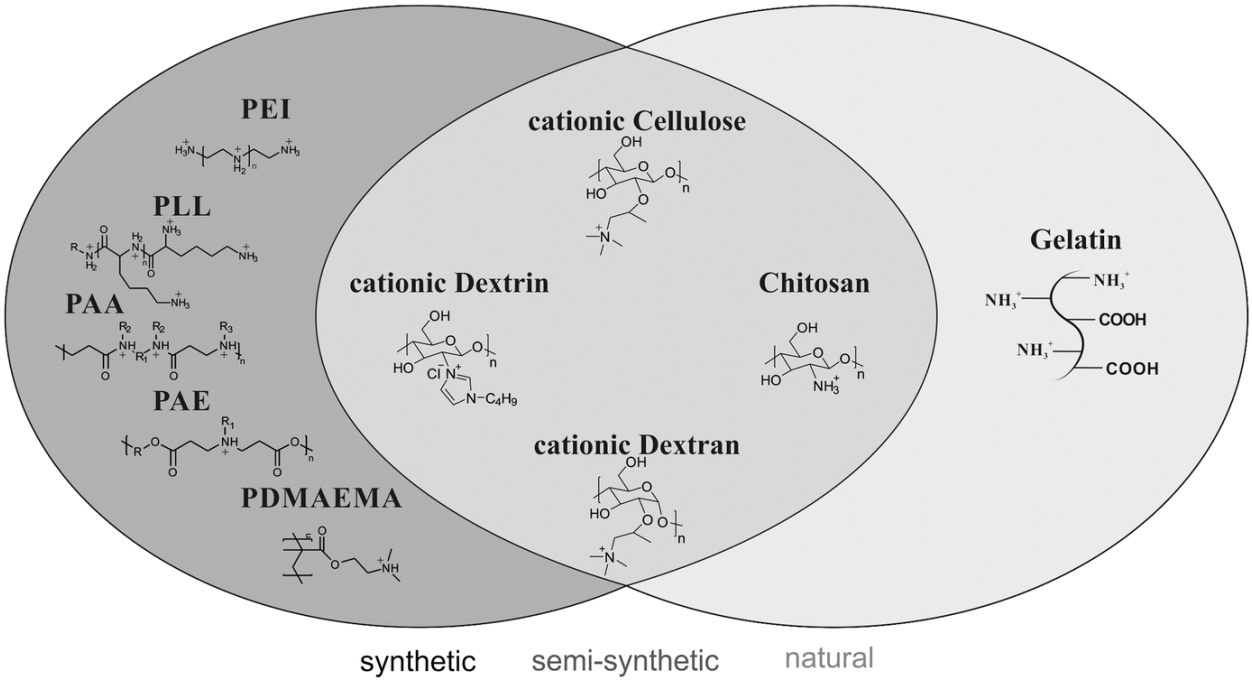

Figure 1.5: Classification of cationic polymers on the source of origin.[72]

1.3.3.1.1. Natural polymers

Natural cationic polymers possess intrinsic positive charge and are obtained from renewable sources. These are mainly biodegradable, biocompatible, often possess low immunogenicity and low toxicity. Most of the natural cationic polymers have reactive sites that can be further modified to improve their properties for the therapeutic effect. The most common natural

cationic polymers used in biomedical applications are cationic gelatin,[74] cationic chitosan,[75] cationic cellulose,[76] and cationic dextran.[77]

1.3.3.1.2. Semi-synthetic polymers

These polymers were obtained from nature, but they need further modification to acquire positive charge. These polymers could retain the properties of the natural polymers like biodegradability, though the introduced positive charge could lead to increased cytotoxicity and decrease in biocompatibility. One can control the charge and thus can improve their properties with further modifications. The most commonly known semi-synthetic cationic polymers are chitosan,[78] cationic cyclodextrin,[79] and cationic dextran.[80]

1.3.3.1.3. Synthetic polymers

In recent decades, synthetic polymers have received great attention in biomedical applications, drug delivery systems and as well as in tissue engineering as they can overcome the problem associated with batch-to-batch variation of natural polymers. They can be easily modified with some specific functional and bioactive moieties; molecular weight could be controlled, and their degradation behavior can also be improved. The most commonly used synthetic cationic polymers in biomedical applications includes polyethyleneimine (PEI),[81] poly-L-lysine,[82] polyamidoamine,[83] poly[2-(N,N-dimethylamino)ethyl methacrylate (PDMAEMA). [84]

1.3.3.2. Anticancer cationic peptides

Peptides consist of short chains of 5–50 amino acids linked via peptide bonds and are mainly arranged as α-helices or β-sheets—the major secondary structures. In addition, peptides possess some distinctive features, such as hydrophobicity and high cationic charges, which facilitate the formation of amphiphilic structures and interactions with cancer cells.[85, 86] Materials based on these peptides have been found to be promising for use as cancer therapeutics with a number of activities such as drug delivery, sensing, fate control, tumor tissue perforation, and generation of immunological responses for anticancer therapeutics.[87-90] Tumor cells differ

from normal cells in their morphological appearance, have different chemical compositions and cellular membranes, and lose their original function. Anionic molecules such as phospholipid phosphatidylserine, O-glycosylated mucins, heparin sulfate, and sialylated gangliosides are overexpressed by the cancer cell membranes, resulting in a net negative charge as compared to normal cells. Because of these key differences between normal and cancer cells, it has been predicted that cancer cells are more vulnerable to anticancer cationic peptides (ACPs), resulting in the likelihood of selectivity. Peptides with membrane-disrupting lytic modes of action serve as defense molecules in plants, invertebrates, vertebrates, bacteria, insects, and humans. These membrane lytic peptides have gained recognition as antimicrobial peptides and can affect both eukaryotic and prokaryotic cells. Subsequently, the sensitivity of tumor cells to ACPs was discovered. As discussed above, the negatively charged membranes of cancer cells bind to ACPs through electrostatic interactions, ultimately leading to cell membrane lysis. ACPs can interact with cancer cells through different mechanisms, such as the barrel-stave model, carpet-like mechanism, toroidal pore model, in-plane diffusion model, and detergent-like effect model **(Table 1.2, Figure 1.6)** .[91]

Table 1.2. Membranolytic modes of anticancer peptides

Model	**Membrane lytic mechanism**	**Peptide**	**Reference**
Barrel-stave model	α-Helices of amphipathic lytic peptides are inserted into the hydrophobic core of the bilayer membrane and form transmembrane pores	Alamethicin, melittin, and hemolysin	[92, 93]
Toroidal or two-state model	Peptides associate with lipid headgroups, which line the inside of the pore with the helical axis parallel to the interface	Magainin	[94]
In-plane diffusion model	Short peptides are inserted in-plane, which disrupt the bilayer packing, reduce the membrane thickness, and eventually form transient pores	Mastoparan and cecropin-melittin hybrids	[93, 95, 96]
Carpet model	Perpendicular binding of peptides to the membrane in a carpet-like manner via interactions with the lipid head groups of the membrane without insertion into the hydrophobic core	Dermaseptin and magainin	[97, 98]
Detergent-like effect model	Disruption of the bilayer by the release of micellar structures from membrane	Melittin, apolipoproteins, myelin basic protein, and glucagon	[99-102]

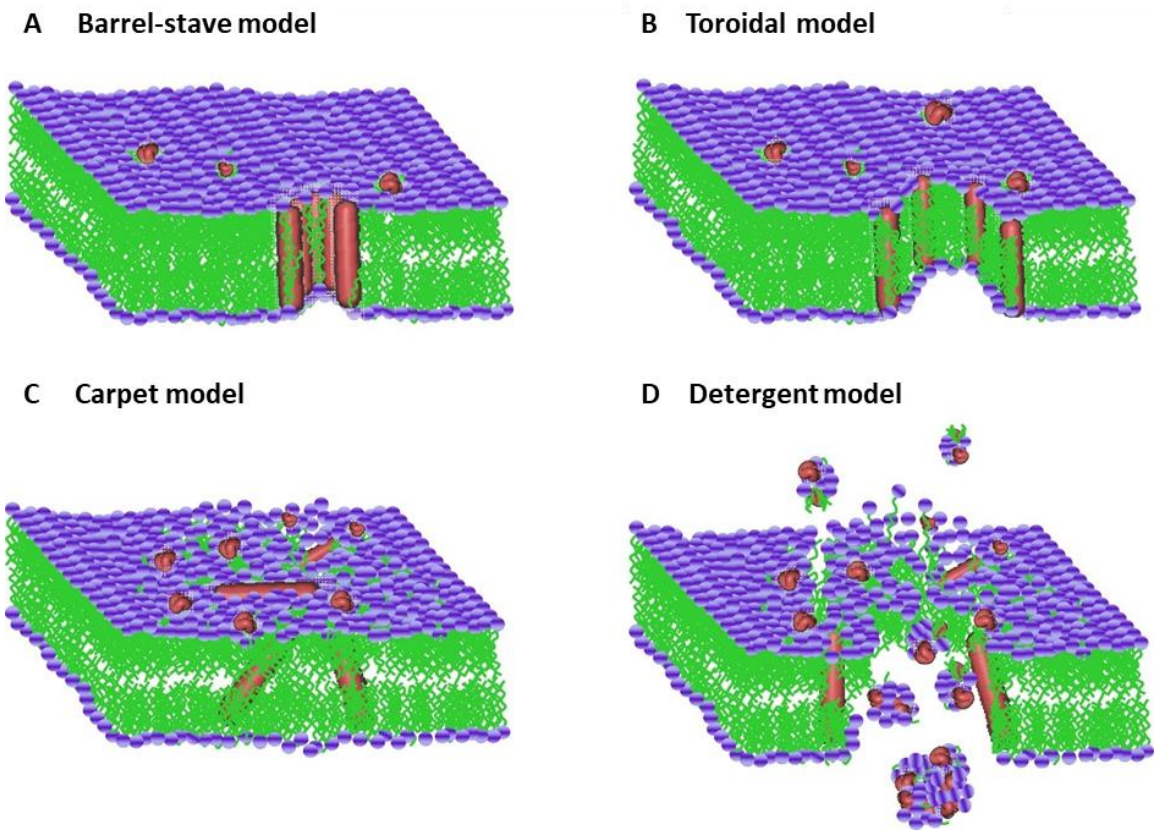

Figure 1.6: Proposed mechanisms with which ACPs can interact with cancer cells. (A) Barrel-stave model, (B) toroidal pore model, (C) carpet-like mechanism, and (D) detergent-like effect model.[103]

Overall, serial analysis and research on anticancer peptides is a constructive work for the research and development of new anticancer drugs; however, every method has its own limitations. ACPs are as expensive as cancer treatments, and thus researchers are exploring cationic polymers.

1.3.3.3. Cationic polymers for cancer treatment

Several studies have reported that cancer cells have an additional negative charge compared to normal cells due to the overexpression of phosphatidyl serine and sialic acid on their cell surface,[104-107] similar to bacterial cell membranes, and antimicrobial peptides have been attributed to their elevated selectivity and potency against cancer cells due to their anionic nature. This negatively charged cell surface in cancer cells opens a way to potential drug targets.

Gakhar et al.[108] reported polymers from three families of cationic, natural, and synthetic polymers. Chitosan and dextran from the polysaccharide family, Lys and Arg-based poly(ester amides) from amino acid-based poly(ester amides) (AA-PEA) family and PolyAETA(2-(acryloxy)ethyl-trimethylammonium chloride) vinyl-based monomer (from the vinyl family to inhibit the growth of prostate cancer cells in comparison to normal prostate epithelial cells (RWPE-1).

In another study, Park et al.[109] designed a macromolecular chemotherapeutic with three principal components: a hydrophilic polyethylene glycol (PEG) block, a linking group, and a cationic block that interacts with the negatively charged lipid membranes. Polycarbonate with pendant benzyl chloride was selected as the cationic block, offering an excellent platform to introduce cationic charge and the essential functional groups that enable the polymeric molecules to self-assemble into micellar structures critical for the proposed mechanism. With an improved EPR effect, the nanoparticles formed will flow through the blood stream and selectively attack the tumor tissue.

In another study, Zhong et al.[110] synthesized guanidinium-functionalized macromolecular anticancer polymers. A series of triblock copolymers of PEG, guanidinium-functionalized polycarbonate, and polylactide (PEG-PGCm-PLAn) were prepared using organocatalytic ring-opening polymerization (OROP) The cytotoxicity of these polymers was tested on different cancer cell lines, BCap37, HepG2, A549, HL-7702, and A431, along with MDR cells. Their selectivity was estimated using normal human cell lines (a human hepatic HL-7702 cell line and primary human dermal fibroblasts) for comparison.

Based on this membrane-targeting mechanism, Takahashi et al.[111] published a report on the design of a new class of anticancer polymers. The authors designed and synthesized a series of new anticancer cationic polymers, which were effective in killing dormant prostate cancer (PCa) cells instigated by membrane-active host defense peptides [112-114]

These findings expand the use of cationic polymers and provide new opportunities for the use of cancer chemotherapeutics and antibiotics in combination with cationic polymers for selective and effective treatment of cancer.

1.4. Objective of the thesis

In my doctoral research thesis, the polymers were checked for their anti-cancerous properties. In this thesis the polymers were used as anticancer agents in itself without the usage of any additional drugs like doxorubicin, paclitaxel, etc. To achieve this purpose, the polymers carrying the cationic charge were synthesized by the RAFT polymerization. These synthesized polymers were checked for their anticancer properties along with their mechanism of action.

1.4.1. Chapter 2

Background: The development of the molecules effective for killing cancer cells is still a persistent issue in drug discovery. With all the known limitations of the small molecules and the nanotechnology-based drug delivery systems which hinders the development of chemotherapeutic drug, the potential of polymeric molecules as anticancer drug was investigated. The use of cationic polymers as antimicrobials has been extensively studied due to the selective binding of cationic group with the anionic membranes of the bacterial cells. On the basis of these findings recently, cationic polymers have proven to be very promising and found to be effective against various cancer cell lines, even in the killing of multi-drug resistant cancer cells. Although, these literatures reported the use of cationic polymers, the effect of hydrophobicity and its interaction with the cancer cell membrane was not extensively studied.

Outline: The design and synthesis of novel anticancer polymers containing hydrophobic groups were described. The fact that the cationic homopolymer poly(3-acrylamidopropyl)trimethylammonium chloride (PAMPTMA) does not show any anticancer activity on its own; however, the insertion of hydrophobic moieties in copolymers

(PAMPTMA-*r*-BuMA, PAMPTMA-*r*-HexMA, and PAMPTMA-*r*-OctMA) [BuMa: butyl methacrylate, HexMA: hexyl methacrylate, OctMA: octyl methacrylate] enhances their anticancer activity with very low IC_{50} value was established. Mechanistic investigations were carried out using LDH leakage assay, cellular uptake, and DOSY NMR to study the interaction between the polymer and the cell membrane as well as the role of hydrophobicity in enhancing this interaction. The results demonstrated that polymers are attracted by the anionic cancer cell membrane, which then leads to the insertion of hydrophobic groups inside the cell membrane, causing its disruption and ultimate lysis of the cell. This study demonstrates a novel and better approach for the rational design and discovery of new polymeric anticancer agents with improved efficacy.

1.4.2. Chapter 3

Background: In chapter 2, the efficacy of the cationic polymers with some hydrophobicity towards the cancer cell line was proved. The designed polymeric models work well, also gave us insights regarding the mechanism involved during the interaction towards the cancer cell membrane. However, the selectivity towards the normal cell was not explained, which is very important for the anticancer systems to work with. Selectivity is the one of the major issues when it comes to cancer treatment along with drug resistance development and the tumor metastasis. In the present scenario, the invention of an anticancer agent with negligible cytotoxicity towards the normal cells and mitigating the multidrug resistance (MDR) issue along with the metastasis is a great challenge.

Outline: To surmount these challenges a series of poly-L-lysine (PLL) and nicotinic acid (NA) based polymers with varying amount of dodecylsuccinic anhydride (DDSA) was synthesized. In order to obtain the selectivity, the cationic charge of polymers was concealed/masked by coordination with the Zn^{2+} ions. These Zn-bound polymers were found to be highly effective

against liver cancer (HepG2) and colon cancer (colon 26) and also prevented cancer cell migration. These anticancer polymers are designed to target the anionic membranes of the cancer cells owing to the overexpression of the various lipids on their surface and therefore act by disrupting the cancer cell membranes. As a consequence of this mechanism, they exhibited potent anticancer activity against the drug resistance cell lines (COR-L23/R). The experiments with the small molecule drug like doxorubicin (DOX) showed lack of selectivity and its efficacy towards the drug resistance cell lines and failure in preventing the tumor metastasis. Overall, the designed polymers show great promise in cancer treatment along with mitigating the issue of drug resistance and tumor metastasis, and therefore could be a new and novel approach in designing the cancer therapeutics using the macromolecules.

1.4.3. Chapter 4

Background: In chapter 2 and 3, the use of cationic polymers in cancer treatment was investigated. I also focused on the surface morphological properties of the cancer cell and how they behaved when they come in contact of the cationic polymers. The previous chapter made us understand the importance of selectivity and how it can be achieved by masking the cationic charge in them. On the basis of the knowledge, information obtained, and the potential benefits known for cationic polymers from the previous chapters we decided to convert one of the bioactive anticancer compound methyl jasmonate (MJ) to the cationic polymer or to copolymerize it with known cationic polymers. Hence in this chapter, the synthesis of MJ based monomer and then further copolymerized it with cationic monomers was carried out.

Outline: In order to achieve that, the MJ based monomer were synthesized by developing various synthetic routes and finally selecting with lesser number of steps, essay preparation methods. The obtained MJ based monomer was further copolymerized with varying amounts of the (3-acrylamidopropyl)trimethylammonium chloride as a cationic monomer. The synthesis

of the obtained monomer and the copolymers were confirmed by the proton NMR. The obtained polymers were tested against the cancer cell line to determine their anticancer efficacy. The results demonstrated the enhancement of the anticancer activity with polymerized MJ as compared to the MJ as a small molecular drug.

1.5. References

1. World Health Organisation, 2021**,** https://gco.iarc.fr/.
2. Kumar, N.; Fazal, S.; Miyako, E.; Matsumura, K.; Rajan, R., *Materials Today* **2021**, *51*, 317-349.
3. Samatov, T. R.; Galatenko, V. V.; Block, A.; Shkurnikov, M. Y.; Tonevitsky, A. G.; Schumacher, U., *Semin Cancer Biol* **2017**, *45*, 50-57.
4. Vallabhapurapu, S. D.; Blanco, V. M.; Sulaiman, M. K.; Vallabhapurapu, S. L.; Chu, Z.; Franco, R. S.; Qi, X., *Oncotarget* **2015**, *6*, (33), 34375-88.
5. Yoon, W. H.; Park, H. D.; Lim, K.; Hwang, B. D., *Biochem Biophys Res Commun* **1996**, *222*, (3), 694-9.
6. Burdick, M. D.; Harris, A.; Reid, C. J.; Iwamura, T.; Hollingsworth, M. A., *J Biol Chem* **1997**, *272*, (39), 24198-202.
7. Lee, H. S.; Park, C. B.; Kim, J. M.; Jang, S. A.; Park, I. Y.; Kim, M. S.; Cho, J. H.; Kim, S. C., *Cancer Lett* **2008**, *271*, (1), 47-55.
8. Kleeff, J.; Ishiwata, T.; Kumbasar, A.; Friess, H.; Büchler, M. W.; Lander, A. D.; Korc, M., *J Clin Invest* **1998**, *102*, (9), 1662-73.
9. Hoskin, D. W.; Ramamoorthy, A., *Biochim Biophys Acta* **2008**, *1778*, (2), 357-75.
10. Chan, S. C.; Hui, L.; Chen, H. M., *Anticancer Res* **1998**, *18*, (6a), 4467-74.
11. Warburg, O., *Science* **1956**, *123*, (3191), 309-314.
12. Bhardwaj, V.; Rizvi, N.; Lai, M. B.; Lai, J. C.; Bhushan, A., *Anticancer Res* **2010**, *30*, (3), 743-9.
13. Chen, B.; Le, W.; Wang, Y.; Li, Z.; Wang, D.; Ren, L.; Lin, L.; Cui, S.; Hu, J. J.; Hu, Y.; Yang, P.; Ewing, R. C.; Shi, D.; Cui, Z., *Theranostics* **2016**, *6*, (11), 1887-1898.
14. J. H. Breasted, *The Edwin Smith Surgical Papyrus,*, University of Chicago Press,, 1930.
15. Hajdu, S. I., *Cancer* **2004**, *100*, (10), 2048-51.
16. Castiglioni A, *Histoire de la Medecine*, 1931.

17. National Cancer Institute Surgery to treat cancer https://www.cancer.gov/about-cancer/treatment/types/surgery.

18. Dayes, I. S.; Whelan, T. J.; Julian, J. A.; Kuettel, M. R.; Regmi, D.; Okawara, G. S.; Patel, M.; Reiter, H. I.; Dubois, S., *Curr Oncol* **2006**, *13*, (4), 124-129.

19. Nutting, C. M.; Bedford, J. L.; Cosgrove, V. P.; Tait, D. M.; Dearnaley, D. P.; Webb, S., *Radiother Oncol* **2001**, *61*, (2), 157-63.

20. Lo, S. S.; Fakiris, A. J.; Chang, E. L.; Mayr, N. A.; Wang, J. Z.; Papiez, L.; Teh, B. S.; McGarry, R. C.; Cardenes, H. R.; Timmerman, R. D., *Nat Rev Clin Oncol* **2010**, *7*, (1), 44-54.

21. Huang, C. Y.; Ju, D. T.; Chang, C. F.; Muralidhar Reddy, P.; Velmurugan, B. K., *Biomedicine (Taipei)* **2017**, *7*, (4), 23.

22. Schirrmacher, V., *Int J Oncol* **2019**, *54*, (2), 407-419.

23. Rajan, R.; Matsumura, K., Development and Application of Cryoprotectants. In *Survival Strategies in Extreme Cold and Desiccation: Adaptation Mechanisms and Their Applications*, Iwaya-Inoue, M.; Sakurai, M.; Uemura, M., Eds. Springer Singapore: Singapore, 2018; pp 339-354.

24. Glassman, P. M.; Muzykantov, V. R., *Journal of Pharmacology and Experimental Therapeutics* **2019**, *370*, (3), 570-580.

25. Wang, H.; Evans, C. L., Chapter 11 - Coherent Raman Scattering Microscopy in Dermatological Imaging. In *Imaging in Dermatology*, Hamblin, M. R.; Avci, P.; Gupta, G. K., Eds. Academic Press: Boston, 2016; pp 103-117.

26. Ernsting, M. J.; Murakami, M.; Roy, A.; Li, S. D., *Journal of Controlled Release* **2013**, *172*, (3), 782-794.

27. Torchilin, V., *Advanced Drug Delivery Reviews* **2011**, *63*, (3), 131-135.

28. Hasan, W.; Chu, K.; Gullapalli, A.; Dunn, S. S.; Enlow, E. M.; Luft, J. C.; Tian, S.; Napier, M. E.; Pohlhaus, P. D.; Rolland, J. P.; Desimone, J. M., *Nano Letters* **2012**, *12*, (1), 287-292.

29. Hu, Q.; Gao, X.; Gu, G.; Kang, T.; Tu, Y.; Liu, Z.; Song, Q.; Yao, L.; Pang, Z.; Jiang, X.; Chen, H.; Chen, J., *Biomaterials* **2013**, *34*, (22), 5640-5650.

30. Pan, Q.; Tian, J.; Zhu, H.; Hong, L.; Mao, Z.; Oliveira, J. M.; Reis, R. L.; Li, X., *ACS Biomaterials Science and Engineering* **2020**, *6*, (4), 2175-2185.

31. Strand, M. S.; Krasnick, B. A.; Pan, H.; Zhang, X.; Bi, Y.; Brooks, C.; Wetzel, C.; Sankpal, N.; Fleming, T.; Peter Goedegebuure, S.; DeNardo, D. G.; Gillanders, W. E.; Hawkins, W. G.; Wickline, S. A.; Fields, R. C., *Oncotarget* **2019**, *10*, (46), 4761-4775.

32. Wohlfart, S.; Khalansky, A. S.; Gelperina, S.; Maksimenko, O.; Bernreuther, C.; Glatzel, M.; Kreuter, J., *PLoS ONE* **2011**, *6*, (5).

33. Song, C.; Xiao, Y.; Ouyang, Z.; Shen, M.; Shi, X., *Journal of Materials Chemistry B* **2020**, *8*, (14), 2768-2774.

34. Patterson, C. M.; Balachander, S. B.; Grant, I.; Pop-Damkov, P.; Kelly, B.; McCoull, W.; Parker, J.; Giannis, M.; Hill, K. J.; Gibbons, F. D.; Hennessy, E. J.; Kemmitt, P.; Harmer, A. R.; Gales, S.; Purbrick, S.; Redmond, S.; Skinner, M.; Graham, L.; Secrist, J. P.; Schuller, A. G.; Wen, S.; Adam, A.; Reimer, C.; Cidado, J.; Wild, M.; Gangl, E.; Fawell, S. E.; Saeh, J.; Davies, B. R.; Owen, D. J.; Ashford, M. B., *Communications Biology* **2021**, *4*, (1).

35. Kaminskas, L. M.; McLeod, V. M.; Kelly, B. D.; Sberna, G.; Boyd, B. J.; Williamson, M.; Owen, D. J.; Porter, C. J. H., *Nanomedicine: Nanotechnology, Biology, and Medicine* **2012**, *8*, (1), 103-111.

36. Dong, Y.; Yu, T.; Ding, L.; Laurini, E.; Huang, Y.; Zhang, M.; Weng, Y.; Lin, S.; Chen, P.; Marson, D.; Jiang, Y.; Giorgio, S.; Pricl, S.; Liu, X.; Rocchi, P.; Peng, L., *Journal of the American Chemical Society* **2018**, *140*, (47), 16264-16274.

37. Cui, Y.; Sui, J.; He, M.; Xu, Z.; Sun, Y.; Liang, J.; Fan, Y.; Zhang, X., *ACS Applied Materials and Interfaces* **2016**, *8*, (3), 2193-2203.

38. Zhang, Y.; Renssen, H.; Seppä, H., *Clim. Past* **2016**, *12*, (5), 1119-1135.

39. Park, E. K.; Kim, S. Y.; Lee, S. B.; Lee, Y. M. In *Folate-conjugated methoxy poly(ethylene glycol)/poly(ε-caprolactone) amphiphilic block copolymeric micelles for tumor-targeted drug delivery*, Journal of Controlled Release, 2005; pp 158-168.

40. Li, Y.; Jin, M.; Shao, S.; Huang, W.; Yang, F.; Chen, W.; Zhang, S.; Xia, G.; Gao, Z., *BMC Cancer* **2014**, *14*, (1), 329.

41. Alibolandi, M.; Abnous, K.; Hadizadeh, F.; Taghdisi, S. M.; Alabdollah, F.; Mohammadi, M.; Nassirli, H.; Ramezani, M., *Journal of Controlled Release* **2016**, *241*, 45-56.

42. Zhu, D.; Fan, F.; Huang, C.; Zhang, Z.; Qin, Y.; Lu, L.; Wang, H.; Jin, X.; Zhao, H.; Yang, H.; Zhang, C.; Yang, J.; Liu, Z.; Sun, H.; Leng, X.; Kong, D.; Zhang, L., *Acta Biomaterialia* **2018**, *75*, 386-397.

43. Yang, X.; Grailer, J. J.; Rowland, I. J.; Javadi, A.; Hurley, S. A.; Matson, V. Z.; Steeber, D. A.; Gong, S., *ACS Nano* **2010**, *4*, (11), 6805-6817.

44. Du, Y.; Chen, W.; Zheng, M.; Meng, F.; Zhong, Z., *Biomaterials* **2012**, *33*, (29), 7291-7299.

45. Chiang, W. H.; Ho, V. T.; Huang, W. C.; Huang, Y. F.; Chern, C. S.; Chiu, H. C., *Langmuir* **2012**, *28*, (42), 15056-15064.

46. Desale, S. S.; Raja, S. M.; Kim, J. O.; Mohapatra, B.; Soni, K. S.; Luan, H.; Williams, S. H.; Bielecki, T. A.; Feng, D.; Storck, M.; Band, V.; Cohen, S. M.; Band, H.; Bronich, T. K., *Journal of Controlled Release* **2015**, *208*, 59-66.

47. Qiao, Z. Y.; Zhang, R.; Du, F. S.; Liang, D. H.; Li, Z. C., *Journal of Controlled Release* **2011**, *152*, (1), 57-66.

48. Maciel, D.; Figueira, P.; Xiao, S.; Hu, D.; Shi, X.; Rodrigues, J.; Tomás, H.; Li, Y., *Biomacromolecules* **2013**, *14*, (9), 3140-3146.

49. Schiffelers, R. M.; Koning, G. A.; Ten Hagen, T. L. M.; Fens, M. H. A. M.; Schraa, A. J.; Janssen, A. P. C. A.; Kok, R. J.; Molema, G.; Storm, G. In *Anti-tumor efficacy of tumor vasculature-targeted liposomal doxorubicin*, Journal of Controlled Release, 2003; pp 115-122.

50. Camacho, K. M.; Menegatti, S.; Vogus, D. R.; Pusuluri, A.; Fuchs, Z.; Jarvis, M.; Zakrewsky, M.; Evans, M. A.; Chen, R.; Mitragotri, S., *Journal of Controlled Release* **2016**, *229*, 154-162.

51. Battaglia, L.; Muntoni, E.; Chirio, D.; Peira, E.; Annovazzi, L.; Schiffer, D.; Mellai, M.; Riganti, C.; Salaroglio, I. C.; Lanotte, M.; Panciani, P.; Capucchio, M. T.; Valazza, A.; Biasibetti, E.; Gallarate, M., *Nanomedicine* **2017**, *12*, (6), 639-656.

52. Rosière, R.; Van Woensel, M.; Gelbcke, M.; Mathieu, V.; Hecq, J.; Mathivet, T.; Vermeersch, M.; Van Antwerpen, P.; Amighi, K.; Wauthoz, N., *Molecular Pharmaceutics* **2018**, *15*, (3), 899-910.

53. Kim, J. H.; Kim, Y.; Bae, K. H.; Park, T. G.; Lee, J. H.; Park, K., *Molecular Pharmaceutics* **2015**, *12*, (4), 1230-1241.

54. Deirram, N.; Zhang, C.; Kermaniyan, S. S.; Johnston, A. P. R.; Such, G. K., *Macromolecular Rapid Communications* **2019**, *40*, (10), 1800917.

55. Li, Y.; Xiao, K.; Luo, J.; Xiao, W.; Lee, J. S.; Gonik, A. M.; Kato, J.; Dong, T. A.; Lam, K. S., *Biomaterials* **2011**, *32*, (27), 6633-6645.

56. Gobin, E.; Bagwell, K.; Wagner, J.; Mysona, D.; Sandirasegarane, S.; Smith, N.; Bai, S.; Sharma, A.; Schleifer, R.; She, J. X., *BMC Cancer* **2019**, *19*, (1).

57. Yuan, C.; Ji, W.; Xing, R.; Li, J.; Gazit, E.; Yan, X., *Nature Reviews Chemistry* **2019**, *3*, (10), 567-588.

58. Li, S.; Zhang, W.; Xue, H.; Xing, R.; Yan, X., *Chemical Science* **2020**, *11*, (33), 8644-8656.

59. Chang, R.; Yan, X., *Small Structures* **2020**, *1*, (2), 2000068.

60. Mandal, A.; Boopathy, A. V.; Lam, L. K. W.; Moynihan, K. D.; Welch, M. E.; Bennett, N. R.; Turvey, M. E.; Thai, N.; Van, J. H.; Love, J. C.; Hammond, P. T.; Irvine, D. J., *Sci. Transl. Med.* **2018**, *10*, 467.

61. Chen, Daniel S.; Mellman, I., *Immunity* **2013**, *39*, (1), 1-10.

62. Ahmed, S.; Rai, K. R., *Best Practice and Research: Clinical Haematology* **2003**, *16*, (1), 69-81.

63. Menon, S., *Cancers (Basel)* **2016**, *8*, 12.

64. Stephan, S. B.; Taber, A. M.; Jileaeva, I.; Pegues, E. P.; Sentman, C. L.; Stephan, M. T., *Nature Biotechnology* **2015**, *33*, (1), 97-101.

65. Riley, R. S.; June, C. H.; Langer, R.; Mitchell, M. J., *Nature Reviews Drug Discovery* **2019**, *18*, (3), 175-196.

66. Guo, L.; Yan, D. D.; Yang, D.; Li, Y.; Wang, X.; Zalewski, O.; Yan, B.; Lu, W., *ACS Nano* **2014**, *8*, (6), 5670-5681.

67. Wu, L.; Huang, J.; Pu, K.; James, T. D., *Nature Reviews Chemistry* **2021**, *5*, (6), 406-421.

68. Zhang, C.; Zeng, Z.; Cui, D.; He, S.; Jiang, Y.; Li, J.; Huang, J.; Pu, K., *Nature Communications* **2021**, *12*, (1).

69. Jiang, Y.; Huang, J.; Xu, C.; Pu, K., *Nature Communications* **2021**, *12*, (1).

70. Zhang, C.; Pu, K., *Chemical Society Reviews* **2020**, *49*, (13), 4234-4253.

71. Zhang, Y.; Xu, C.; Yang, X.; Pu, K., *Advanced Materials* **2020**, *32*, (34), 2070252.

72. Tabujew, I.; Peneva, K., CHAPTER 1 Functionalization of Cationic Polymers for Drug Delivery Applications. In *Cationic Polymers in Regenerative Medicine*, The Royal Society of Chemistry: 2015; pp 1-29.

73. Farshbaf, M.; Davaran, S.; Zarebkohan, A.; Annabi, N.; Akbarzadeh, A.; Salehi, R., *Artificial Cells, Nanomedicine, and Biotechnology* **2018**, *46*, (8), 1872-1891.

74. Lee, W. F.; Lee, S. C., (0957-4530 (Print)).

75. Lee, J.; Yun, K.-S.; Choi, C. S.; Shin, S.-H.; Ban, H.-S.; Rhim, T.; Lee, S. K.; Lee, K. Y., *Bioconjugate Chemistry* **2012**, *23*, (6), 1174-1180.

76. Song, Y.; Zhang, L.; Gan, W.; Zhou, J.; Zhang, L., *Colloids and Surfaces B: Biointerfaces* **2011**, *83*, (2), 313-320.

77. Cohen, J. L.; Schubert, S.; Wich, P. R.; Cui, L.; Cohen, J. A.; Mynar, J. L.; Fréchet, J. M. J., *Bioconjugate Chemistry* **2011**, *22*, (6), 1056-1065.

78. Wong, K.; Sun, G.; Zhang; Dai, H.; Liu, Y.; He; Leong, K. W., *Bioconjugate Chemistry* **2006**, *17*, (1), 152-158.

79. Díaz-Moscoso, A.; Vercauteren, D.; Rejman, J.; Benito, J. M.; Ortiz Mellet, C.; De Smedt, S. C.; Fernández, J. M. G., *Journal of Controlled Release* **2010**, *143*, (3), 318-325.

80. Kamiński, K.; Płonka, M.; Ciejka, J.; Szczubiałka, K.; Nowakowska, M.; Lorkowska, B.; Korbut, R.; Lach, R., *Journal of Medicinal Chemistry* **2011**, *54*, (19), 6586-6596.

81. Chen, M.; Tang, Y.; Wang, T.; Long, Q.; Zeng, Z.; Chen, H.; Feng, X., *Materials Science and Engineering: C* **2016**, *69*, 1367-1372.

82. Liu, T.; Xue, W.; Ke, B.; Xie, M.-Q.; Ma, D., *Biomaterials* **2014**, *35*, (12), 3865-3872.

83. Jeong H Fau - Lee, E.-S.; Lee Es Fau - Jung, G.; Jung G Fau - Park, J.; Park J Fau - Jeong, B.; Jeong B Fau - Ryu, K. H.; Ryu Kh Fau - Hwang, N. S.; Hwang Ns Fau - Lee, H.; Lee, H., (1550-7033 (Print)).

84. Han, S.; Cheng, Q.; Wu, Y.; Zhou, J.; Long, X.; Wei, T.; Huang, Y.; Zheng, S.; Zhang, J.; Deng, L.; Wang, X.; Liang, X.-J.; Cao, H.; Liang, Z.; Dong, A., *Biomaterials* **2015**, *48*, 45-55.

85. Lind, M. J., *Medicine* **2008**, *36*, (1), 19-23.

86. Lohner, K.; Blondelle, S. E., *Comb Chem High Throughput Screen* **2005**, *8*, (3), 241-56.

87. Sun, H.; Dong, Y.; Feijen, J.; Zhong, Z., *J Control Release* **2018**, *290*, 11-27.

88. Tang, W.; Becker, M. L., *Chem Soc Rev* **2014**, *43*, (20), 7013-39.

89. Komin, A.; Russell, L. M.; Hristova, K. A.; Searson, P. C., *Adv Drug Deliv Rev* **2017**, *110-111*, 52-64.

90. Zhao, J.; Li, Q.; Hao, X.; Ren, X.; Guo, J.; Feng, Y.; Shi, C., *Journal of Materials Chemistry B* **2017**, *5*, (40), 8035-8051.

91. Leuschner, C.; Hansel, W., *Curr Pharm Des* **2004**, *10*, (19), 2299-310.

92. Sui, S. F.; Wu, H.; Guo, Y.; Chen, K. S., *J Biochem* **1994**, *116*, (3), 482-7.

93. Bechinger, B., *Biochim Biophys Acta* **1999**, *1462*, (1-2), 157-83.

94. Huang, H. W., *Biochemistry* **2000**, *39*, (29), 8347-52.

95. Mellor, I. R.; Sansom, M. S., *Proc R Soc Lond B Biol Sci* **1990**, *239*, (1296), 383-400.

96. Merrifield, E. L.; Mitchell, S. A.; Ubach, J.; Boman, H. G.; Andreu, D.; Merrifield, R. B., *International Journal of Peptide and Protein Research* **1995**, *46*, (3-4), 214-220.

97. Ludtke, S. J.; He, K.; Wu, Y.; Huang, H. W., *Biochim Biophys Acta* **1994**, *1190*, (1), 181-4.

98. Pouny, Y.; Rapaport, D.; Mor, A.; Nicolas, P.; Shai, Y., *Biochemistry* **1992**, *31*, (49), 12416-23.

99. Dufourcq, J.; Faucon, J. F.; Fourche, G.; Dasseux, J. L.; Le Maire, M.; Gulik-Krzywicki, T., *Biochim Biophys Acta* **1986**, *859*, (1), 33-48.

100. Dempsey, C. E.; Sternberg, B., *Biochimica et Biophysica Acta (BBA) - Biomembranes* **1991**, *1061*, (2), 175-184.

101. Segrest, J. P.; Garber, D. W.; Brouillette, C. G.; Harvey, S. C.; Anantharamaiah, G. M., *Adv Protein Chem* **1994**, *45*, 303-69.

102. Roux, M.; Nezil, F. A.; Monck, M.; Bloom, M., *Biochemistry* **1994**, *33*, (1), 307-311.

103. Engler, A. C.; Wiradharma, N.; Ong, Z. Y.; Coady, D. J.; Hedrick, J. L.; Yang, Y.-Y., *Nano Today* **2012**, *7*, (3), 201-222.

104. Holmberg, A. R.; Wilchek, M.; Márquez, M.; Westlin, J. E.; Du, J.; Nilsson, S., *Clin Cancer Res* **1999**, *5*, (10 Suppl), 3056s-3058s.

105. Kawai, T.; Kato, A.; Higashi, H.; Kato, S.; Naiki, M., *Cancer Res* **1991**, *51*, (4), 1242-6.

106. Kökoğlu, E.; Sönmez, H.; Uslu, E.; Uslu, I., *Cancer Biochem Biophys* **1992**, *13*, (1), 57-64.

107. Lin, S.; Kemmner, W.; Grigull, S.; Schlag, P. M., *Exp Cell Res* **2002**, *276*, (1), 101-10.

108. Gakhar, G.; Liu, H.; Shen, R.; Scherr, D.; Wu, D.; Nanus, D.; Chu, C. C., *Anticancer Res* **2014**, *34*, (8), 3981-9.

109. Park, N. H.; Cheng, W.; Lai, F.; Yang, C.; Florez de Sessions, P.; Periaswamy, B.; Wenhan Chu, C.; Bianco, S.; Liu, S.; Venkataraman, S.; Chen, Q.; Yang, Y. Y.; Hedrick, J. L., *Journal of the American Chemical Society* **2018**, *140*, (12), 4244-4252.

110. Zhong, G.; Yang, C.; Liu, S.; Zheng, Y.; Lou, W.; Teo, J. Y.; Bao, C.; Cheng, W.; Tan, J. P. K.; Gao, S.; Park, N.; Venkataraman, S.; Huang, Y.; Tan, M. H.; Wang, X.; Hedrick, J. L.; Fan, W.; Yang, Y. Y., *Biomaterials* **2019**, *199*, 76-87.

111. Takahashi, H.; Yumoto, K.; Yasuhara, K.; Nadres, E. T.; Kikuchi, Y.; Buttitta, L.; Taichman, R. S.; Kuroda, K., *Sci Rep* **2019**, *9*, (1), 1096.

112. Papo, N.; Shai, Y., *Cell Mol Life Sci* **2005**, *62*, (7-8), 784-90.

113. Riedl, S.; Zweytick, D.; Lohner, K., *Chem Phys Lipids* **2011**, *164*, (8), 766-81.

114. Yeung, A. T. Y.; Gellatly, S. L.; Hancock, R. E. W., *Cellular and Molecular Life Sciences* **2011**, *68*, (13), 2161.

Chapter 2

Mechanistic insights and importance of hydrophobicity in cationic polymers for cancer therapy

2.1. Introduction

With the gradual recovery of the world from the global pandemic of Covid-19, there is a compelling need to develop pioneering ways to anticipate and prevent the emergence of new disorders and to treat existing ones such as cancer. Although cancer has become a leading cause of mortality after cardiovascular diseases, its treatment remains a problem for the health care system worldwide.[1, 2] Treatments such as surgical resection, radiation therapy, and chemotherapy have afforded impressive results and improved the overall survival rate of patients, but only to a limited extent.[3, 4] This is because of various issues associated with these traditional treatment regimes, such as pain during surgery, drug resistance, off-target cytotoxicity, insufficient drug accumulation, and rapid clearance from the body.[5-7] To overcome these issues, nanotechnology-based treatments that enable the use of drugs and materials in single platform have been attracting enormous attention, as they can prevent the degradation of the drug inside the body and reduce drug cytotoxicity and its side effects.[8-10] However, these treatment regimens still suffer from the inherited limitation of the drug and rely on the action of the drug itself. In addition, loading of drugs on nanoparticles and material-related limitations are other drawbacks of these systems.[2]

Because of all these known limitations of small molecules and nanoparticle-based drug-delivery systems, there is a compelling need to develop new chemotherapeutics for tumour treatment and mitigating drug resistance and tumour metastasis. Recently, the potential of using polymers as an anticancer drug was investigated. Because cationic polymers selectively bind to the anionic

membrane of the bacterial cells, their usage as antimicrobials has been extensively studied; however, their application as anticancer agents is relatively new.[11-13] Similar to the bacterial cell membrane, the cancer cell membranes are more negatively charged because of the overexpression of anionic lipids, including phosphatidylserine (PS), sialylated gangliosides, and heparan sulfates.[14-17] Consequently, certain antimicrobial peptides (AMPs) and anticancer peptides (ACPs) have shown potent selectivity and apoptotic and anti-proliferative activity against cancer cells.[18-21] Nevertheless, their low bioavailability, short half-life, poor pharmacokinetics, and high production cost when manufactured on a large scale are some notable disadvantages.[22, 23]

Recently, a few studies have reported the use of cationic polymers as anticancer agents while investigating the drug-resistance issue,[23, 24] tumour metastasis,[25] killing of dormant cancer cells, [26] and certain applications in prostate cancer as well.[27] Several factors contribute to the adhesion and subsequent adsorption of anticancer agents into the cell membrane.[28, 29] Although the literature has reported the use of cationic polymers, their adsorption behavior and the role of hydrophobicity on the cancer cell membrane have not been reported yet. From the previous studies on AMPs and ACPs, it is evident that they first selectively bind to the PS lipid-rich membrane of the cancer cell by electrostatic interactions, and then insert the hydrophobic domain of their helix into the cell membrane, resulting in the disruption of the cell membrane and subsequent lysis of the cell.[30] Herein, I investigate whether cationic polymers show enhanced anticancer efficacy because of their hydrophobic groups and form a stronger association with the cell membrane, resulting in cell lysis. Although it has been widely reported that cationic polymers exhibit remarkable anticancer efficacy, it has not yet been established whether synthetic cationic polymers alone show any noticeable anticancer property and whether the presence of a hydrophobic counterpart is a prerequisite. To the best of our knowledge, no extensive study has yet been

conducted to confirm whether the hydrophobicity of cationic polymers plays a role in their anti-cancerous property. In addition, we demonstrated the use of molecular dynamics as a tool to investigate the adsorption behavior, polymer interactions with the cell membrane. A clear understanding of the mechanism will facilitate the rational design of polymeric anticancer agents with improved efficiency.

In this study, the design of new macromolecular anticancer polymers containing a cationic chain and a hydrophobic chain was carried out. A series of cationic homopolymers of (3-acrylamidopropyl)trimethylammonium chloride (AMPTMA) and its copolymers with the hydrophobic co-monomer *n*-butyl methacrylate (BuMA) are synthesized through reversible addition-fragmentation chain transfer (RAFT) polymerization. The composition of the polymers is modulated by varying the amount of BuMA to study the effect of hydrophobicity on anticancer activity. The copolymers containing the *n*-hexyl methacrylate (HexMA) and *n*-octyl methacrylate (OcMA) as co-monomers are also synthesized to study the effect of the size of the hydrophobic group on cytotoxicity. The anti-cancerous activity of the synthesized polymers is studied against various cancer cell lines by the cell-viability assay. The effect of hydrophobicity is systematically investigated by conducting the lactate dehydrogenase (LDH) leakage assay, confocal microscopy, and dye-leakage experiments. Finally, the interaction of the hydrophobic-group-containing polymers with the cell membrane was established by ^{1}H-NMR diffusion ordered spectroscopy (DOSY). In addition to that, modelling and the molecular dynamics simulations were performed to further prove our hypothesis.

2.2. Experimental Section

2.2.1. Materials

4-Cyano-4-[(dodecylsulfanylthiocarbonyl)sulfanyl]pentanoic acid (RAFT agent) and 4,4′-azobis(4-cyanovaleric acid) (ACVA; initiator) were purchased from Sigma-Aldrich (St. Louis, MO) and used as received. A 75% aqueous solution of the monomer (3-acrylamidopropyl)trimethylammonium chloride (AMPTMA), *n*-butyl methacrylate (BuMA), *n*-hexyl methacrylate (HexMA), and *N*-(2-hydroxyethyl) acrylamide (HEAA) was purchased from TCI Japan. BuMA was purified prior to use by passing it through a packed column for removing the inhibitor (Sigma-Aldrich). *n*-Octyl methacrylate (OctMA) was purchased from NOF Corporation (Tokyo, Japan). Egg phosphatidylcholine/L-α-phosphatidylcholine (EPC) and 5(6)-carboxyfluorescein (CF) were purchased from Sigma-Aldrich. Dipalmitoylphosphatidylcholine (DOPC) was obtained from NOF Corporation (Tokyo, Japan).

2.2.2. Synthesis of polymers

2.2.2.1. Synthesis of Poly(AMPTMA). I synthesized PAMPTMA homopolymers **(Scheme 2.1a)**, AMPTMA monomers, a RAFT agent, and an initiator were combined to prepare homopolymers of different molecular weight. As an example, $PAMPTMA_{100}$ was synthesized at a mole feed ratio [AMPTMA]:[RAFT agent]:[ACVA] = 100:1:0.2. In a 100-mL round-bottomed flask, AMPTMA (1.5 g, 7.25 mmol), RAFT agent (29.26 mg, 0.0725 mmol), and initiator ACVA (4.06 mg, 0.0145 mmol) were dissolved in 25 mL of methanol-acetate buffer (7:3 v/v; pH 5.3). The solution was then purged with nitrogen gas for 30 min, sealed with a rubber septum, and stirred at 70 °C for 24 h. The obtained polymer was purified by dialysis using distilled water (4 days) with a 3500 MWCO dialysis membrane (Spectra/Por Dialysis membrane), followed by lyophilisation. The obtained homopolymers were successfully characterized by ^{1}H-NMR and ^{13}C-NMR.

2.2.2.2. Synthesis of Poly(AMPTMA-*r*-BuMA). I synthesized various copolymers **(Scheme 2.1b)** by varying the proportion of BuMA as a co-monomer. As an example, 10% BuMA copolymer comprising 90 mol% AMPTMA and 10 mol% BuMA was synthesized by adding AMPTMA (1 g, 4.837 mmol), BuMA (76.42 mg, 0.537 mmol), a RAFT agent (19.53 mg, 0.048 mmol), and ACVA (2.71mg, 0.0096 mmol) to the round-bottomed flask, followed by adding 25 mL of methanol-acetate buffer (7:3 v/v). The resulting solution was then purged with nitrogen gas for 30 min and stirred at 70 °C for 24 h. To change the hydrophobicity, the amount of BuMA was varied from 5% to 30% of the total monomer amount. The obtained random copolymer was purified by dialysis using distilled water (4 days) with a 3500 MWCO dialysis membrane (Spectra/Por Dialysis membrane), followed by lyophilization.

Similar procedures were followed for the synthesis of the AMPTMA-*r*-HexMA and AMPTMA-*r*-OctMA copolymers **(Scheme 2.1c and 2.1d)**. The obtained copolymers were successfully characterized by ^{1}H-NMR and ^{13}C-NMR.

2.2.2.3. Synthesis of Poly(HEAA-*r*-BuMA) Polymer. Neutral homopolymer (PHEAA) and its copolymers (HEAA-*r*-BuMA) were synthesized following the scheme shown in **Scheme 2.2**. For example, for the synthesis of 10% BuMA copolymer containing 90 mol% HEAA and 10 mol% of BuMA, I added HEAA (1 g, 8.686 mmol), BuMA (137.23 mg, 0.965 mmol), a RAFT agent (35.03 mg, 0.086 mmol), and ACVA (4.87 mg, 0.0173 mmol) to the 100-mL round-bottomed flask equipped with a magnetic stirrer. I then added 25 mL of methanol-acetate buffer (7:3 v/v). The resulting solution was then purged with nitrogen gas for 30 min and stirred at 70 °C for 24 h. To change the hydrophobicity, the amount of BuMA was varied from 0 % to 20 % of the total monomer amount. The obtained random copolymer was purified by dialysis using distilled water

(4 days) with a 3500 MWCO dialysis membrane (Spectra/Por Dialysis membrane), followed by lyophilization. The obtained polymers were successfully characterized by ^{1}H-NMR and ^{13}C-NMR.

2.2.3. Polymer Characterization

^{1}H-NMR and ^{13}C-NMR spectra were of the obtained polymers were recorded on a Bruker Avance NEO 400 spectrometer (400 MHz). The chemical shifts were referenced based on the solvent peak (δ = 4.79 ppm for D_2O). The molecular weight and distribution (polydispersity index, PDI) of the polymers were determined by gel-permeation chromatography (GPC, Waters e2695) using the Ultrahydrogel 250 column and 2414 refractive index detector at 50 °C. A 10% methanol–PBS solution (pH 7.4) was used as the mobile phase (flow rate: 1 mL min^{-1}) and a Shodex standard was used as the standard. Dynamic light scattering (DLS) and zeta-potential measurements were carried out on a Zetasizer Nano-ZS instrument (Malvern, UK) by using disposable folded capillary cells (DTS1070) with a scattering angle of 173°.

2.2.4. Determination of Cytotoxicity

2.2.4.1. Cell Culture. HepG2, Colon 26, and B16F10 cells were purchased from American Type Culture Collection (ATCC). Dulbecco's modified Eagle's medium (DMEM, Sigma-Aldrich) supplemented with 10% fetal bovine serum (FBS, Invitrogen, Singapore) was used for the cell culture at 37 °C in a CO_2 incubator under a humidified atmosphere. After the confluency, the cells were washed with phosphate-buffered saline (PBS) and then further treated with trypsin solution (0.25 % [w/v] trypsin containing 0.02% [w/v] ethylenediaminetetraacetic acid in PBS) to detach the cells. The cells were then collected by centrifugation and further re-suspended in fresh DMEM and subsequently transferred to a new culture plate for subculture.

2.2.4.2. MTT Assay. The cytotoxicity of polymers against various cancer cell lines was studied via 3-(4,5-dimethylthiazol-2-yl)-2,5-diphenyltetrazolium bromide (MTT) assay. The cells were seeded at a density of 3×10^3 cells per well in 0.1 mL of culture media in a 96-well plate for 24 h at 37 °C in a 5 % CO_2 incubator under a humidified atmosphere. The culture medium was then replaced with a fresh medium containing the polymer at various concentrations and incubated for 48 h at 37 °C; subsequently, 0.1 mL (300 μg/mL in DMEM) of the MTT solution was added. After 3 h of incubation, the medium containing MTT was discarded and replaced with 0.1 mL of DMSO to dissolve purple formazan crystals, followed by determination of absorbance at 540 nm using a microplate reader (Infinite 200Pro, Infinite M Nano, Tecan). The experiment was independently repeated three times.

2.2.5. LDH leakage assay

The HepG2 cells were seeded at 3×10^3 cells per well in a 96-well flat-bottom polystyrene cell culture plate for 24 h. Then, the medium was replaced by a serial concentration of the polymer (P3-P11, Table 1) and incubated for 48 h. After 48 h of treatment, 10 μL of the lysis buffer from the Cytotoxicity LDH assay Kit-WST (Dojindo) was added to four wells (positive control indicating 100% lysis) and incubated for 30 min at 37 °C as per manufacturer instructions. Then, 100 μL of the working solution was added to all wells and incubated for 30 min at room temperature. To stop the reaction, 50 μL of the stop solution was added, and absorbance at 490 nm was measured using a microplate reader (Infinite 200Pro, Infinite M Nano, Tecan). The percentage of LDH leakage was determined relative to that of 100 % lysed cells. Each assay was independently repeated three times.

2.2.6. Cellular Uptake Analysis

HepG2 cells were seeded onto a four-well glass-bottom dish (Matsunami), at a density of 30000 cells per well and allowed to attach and grow for 24 h. The medium was then replaced with an equal volume of another medium containing AlexaFluor 488 tagged P3 and P8 (at IC_{50} concentration). After 2 and 24 h of incubation, the cells were washed thrice with PBS for removing any free dye. Next, 4% formaldehyde was used to fix the cells for 15 min at 37 °C. The cells were then washed thrice in PBS. The cells were subsequently stained with Image-IT™ Live Plasma Membrane and Nuclear Labeling Kit (Invitrogen, Singapore), according to the manufacturer's instructions, followed by washing with PBS thrice. The cells were then observed under confocal laser scanning microscopy (Olympus FV1000D, oil immersed 60 × objective lens).

2.2.6.1. Tagging with AlexaFluor 488. A stock solution of the AlexaFluor 488 (melamide for thiol group) is prepared by dissolving it in high quality of the DMSO. This stock solution was added dropwise to the polymer solution (end terminal raft agent was converted to thiol group by using $NaBH_4$ beforehand) approximately 10 mmol of the polymer solution and the rection is kept for stirring for 4 h at 25 ºC with protection from the light. The unreacted dye was removed from the Sephadex G-25 gel filtration column. The solution was dried under vacuum and obtained powder was the AlexaFluor tagged polymer.

2.2.7. Liposome Preparation

In a glass vial, EPC or DOPC (12 mg) was dissolved in chloroform. The organic solvent was then evaporated under a gentle flow of nitrogen gas to produce a thin lipid film. The film was subsequently dried overnight under a vacuum. The resulting lipid film was hydrated in 1 mL of aqueous solution and then sonicated for 30 min at 45 °C. The single unilamellar vesicles were

obtained using a mini-extruder set (Avanti Polar Lipids), which was preheated to 55 °C and extruded 15 times through a membrane (Nuclepore Track-etch Membrane, Whatman) with a 0.1-μm pore size. Liposomes are closed vesicles composed of phospholipid bilayers and enclose an aqueous solution. Hence, they are commonly used as a cell-membrane mimic.

2.2.8. Leakage Experiment

Lipid films of liposomes were prepared as described above. The resulting lipid film was hydrated in 1 mL of 0.05 M of CF/PBS solution (the pH was maintained by adding NaOH for dissolving the CF dye). Uniform liposomes were obtained using a mini-extruder set (Avanti Polar Lipids) and membranes (Nuclepore Track-etch Membrane, Whatman) with a 0.1-μm pore size, as described above. Excess CF dye was removed by passing the liposome though a Sephadex G-25 column (NAP-10, Cytiva). The obtained liposomes were then treated with polymer solutions and the CF fluorescence was measured with a JASCO FP-8600 spectrofluorometer using an excitation wavelength of 450 nm and a detection wavelength of 520 nm at different time intervals. An increase in fluorescence intensity with time represents the membrane damage caused by the release of CF into the surrounding buffer.

2.2.9. ^{1}H Diffusion-Ordered NMR Spectroscopy (DOSY)

To understand the interaction between polymers and the cell membrane, ^{1}H diffusion-ordered NMR spectroscopy (DOSY) measurements were performed using a JEOL JNM-ECZ 400 spectrometer by employing DOPC liposomes as a model membrane. The DOSY spectrum was acquired at 25 °C. One-dimensional (1D) data were analysed with the Delta 5.3.1 software. In DOSY, the gradient strength (G) was varied from 0.1 to 0.9 Tm^{-1} at 25 °C. The diffusion time (Δ) and magnetic field gradient pulse width (δ) were determined for each polymer solution. Equation

1 shows the relationship between the diffusion coefficient (*D*) as a function of gradient strength, where I_0 and I are intensities at $G = 0$ and arbitrary G, respectively.

$$I(G,\delta,\Delta) = I_0 \times \exp\left(-D\gamma^2G^2\delta^2(\Delta - \delta/3)\right) \quad (1)$$

Additional species can be accounted by expanding Eqn. 1 as a sum of exponentials, as shown in Eqn. (2).

$$\ln(I/I_0) = -D\gamma^2G^2\delta^2(\Delta - \delta/3) \quad (2)$$

Therefore, when plotting $\gamma^2G^2\delta^2(\Delta - \delta/3)$ on the horizontal axis and $\ln(I/I_0)$ on the vertical axis, the slope of the straight line can be obtained as the *D* value. The hydrodynamic radius (R_h) of each component was determined by using the Stokes–Einstein (Eqn. 3), where *k* is the Boltzmann constant, *T* is the temperature and η is dynamic viscosity.

$$R_h = kT/6\pi\eta D \quad (3)$$

2.2.10. Modeling and Molecular Dynamics Simulations

The AMPTMA homopolymer was modeled as 15-mer, whereas the PAMPTMA-*r*-BuMA copolymer was constructed randomly from 10 AMPTMA and 5 BuMA monomers. The membrane was modeled as a lipid bilayer consisting of 1-palmitoyl-2-oleoyl-sn-glycero-3-phosphocholine (POPC) molecules. Our polymer-membrane systems were fully solvated with aqueous KCl solutions at 0.15 M, where the PAMPTMA-and PAMPTMA-*r*-BuMA-POPC systems contains 25,027 and 25,038 water molecules with K^+ and Cl^- ions, respectively, in simulation cells of 9.5 nm×9.5 nm×12.5 nm dimensions. A general AMBER force field (GAFF) was applied to the polymers and K^+/Cl^- ions; the Lipid17 and TIP3P force fields were applied to the POPC and water, respectively; point charges were assigned by the restrained electrostatic potential (RESP) approach.

All the MD simulations in the present study were performed using the GROMACS (version 2021.4) package. For equilibration, the MD simulations were first carried out for the NVT ensemble with Nose-Hoover36 thermostat at 310 K for 0.5 ns (2 fs time step). Next, the MD simulations in the NPT ensemble with Nose-Hoover thermostat at 310 K and Parrinello-Rahman barostat at 1 bar were done for 10 ns (2 fs time step), thereby analyzing the MD trajectories. To calibrate the strength of interaction between the polymer and membrane, we evaluated the number of "contact" atoms within an interatomic distance $\leqq$ 4 Å (N_{count}) at each simulation step using "gmx mindist" tool in the GROMACS package. Here the contact atoms are defined as two atoms, one belonging to the polymer and the other to the membrane.

2.2.10.1. Modeling of polymers

PAMPTMA and PAMPTMA-*r*-BuMA polymers were modeled using Polymer Builder tool in Materials Studio 2022.[31] The PAMPTA homopolymer consists of 15 AMPTMA monomer units, whereas the PAMPTMA-*r*-BuMA random copolymer are constructed from 10 AMPTA and 5 BuMA monomer units. To perform their MD simulations, force fields and point charges should be assigned to the resulting polymer structures.

To assign point charges to the polymer, we first divided the polymer into the constituent monomer fragments and then allocated point charges into the fragments. The point charges of the fragment were calculated by the restrained electrostatic potential (RESP) approach[32]: The monomers were first optimized with DFT calculations at the B3LYP[33, 34]/6-31G(d,p)[34, 35] level of theory using Gaussian 2016[36]; their single point energy calculations for the electrostatic potentials were done using the same level of theory; the computed ESPs were converted to RESP charges using the

antechmaber program in Ambertools21; the resultant monomer RESP charges were assigned into the polymer.

A general AMBER force field (GAFF)[37] was applied to the PAMPTMA and PAMPTMA-*r*-BuMA polymers with the RESP charges by using the antechamber[38, 39] and parmchk2[39]programs in Ambertools20.[39] Note that the Cl^- ions were excluded from the polymers when applying GAFF to the polymers. The Cl anion was constrained to bind with the N cation in a harmonic potential with the equilibrium distance between the ions of 3.57 Å and the coupling constant of 10 kcal/mol A^{-2}, which was obtained from the DFT simulation of the monomer fragment.

The PAMPTMA and PAMPTA-*r*-BuMA polymers were placed in a 10 nm × 10 nm × 10 nm simulation cell. The polymers were solvated with aqueous KCl solution at 0.15 M, where 32,441 and 32,449 water molecules were included in the PAMPTMA and PAMPTMA-*r*-BuMA cases, respectively. A TIP3P force field and GAFF were applied to water molecules and K^+/Cl^- ions, respectively.

To obtained equilibrium structures of PAMPTMA and PAMPTMA-*r*-BuMA, we performed the NVT MD simulations with the Nose-Hoover thermostat at 310 K for 0.5 ns, followed by the NPT MD simulations with the Nose-Hoover thermostat at 310K and the Parrinello-Rahman barostat at 1 bar for 50 ns. These equilibrated structures were used for constructing the polymer-membrane systems.

2.2.10.2. Modeling of membrane

The membrane was treated as a lipid bilayer sheet composed of 1-palmitoyl-2-oleoyl-sn-glycero-3-phosphocholine (POPC). Using Membrane Builder[40-43] in CHARMM-GUI,[37] the bilayer was modeled and packed into a MD simulation cell of 9.4 nm × 9.4 nm × 14.0 nm. Here two monolayers

are located at the center of the simulation cell in z-direction, where the monolayer consists of 128 POPC monomer units. The membrane was fully solvated with aqueous KCl solutions at 0.15 M, where 26,702 water molecules were included in the MD simulation cell. The Lipid17 force field was applied to the membrane. We performed the MD simulation in the NVT ensemble with the Berendsen thermostat at 310 K for 0.25 ns (2 fs time step), followed by the NPT ensemble with the Berendsen thermostat and barostat at 1 bar for 2.5 ns (2 fs time step). Furthermore, the equilibration of the membrane structure was performed using the MD simulations in the NPT ensemble with Nose-Hoover thermostat at 310 K and Parrinello-Rahman barostat at 1 bar for 2.5 ns (2 fs time step). Input files including NVT/NPT MD parameters were prepared by CHARMM-GUI Input Generator.[43, 44] The equilibrated membrane structure is used to perform the MD simulations of the polymer-membrane systems.

2.2.11. Statistical Analysis

All data are expressed as the mean±standard deviation (SD). All experiments were conducted in triplicate. To compare the data, an ordinary two-way analysis of variance with Tukey's multiple comparison test was used. Differences were considered statistically significant at $P < .05$.

2.3. Results and Discussion

2.3.1. Polymer Characterization

A series of PAMPTMA homopolymers of different molecular weights were synthesized by RAFT polymerization (**Scheme 2.1a**). The repeating units of the monomer were controlled by varying the RAFT/monomer ratio (**Table 2.1**). The formation of the homopolymers was confirmed by the loss of vinyl protons (δ = 5.0–5.5 ppm). The degree of polymerization was determined by comparing the integral value of the methyl protons (δ = 1.2–1.3 ppm) of the raft agent with the methylene peak (δ = 1.9–2.3 ppm) of AMPTMA using ^{1}H-NMR (**Figure 2.1**). The random

copolymers (PAMPTMA-*r*-BuMA) were synthesized by varying the amount of BuMA from 5% to 30% **(Scheme 2.1b)**. Their formation was confirmed by the appearance of a characteristic peak (δ = 4.0–4.2 ppm) related to the methylene proton of BuMA. The amount of BuMA added and inserted in each copolymer was calculated by comparing the integral value of the above peak and methylene peak of AMPTMA (δ = 3.0–3.5 ppm) in ^{1}H-NMR (**Figures 2.2–2.5, Table 2.1**). Figure 2.6 shows the comparison of the homopolymer and the copolymer containing different amounts of BuMA; when the amount of BuMA was increased, the intensity of the BuMA peak also increased (δ = 4.0–4.2 ppm). The incorporation of BuMA was easily controlled by changing the initial feed amount. In addition, we synthesized random copolymers by varying the size of their hydrophobic group. PAMPTMA-*r*-HexMA and PAMPTMA-r-OctMA (**Scheme 2.1c and 2.1d**) and their formation were confirmed by ^{1}H-NMR (**Figures 2.7 and 2.8**). In addition, we prepared a homopolymer of HEAA and its subsequent copolymers (HEAA-*r*-BuMA) by varying the amount of BuMA (**Scheme 2.2**). Their formation was confirmed by ^{1}H-NMR and ^{13}C NMR (**Figure 2.9-2.11**). Based on the GPC results, we calculated the number-average molecular weight (M_n) and weight-average molecular weight (M_w) values, which range from 10.0×10^3 to 13.0×10^3 g/mol. The polydispersity index (PDI) values were found to be in good range (1.1–1.3; **Table 2.1**). The obtained polymers were well soluble in both water and the cell-culture media.

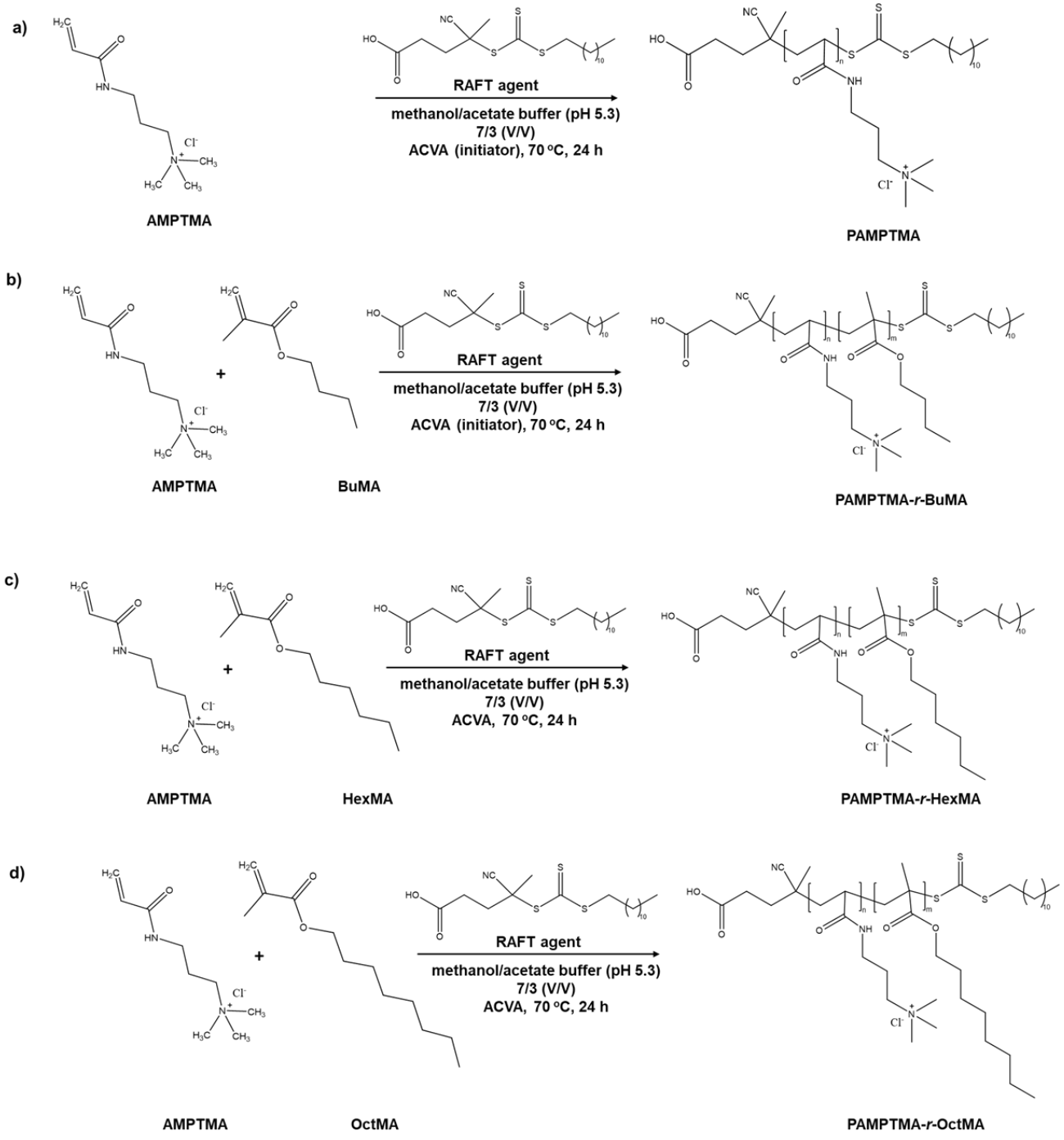

Scheme 2.1: Reaction scheme for the synthesis via RAFT polymerization of (a) homopolymers of the AMPTMA, (b) copolymers of PAMPTMA-*r*-BuMA, (c) copolymer of PAMPTMA-*r*-HexMA, and (d) copolymer of PAMPTMA-*r*-OctMA.

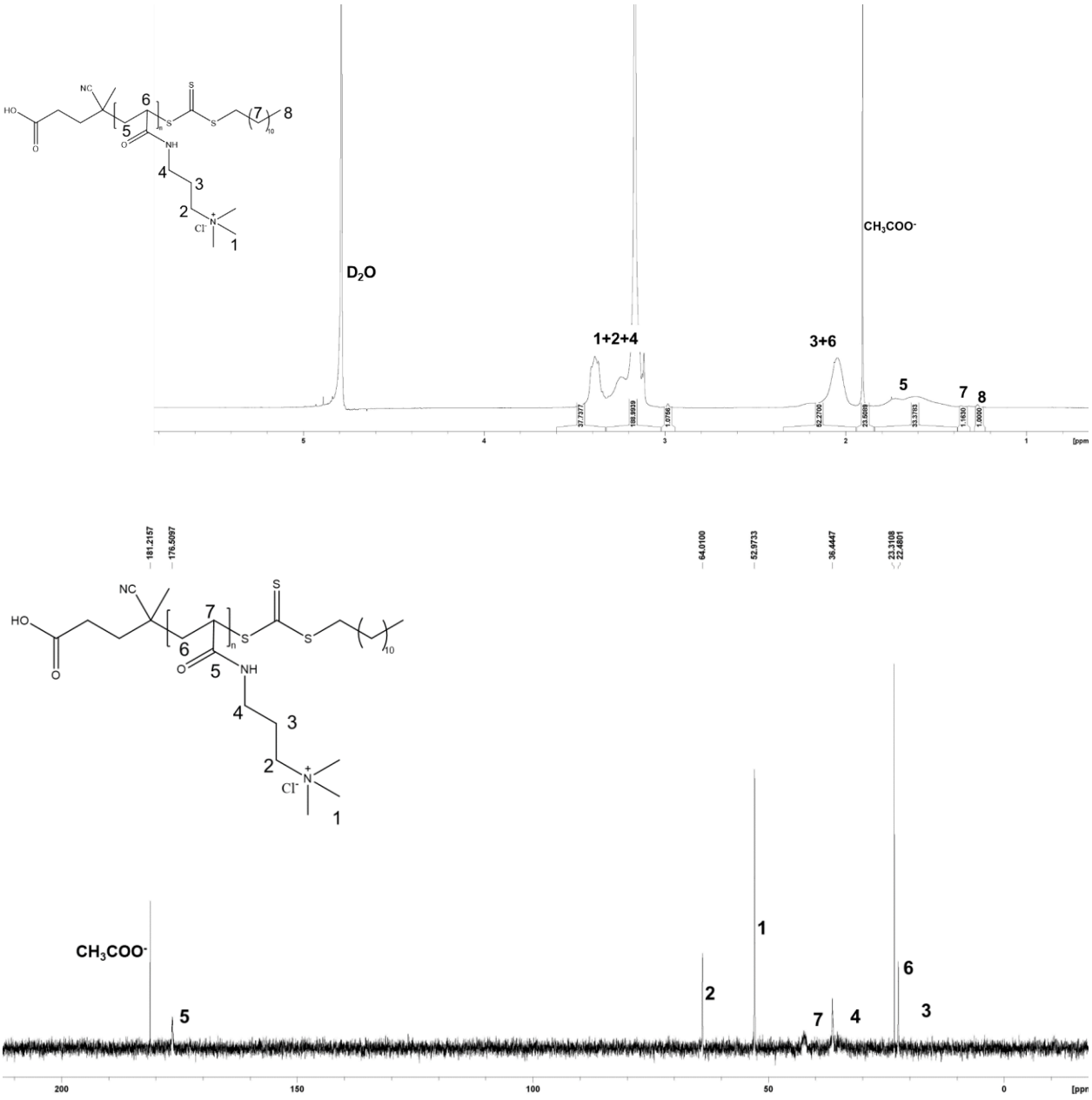

Figure 2.1: ^{1}H-NMR and ^{13}C-NMR of homopolymer of AMPTMA.

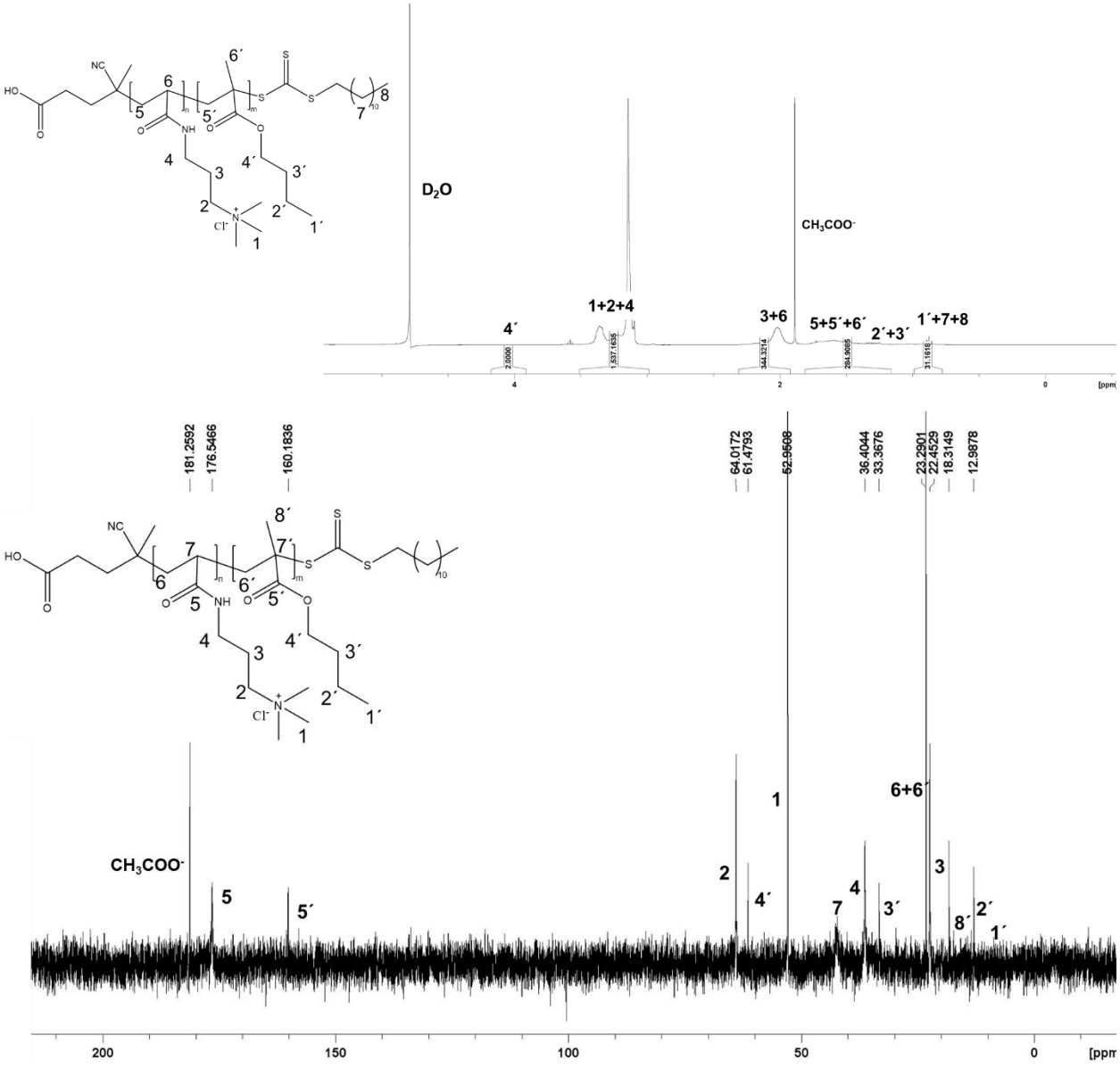

Figure 2.2: ^{1}H-NMR and ^{13}C-NMR of copolymer PAMPTMA-*r*-BuMA with 5 mol% of BuMA.

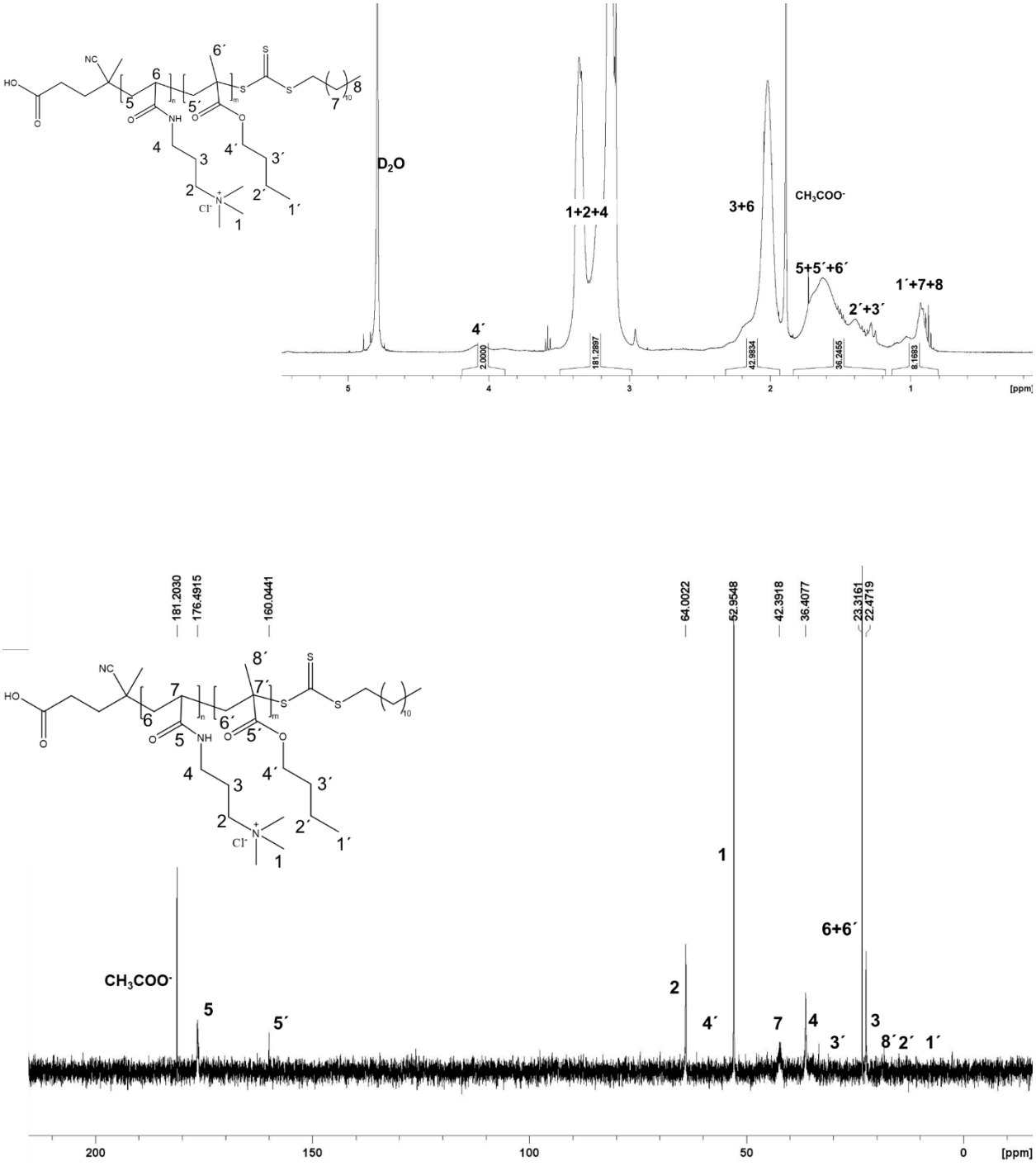

Figure 2.3: ^{1}H-NMR and ^{13}C-NMR of copolymer PAMPTMA-*r*-BuMA with 10 mol% of BuMA. A few small peaks at 2.9 ppm and 3.6 ppm in ^{1}H-NMR was appeared from the monomers AMPTMA and BuMA respectively.

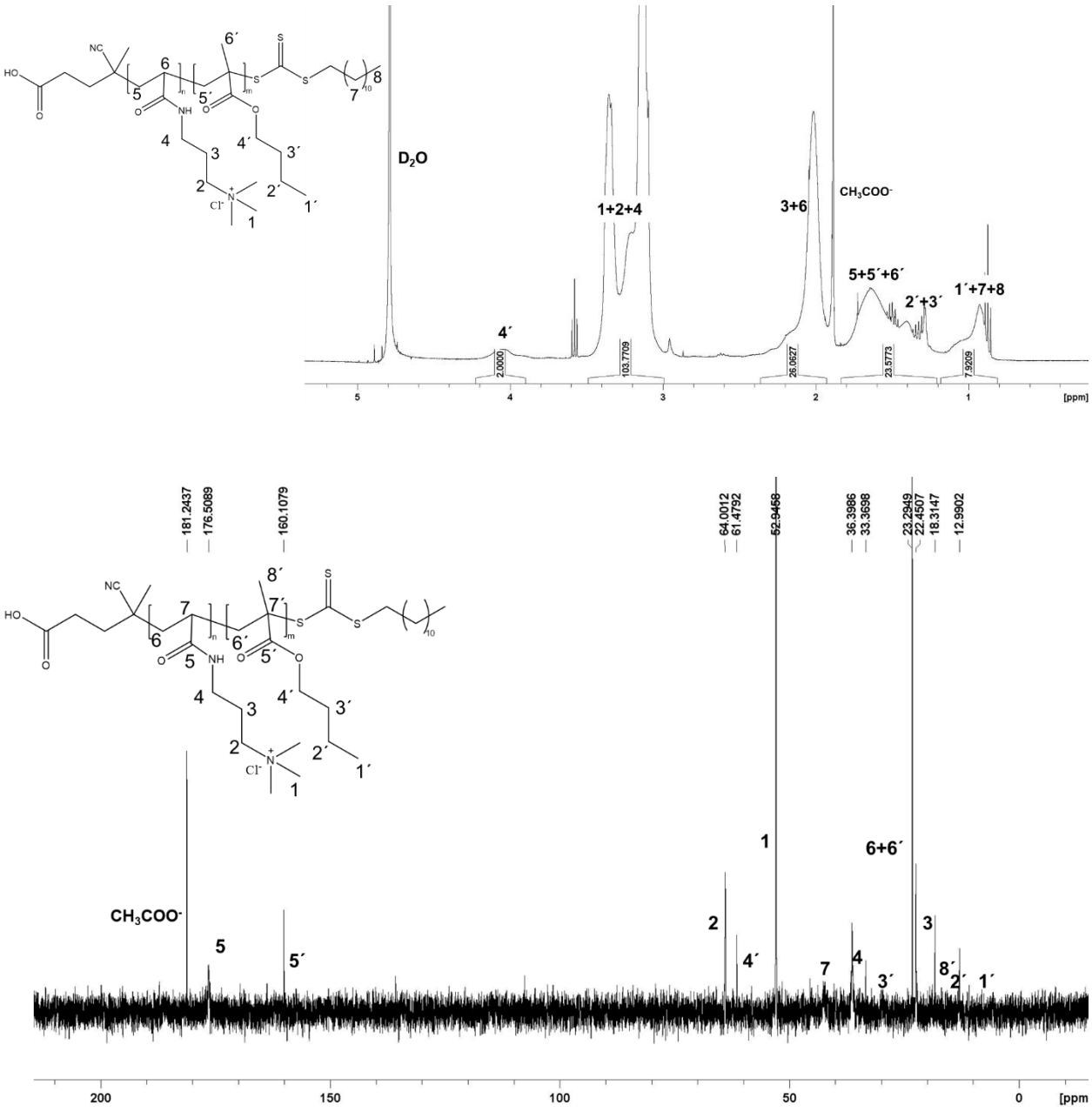

Figure 2.4: ^{1}H-NMR and ^{13}C-NMR of copolymer PAMPTMA-*r*-BuMA with 20 mol% of BuMA.

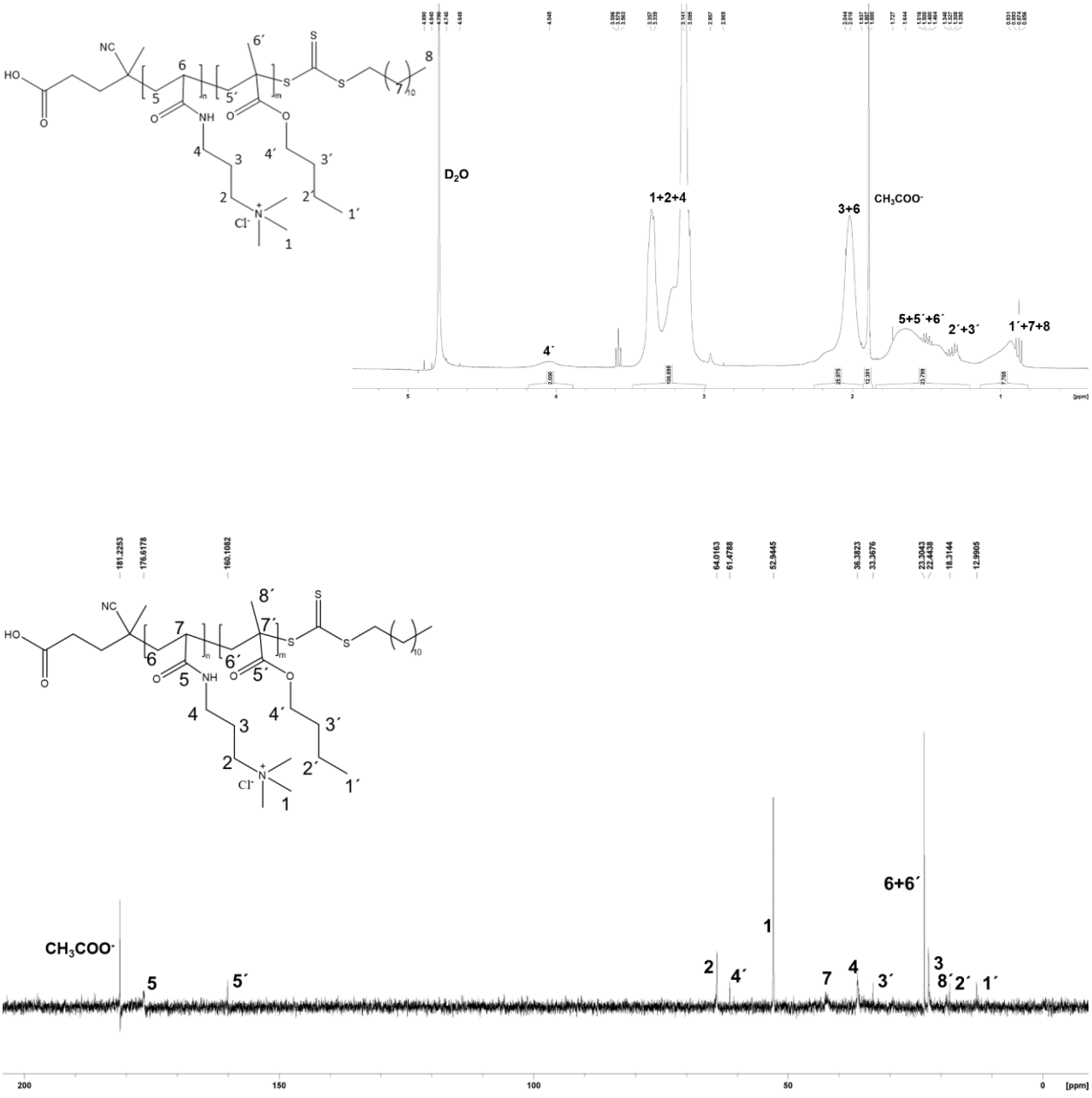

Figure 2.5: ^{1}H-NMR and ^{13}C-NMR of copolymer PAMPTMA-*r*-BuMA with 30 mol% of BuMA.

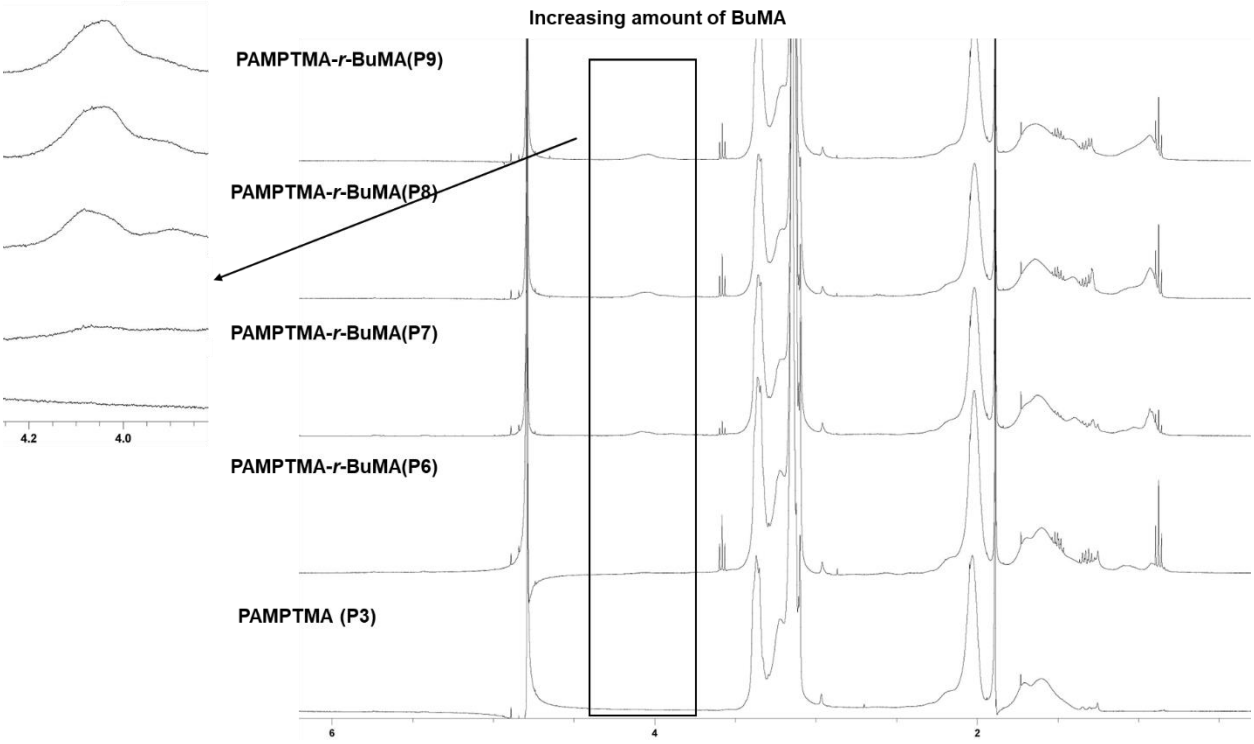

Figure 2.6: Confirmation of the increase in hydrophobicity with the addition of the BuMA.

Figure 2.7: ^{1}H-NMR and ^{13}C-NMR of the copolymer of PAMPTMA-*r*-HexMA.

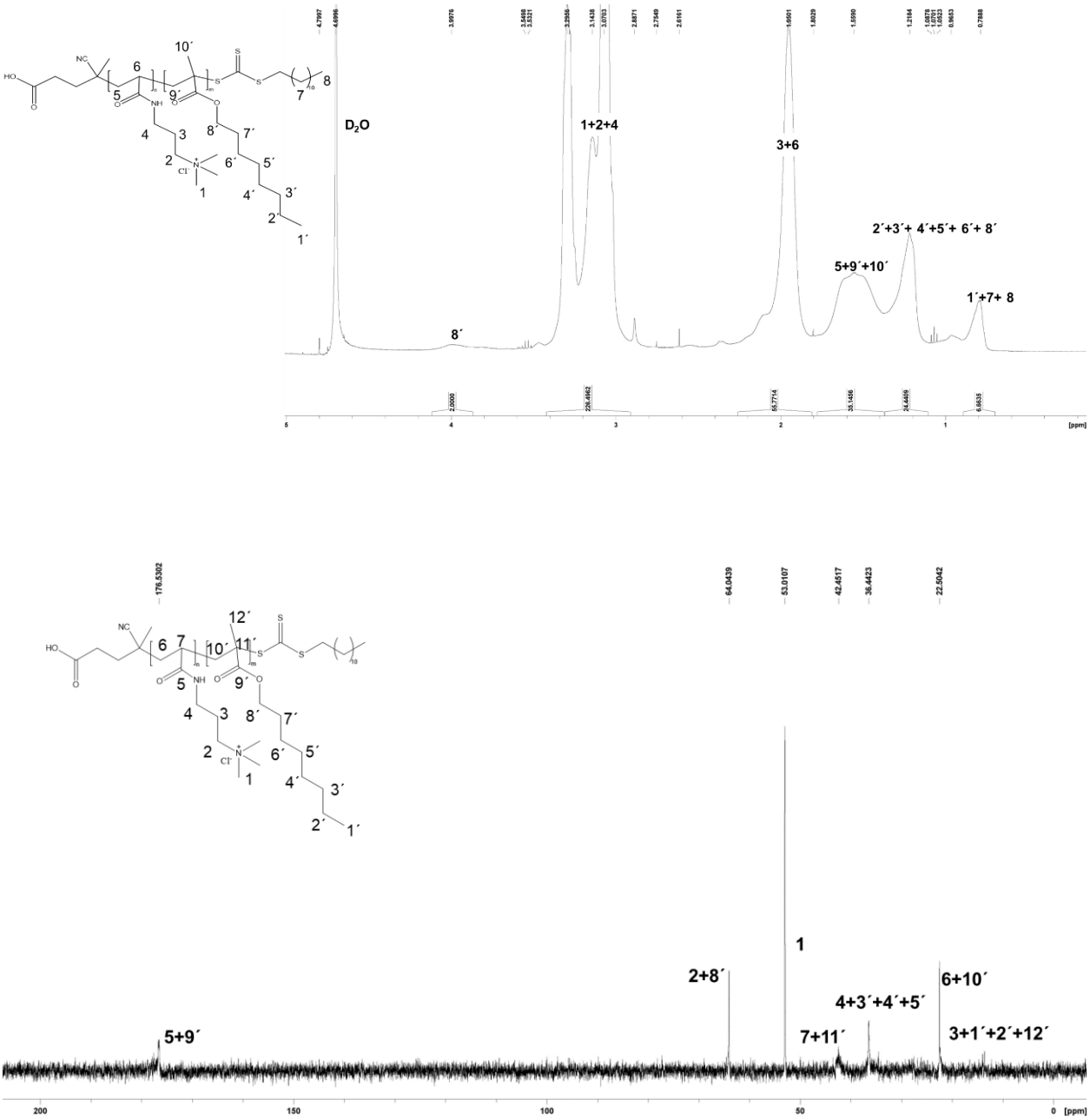

Figure 2.8: ^{1}H-NMR and ^{13}C-NMR of the copolymer of PAMPTMA-*r*-OctMA.

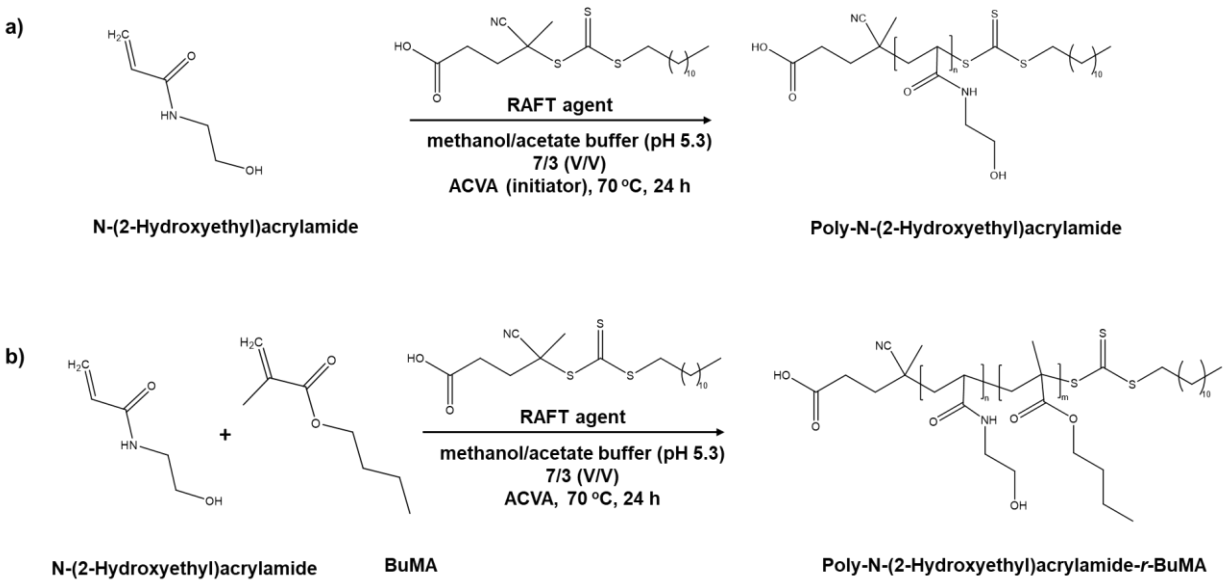

Scheme 2.2: Reaction scheme for the synthesis (a) homopolymers of N-(2-hydroxyethyl)acrylamide (HEAA), and (b) copolymers of N-(2-Hydroxyethyl)acrylamide-*r*-BuMA.

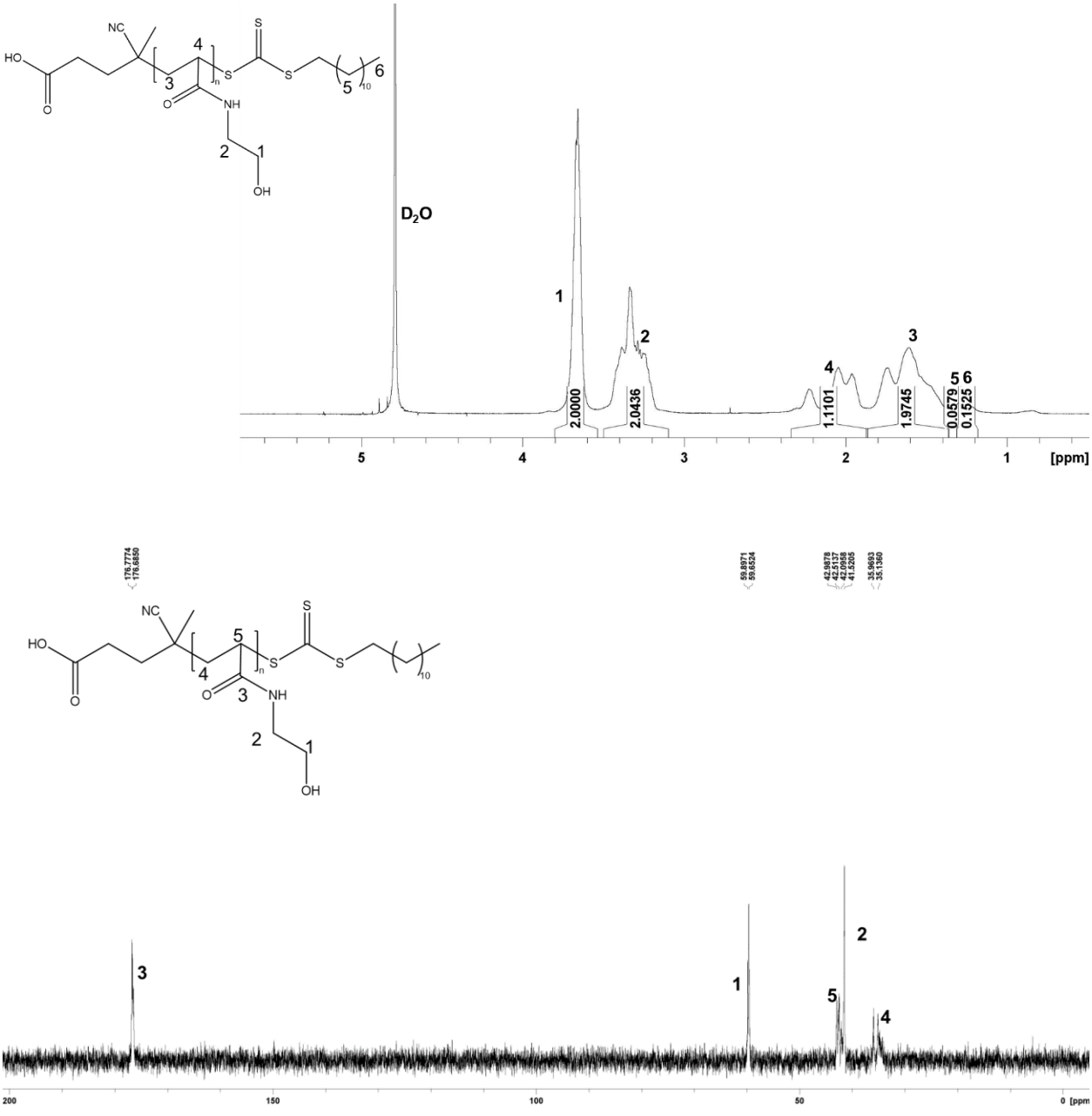

Figure 2.9: ^{1}H-NMR and ^{13}C-NMR of homopolymer of HEAA.

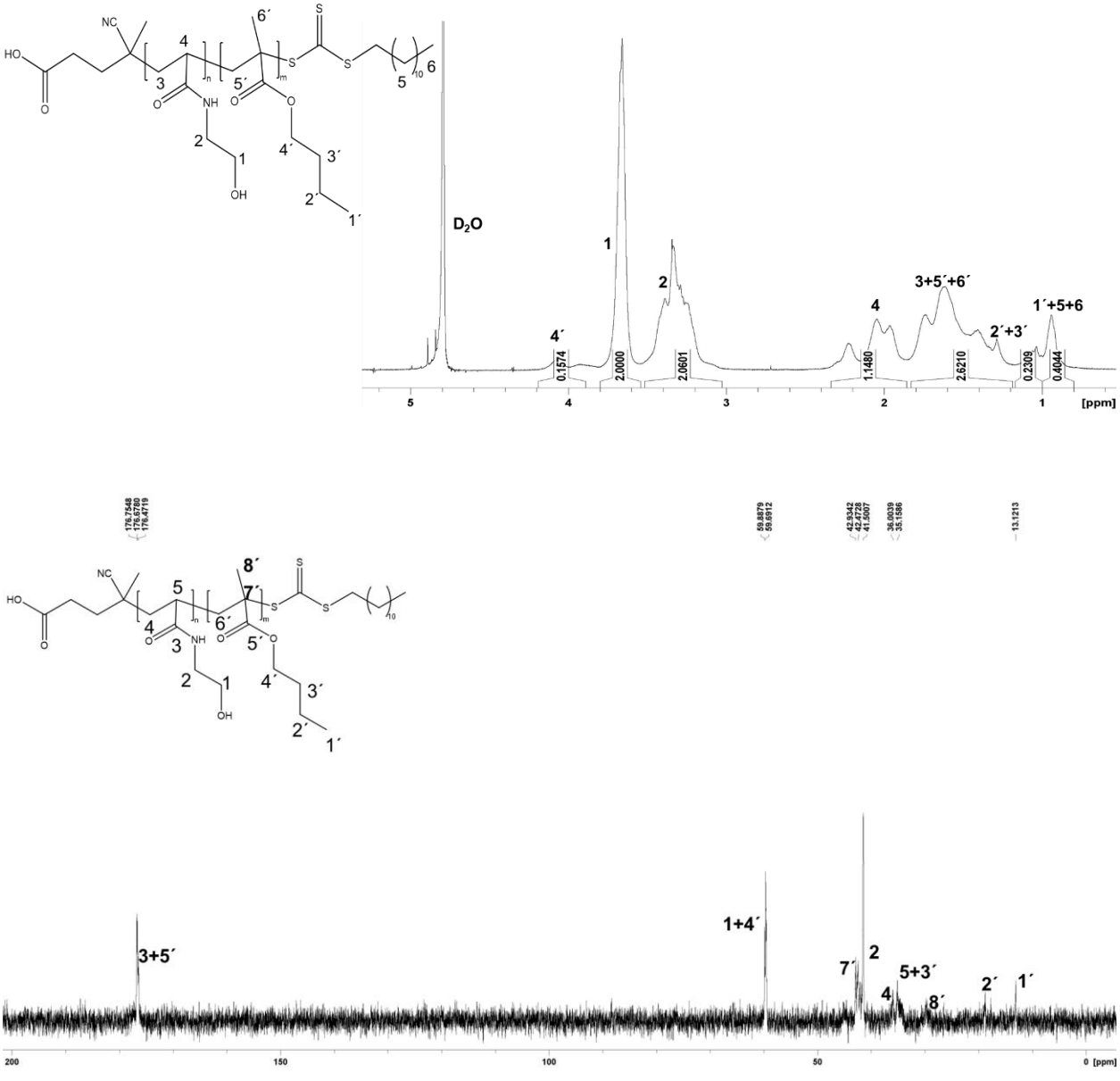

Figure 2.10: ^{1}H-NMR and ^{13}C-NMR of copolymer of HEAA with 10 mol% BuMA.

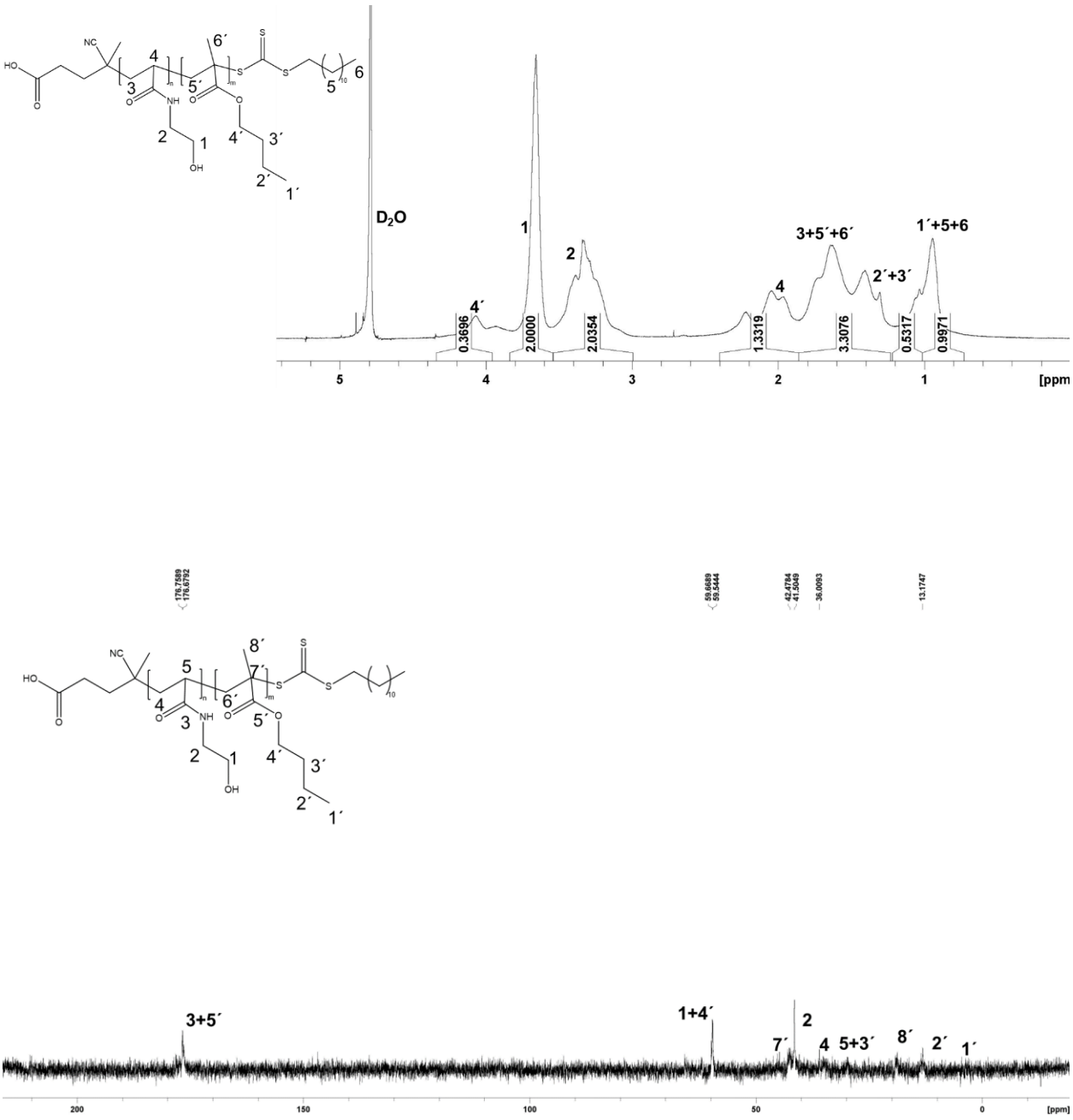

Figure 2.11: ^{1}H-NMR and ^{13}C-NMR of copolymer of HEAA with 20 mol% BuMA.

Table 2.1. Characteristics of the polymers prepared.

Entry	Polymer		Composition				Molar ratio[b]	Zeta Potential (mV)	M ×10^{3,} [c]	M_w/ M_n [c]
			AMPTMA	BuMA	HexMA	OctMA				
1.	P1	In feed In polymer[a]	100	0 0	0 0	0 0	100:4:0.8	60.3±3.7	8.0	1.04
2.	P2	In feed In polymer[a]	100	0 0	0 0	0 0	100:2:0.4	67.6±6.4	8.7	1.06
3.	P3	In feed In polymer[a]	100	0 0	0 0	0 0	100:1:0.2	71.5±4.2	9.5	1.15
4.	P4	In feed In polymer[a]	100	0 0	0 0	0 0	100:0.5:0.1	68.3±5.4	14.3	1.20
5.	P5	In feed In polymer[a]	100	0 0	0 0	0 0	100:0.3:0.6	75.8±3.0	22.1	1.34
6.	P6	In feed In polymer[a]	95 98.2	5 1.8	0 0	0 0	100:1:0.2	69.3±7.0	10.1	1.13
7.	P7	In feed In polymer[a]	90 90.9	10 9.1	0 0	0 0	100:1:0.2	52.6±7.9	10.7	1.14
8.	P8	In feed In polymer[a]	80 83.8	20 16.2	0 0	0 0	100:1:0.2	62.6±3.7	11.8	1.20
9.	P9	In feed In polymer[a]	70 79.1	30 20.9	0 0	0 0	100:1:0.2	55.5±1.8	13.0	1.24
10.	P10	In feed In polymer[a]	90 91.1	0 0	10 8.9	0 0	100:1:0.2	58.0±0.8	16.1	1.27
11.	P11	In feed In polymer[a]	90 91.2	0 0	0 0	10 8.8	100:1:0.2	53.8±1.1	13.3	1.23
Entry	**Polymer**		**HEAA**	**BuMA**	**HexMA**	**OctMA**	**Molar ratio[b]**	**Zeta Potential (mV)**	**M_n× 10^{3,} [c]**	**M_w/ M_n [c]**
12.	P12	In feed In polymer[a]	100	0	0 0	0 0	100:1:0.2	-9.9±0.8	13.0	1.16
13.	P13	In feed In polymer[a]	90 92.2	10 7.8	0 0	0 0	100:1:0.2	-12.6±0.8	11.1	1.15
14.	P14	In feed In polymer[a]	80 81.5	20 18.5	0 0	0 0	100:1:0.2	-16.6±0.4	10.6	1.15

[a] Determined by ^{1}H NMR; [b] [Monomer]:[RAFT agent]:[Initiator]; [c] Determined by GPC.

2.3.2. *In vitro* cytotoxicity determination

MTT Assay. The anticancer activity of the polymers was evaluated against three cancer cell lines-HepG2, colon 26, and B16F10 using the MTT assay. Cancer cells have more negative charges than those of normal cells because of the overexpression of phospholipids on the surface of cancer cells. Initially, the cytotoxicity of cationic homopolymers with different molecular weights on the cancer cells was determined.[45] Homopolymers PAMPTMA (P1–P5) showed very less cytotoxicity against all cancer cells, including the HepG2 cancer cell line even when up to 2000 µg/mL of polymer concentration was used **(Figure 2.12a)**. When the molecular weights of P1–P5 was increased, the cytotoxicity did increase but to a lesser extent. However, IC_{50} values could not be determined for these polymers in case of HepG2 cells **(Table 2.2)**. These homopolymers were further evaluated for their cytotoxicity against the B16F10 and Colon 26 cancer cells **(Figure 2.12b & 2.12c)**. P1–P3 showed very high or no IC_{50} values at all for both cell lines, whereas P4 and P5 showed slightly lower IC_{50}, probably owing to the increase in the cationic chain length **(Table 2.2)**. The cationic charge present in the homopolymers can attract/bind toward the PS lipid-rich membrane of the cancer cell by electrostatic interactions; when the chain length is increased, the cationic charge also increases **(Table 2.1)**, resulting in greater interaction and higher cytotoxicity. However, the lower IC_{50} values in these results suggested that cationic polymers or cationic charge in itself may not be sufficient for killing cancer cells.

Table 2.2. In vitro anticancer activity (IC_{50}) values of the polymers synthesized against the cancer cell lines.

Entry	Polymer	IC_{50} (µg/mL)		
		HepG2	**Colon 26**	**B16F10**
1.	P1	N.D.[a]	N.D.	1815
2.	P2	N.D.	1179	N.D.
3.	P3	N.D.	402	N.D.
4.	P4	N.D.	37	44
5.	P5	N.D.	22	25
6.	P6	N.D.	315	N.D.
7.	P7	N.D.	118	359
8.	P8	582	41	89
9.	P9	210	24	43
10.	P10	167	22	16
11.	P11	60	7	16
12.	P12	865	418	631
13.	P13	N.D.	638	816
14.	P14	N.D.	688	1554

[a]N.D.: not determined upto the concentration of polymer used 2000 µg/mL.

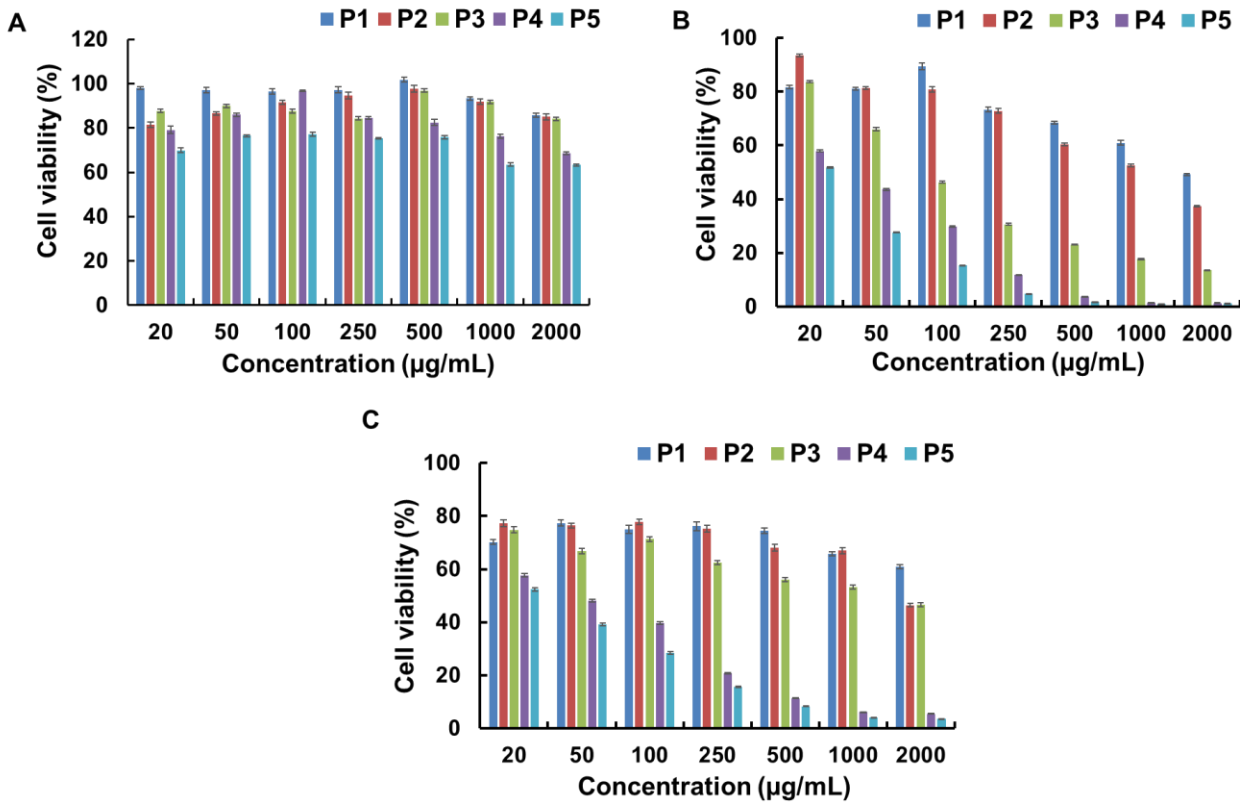

Figure 2.12: MTT cytotoxicity assay of Homopolymers PAMPTMA with different molecular weights on; a) HepG2 cells, b.) Colon 26 cancer cell line, c.) and B16F10 cancer cell line.

Therefore, next I synthesized the copolymers by varying the amount of the hydrophobic co-monomer (BuMA) of similar molecular weight (**Table 2.1**) by fixing the repeating units of PAMPTMA to 100. The MTT cytotoxicity assay was performed on various cancer cell lines using these copolymers. The obtained copolymers demonstrated significantly higher anticancer activity than that exhibited by homopolymers. The IC_{50} value of the homopolymer was >2000 µg/mL. The IC_{50} of some copolymers was <100 µg/mL. Hence, it is clear that the anticancer activity of the obtained copolymers is almost 20 times that of the homopolymers (**Table 2.2**). As the amount of BuMA was increased from P6 to P9, the cytotoxicity also increased against the HepG2 cancer cells (**Figure 2.13a**). Homopolymer P3 with a similar chain length (DP-100) exhibited the highest cell

viability with a high IC_{50} value (not determined), whereas P9 showed the lowest cell viability with a lower IC_{50} value (210 µg/mL) (**Table 2.2**). When the amount of BuMA was increased from 5 to 30 mol% (in feed mol% of BuMA), the anticancer efficacy also enhanced with reduced IC_{50} values across all the cancer cell lines tested (**Figure 2.13b & 2.13c, Table 2.2**). This is likely because after the electrostatic interactions involving the cationic charge, the hydrophobic domain of the polymers inserts into the membranes, which cause membrane disruption and leakage of cellular components, ultimately leading to cell death.

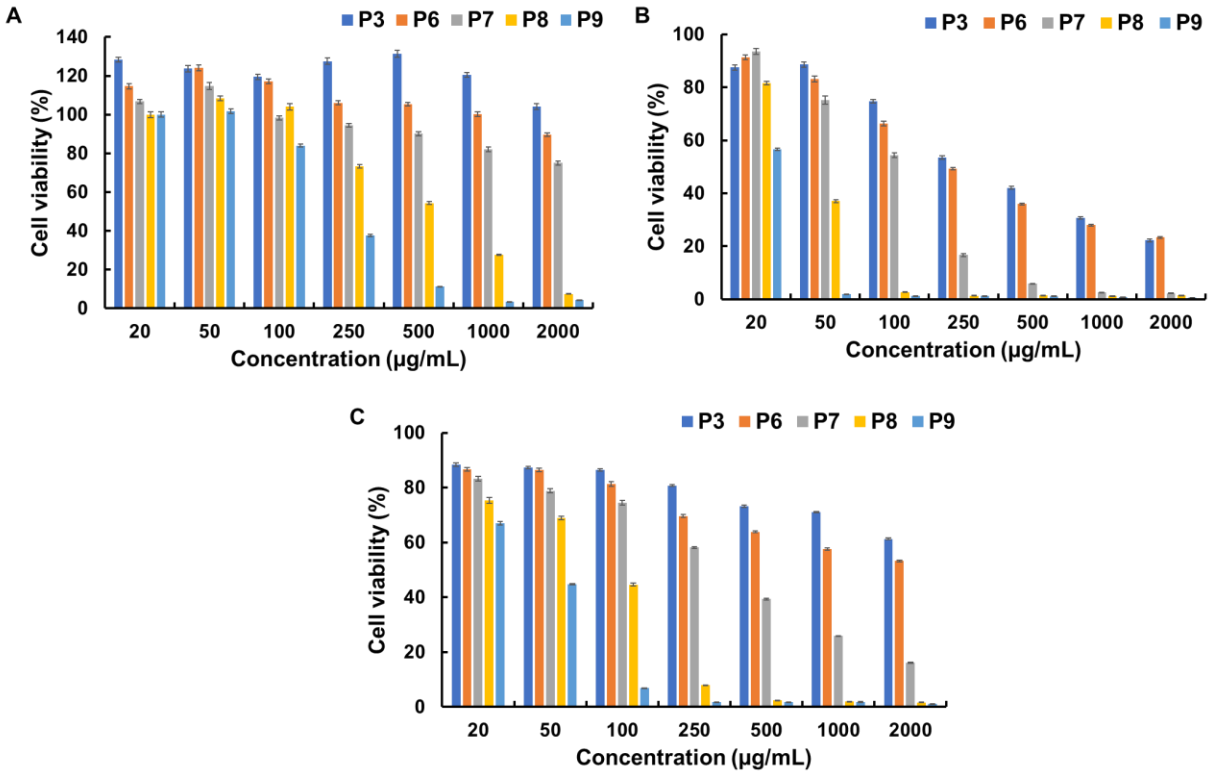

Figure 2.13: MTT cell viability assay of copolymers PAMPTMA-*r*-BuMA, a.) on HepG2 cancer cell line, b.) on Colon 26 cancer cell line, c.) on B16F10 cancer cell line.

To further extend my study and to understand the effect size of hydrophobic groups, we synthesized the copolymers of AMPTMA using HexMA and OctMA of similar hydrophobic content as those of P7 (in 10 mol% feed, **Table 2.1**). The results of the cell viability assay were

compared with those three different types of copolymers—P7, P10, and P11—containing BuMA, HexMA, and OctMA (10 mol % feed) as co-monomers, respectively. As the size of the hydrophobic group increased, the cytotoxicity of the copolymers also increased against the HepG2 cell line (**Figure 2.14a**). Polymer P11 showed the highest cytotoxicity with the lowest IC_{50} (60 µg/mL); in contrast, the IC_{50} of P7 could not be determined (**Table 2.2, Figure 2.14a**). The colon 26 and B16F10 cell lines showed a similar pattern for cell viability and IC_{50} values (**Figure 2.14b & 2.14c, Table 2.2),** probably because of the increased hydrophobic content, which increased the membrane disruption and caused further lysis of the cell. These results confirmed that hydrophobicity is an important factor that determines whether a polymer will exhibit toxicity against cancer cells and that an increase in the hydrophobic chain length further enhances the anticancer activity of the polymer.

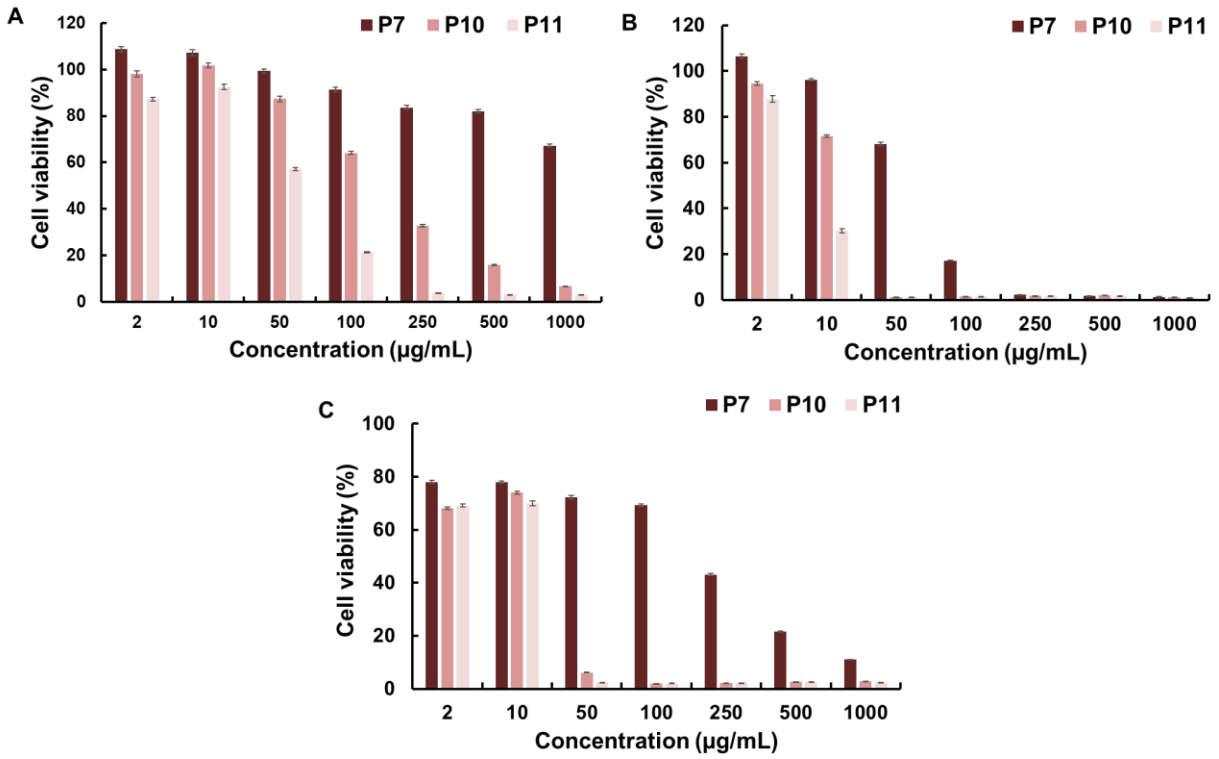

Figure 2.14: MTT cell viability assay of copolymers PAMPTMA-r-BuMA, PAMPTMA-r-HexMA, PAMPTMA-r-OctMA, a.) on HepG2 cancer cell line, b.) on Colon 26 cancer cell line, c.) on B16F10 cancer cell line.

To prove that hydrophobicity alone is not a sufficient condition for the polymers to exhibit anticancer property and that the presence of cationic charge is also required, we prepared a few additional polymers: homopolymer of HEAA (which does not contain any cationic charge) and its copolymer by varying the amount of BuMA used as the hydrophobic group. The obtained polymers showed less cytotoxicity against the HepG2 cell line **(Figure 2.15a)** as well as against other cancer cell lines (**Figure 2.15b & 2.15c**). Interestingly, when the cell viability of these polymers was tested against the HepG2 cell line, polymer P12 (homopolymer) showed more cytotoxicity than its hydrophobic counterparts P13 and P14. This phenomenon is also evident from the higher IC_{50} values of P13 (N.D.) and P14 (N.D.) than that of P12 (865 µg/mL) (**Figure 2.15a, Table 2.2**). Therefore, based on the above results, we can conclude that hydrophobicity alone is not a sufficient requisite to impart anti-cancerous property to a polymer, although its presence can substantially increase the efficacy of cationic polymers against cancer cells, probably because of the increased interaction with the cell membrane. Similarly, although cationic polymers do possess anticancer activity, their efficacy is low and the presence of hydrophobicity significantly augments its property. Therefore, it can be unambiguously established that the presence of both cationic charge and a hydrophobic moiety is paramount for designing an efficient anticancer polymer. For better understanding, we compared the cytotoxicity of PAMPTMA (P3 homopolymer) and copolymer PAMPTMA-*r*-BuMA (P8 copolymer) at a particular concentration on all three cancer cell lines (**Figure 2.16**). Polymer P8 showed a higher cytotoxicity than that exhibited by P3 on all the three cell lines tested.

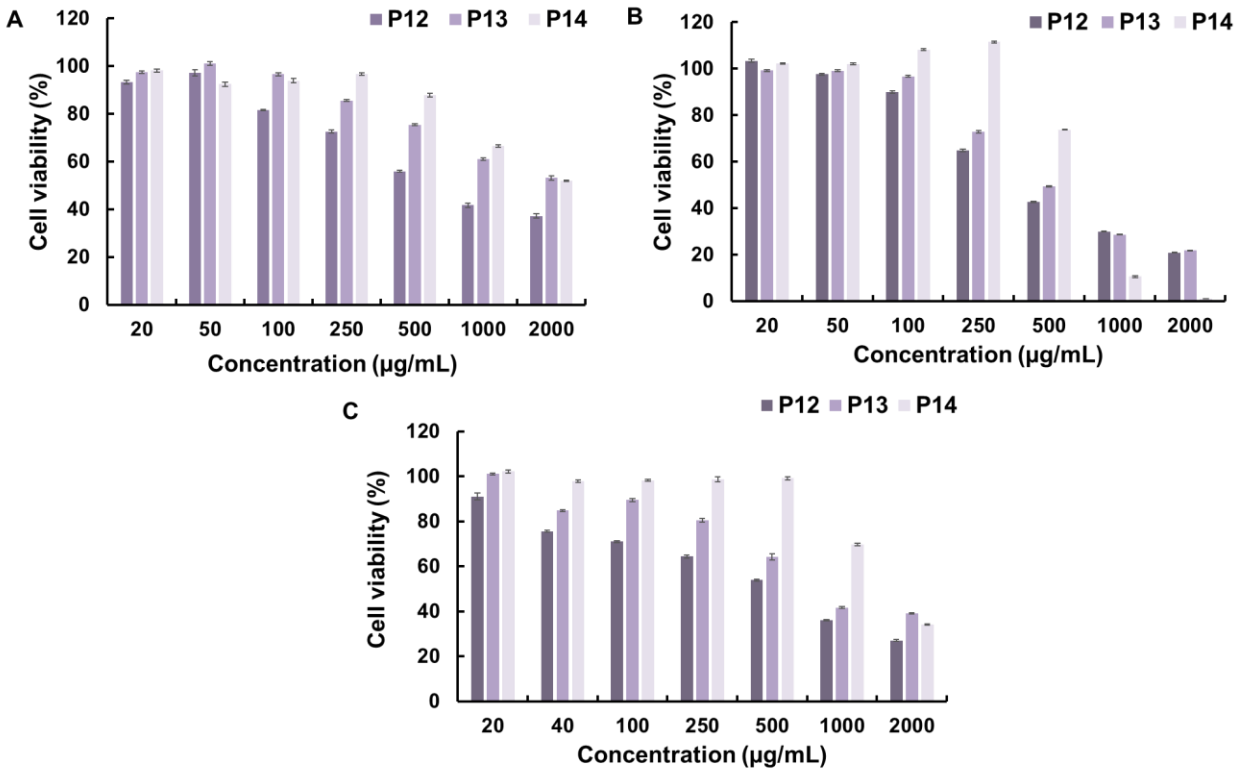

Figure 2.15: MTT cell viability assay of homo- and copolymers of HEAA, a.) on HepG2 cancer cell line and b) on Colon 26 cancer cell line, c) on B16F10 cancer cell line.

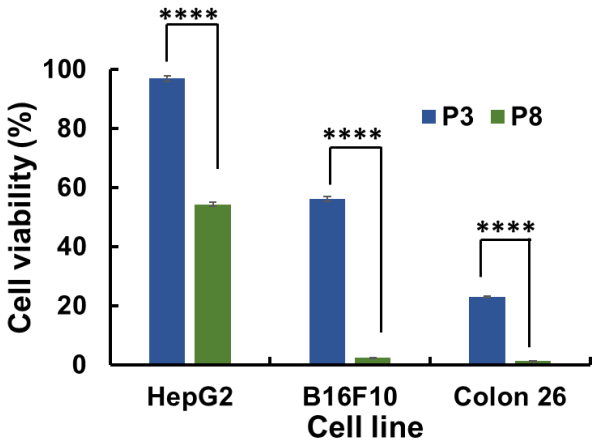

Figure 2.16: Comparison of the cytotoxicity of the homopolymer of PAMPTMA (P3) and one of its copolymers (P8) at 500 μg/mL. Errors bars indicate standard deviation of the mean. ****$P <$ 0.0001, ns: not statistically different.

Overall, the effect of the hydrophobic group was clearly established in cancer-cell treatment. To design an anticancer cationic polymer, both the cationic group and the hydrophobic moiety must be present in the polymer. The cationic charge interacts with the cell membrane, whereas the hydrophobic moiety inserts itself into the cell membranes and kills the cancer cell. To understand the mechanism and to prove our hypothesis, we carried out further investigations in the subsequent sections.

2.3.3. Mechanistic Investigations

2.3.3.1. LDH Leakage Assay. To study the effect of hydrophobicity on the cancer cell membrane and to examine the anticancer mechanism of the polymers, we performed lactate dehydrogenase (LDH) leakage assay. To quantify the damage to the cell membrane by the polymer, the extracellular leakage of the cytoplasmic enzyme LDH from HepG2 cells was examined. I selected P3 as a homopolymer and other cationic copolymers containing the hydrophobic co-monomer with same feed ratio. Homopolymer P3 showed no or significantly low LDH leakage, even at a higher polymer concentration of 2000 μg/mL (**Figure 2.17a**). The increase in the LDH release was observed even with the increased hydrophobicity. Unexpectedly, P8 showed higher LDH leakage than that exhibited by P9 at a higher polymer concentration. The P9 copolymer containing the highest amount of BuMA showed significant LDH leakage at higher concentration as well as at a lower polymer concentration (up to 100 μg/mL) (**Figure 2.17a**). This higher anticancer activity is possibly caused by the insertion of the hydrophobic group inside the cancer cell membrane by membrane disruption. In contrast, when we compared the effect of the size of the hydrophobic group, we noted that as the size of the hydrophobic co-monomer increased from BuMA to HexMA and further to OctMA, the LDH leakage also increased (**Figure 2.17b**). The P11 copolymer containing OctMA as co-monomer showed the highest LDH release, even when the polymer was

used at the minimum concentration (20 µg/mL); in contrast, P7 containing BuMA as a co-monomer showed very low LDH leakage, even at higher polymer concentrations (2000 µg/mL). The extracellular leakage of the cytoplasmic enzyme LDH indicates that the cell membranes of the HepG2 cell were permeabilised. In addition. the IC_{50} values of all the polymers were determined and it was found that their cell viability corresponds well with the LDH-leakage results. These results suggest that the polymer-induced cell death was caused by cell-membrane disruption. Overall, the results obtained clearly established a relationship between the hydrophobicity and the cancer cell membrane.

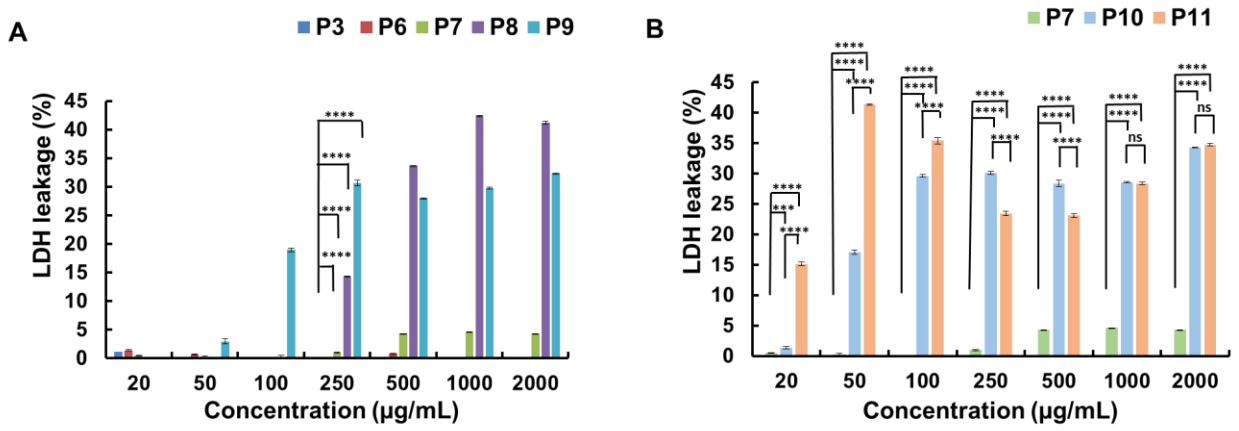

Figure 2.17: LDH leakage on HepG2 cells a) of the homopolymer (P3) and its copolymer containing different amounts of hydrophobic comonomer BuMA, b) for copolymers containing hydrophobic groups of different sizes. Errors bars indicate standard deviation of the mean. ****P < 0.0001, ns: not statistically different.

2.3.3.2. Cellular Uptake. The anticancer mechanism and the effect of hydrophobicity on the cell membrane were further investigated by cellular uptake analysis.[24] To this end, a homopolymer (P3) and a copolymer (P8) were chosen. Both P3 and P8 were labelled with AlexaFluor488. Cellular uptake by HepG2 human liver cancer cells was observed under a confocal microscope.

After 2 h of treatment, no green coloration (AlexaFlour tagged P3/P8) was observed in all three images (**Figure 2.18a**). This result suggested internalization did not occur in either polymer inside the cell membrane. After the 24 h of treatment, P8 was taken up by the cells and can be seen in the cytosol region of the cells; in contrast, no such internalization was observed in P3 and the blank (**Figure 2.18b**). The results indicate the membrane translocation activity of the hydrophobic copolymer due to the initial electrostatic interaction with the cell membrane, damaging the cell membrane and thus resulting into further internalization. Overall, the copolymer was endocytosed by the HepG2 cancer cell, suggesting that the anticancer mechanism shown by the polymers involved membrane lysis, followed by necrosis.

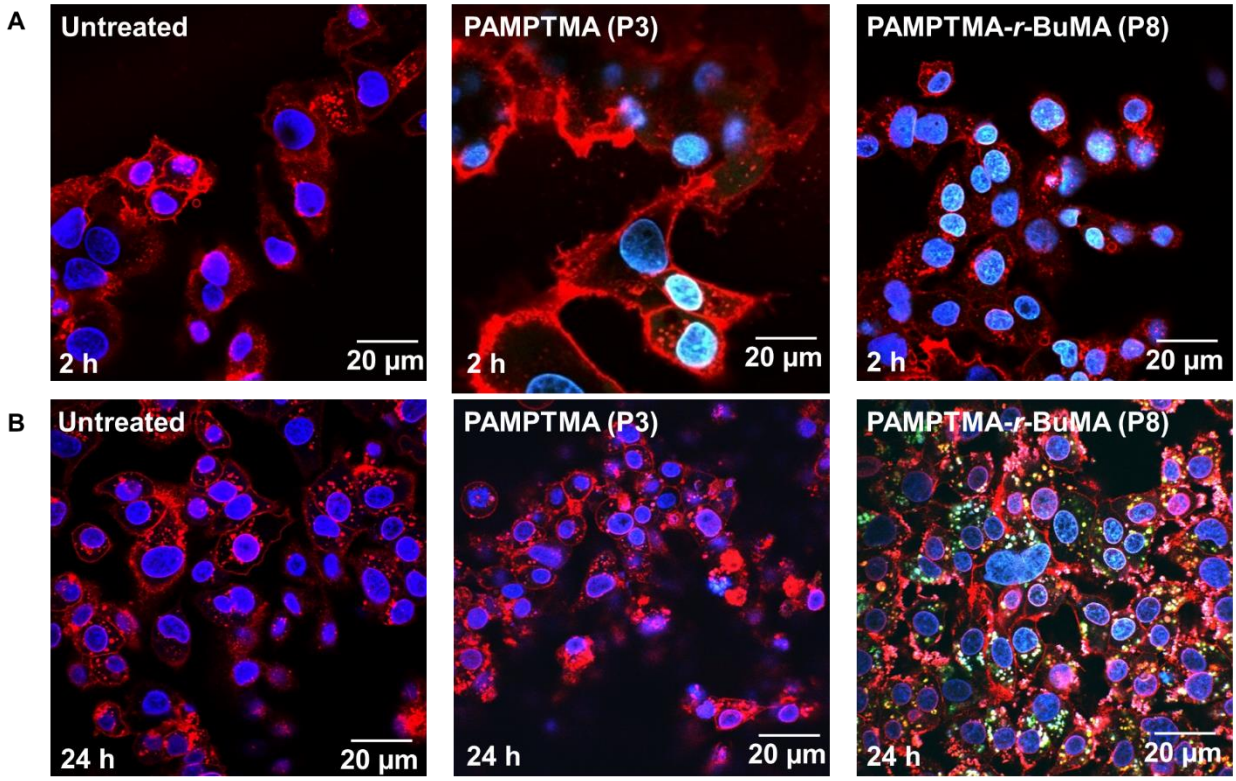

Figure 2.18: Confocal microscopy images of HepG2 cells after treatment with P3/P8 at respective IC_{50}. Hoechst (blue): nucleus; Red: cell membrane; Green: AlexaFluor488-labelled P3/P8. a) at 2-

h treatment with the medium and the tagged polymer b) after 24-h treatment with medium and tagged polymer.

2.3.4. Dye Leakage.

Next, I carried out a dye leakage experiment to confirm the effect of hydrophobicity on membrane interaction and its subsequent damage. Previously, our group has reported the use of soluble fluorescent dye (CF) and its leakage from the liposomes to investigate the membrane damage/lysis.[46, 47] In this experiment, when no polymers were added to the liposomes (PBS), minimum leakage was observed, as very less or no soluble marker (CF) was released from the liposome to the surrounding buffer. In case of homopolymer P3, minimum fluorescence intensity was observed, which kept on increasing with the hydrophobic content of the polymer (**Figure 2.19a**). The highest leakage was observed for P9, which contains the highest amount of the BuMA co-monomer (**Figure 2.19a**). This result is in good agreement with the cytotoxicity and LDH leakage results. Analogously, when similar experiments were performed with the polymer containing hydrophobic groups of different sizes, P11 containing the longest hydrophobic group (OctMA) shows the maximum dye leakage, while P7 containing BuMA as the hydrophobic group shows the minimum leakage (**Figure 2.19b**). The trend observed in the dye leakage experiment is similar to that observed in the MTT and LDH-leakage assays. The increase in dye leakage was observed at different time intervals using polymer P8 (**Figure 2.19c**). The result showed that membrane disruption also depends on time. These results showed a clear effect of the hydrophobic group and its size on membrane disruption; more damage to the membrane was observed with increased hydrophobic content, which supported our hypothesis.

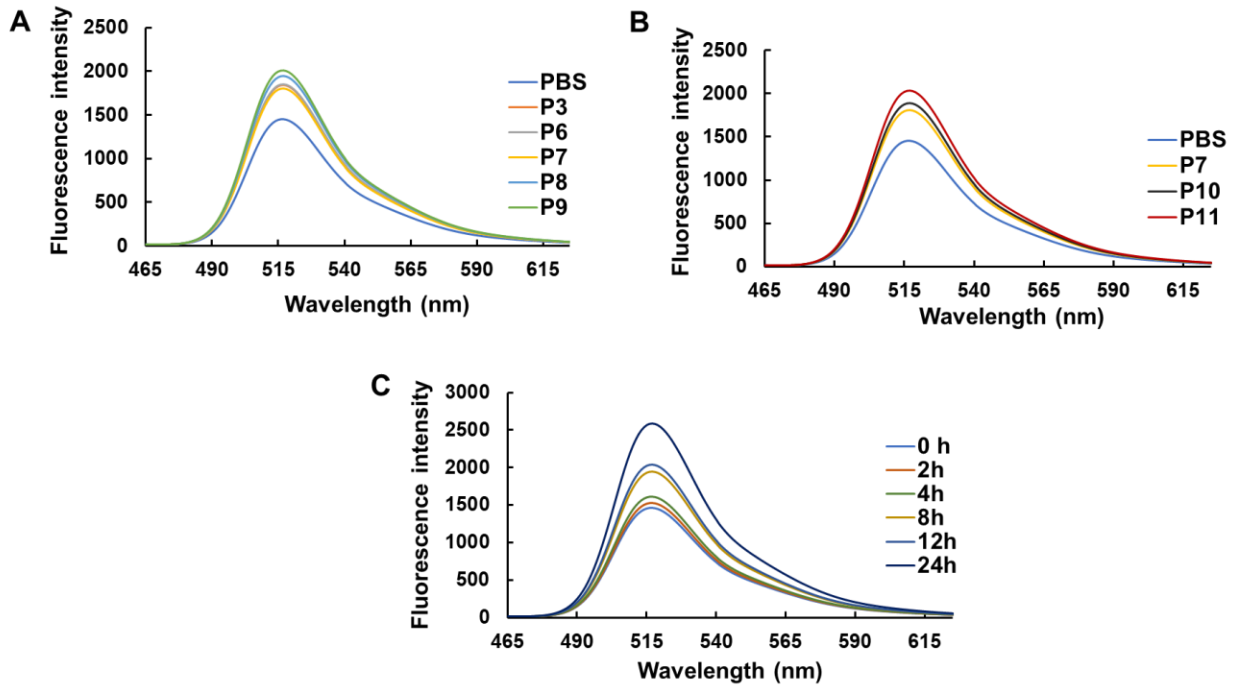

Figure 2.19: Dye-leakage experiments at 150 µg/mL of the polymer concentration. a) Polymers containing homopolymer P3 and copolymers containing BuMA as the hydrophobic group at 8-h time interval. b) Plots showing dye leakage with change in the size of the hydrophobic group at 8-h time interval. c) Leakage of dye was measured at different time intervals for polymer P8.

2.3.5. Diffusion Ordered Spectroscopy (DOSY) Measurements

To determine the interaction between the polymer and the cell membrane, we carried out DOSY experiments using mixtures of DOPC liposomes and copolymers.[48, 49] PAMPTMA (P3), PAMPTMA-*r*-BuMA (P8), and liposome DOPC were each dissolved in heavy water to a concentration of 1 g/L. In Figure 2.20, γ on the horizontal axis is the gyromagnetic ratio (2.68×10^8 rad $s^{-1}T^{-1}$), and I_0 and I on the vertical axis are intensities at $G = 0$ and arbitrary G, respectively. The R_h value was calculated by using the D values from Figure 2.20. The R_h obtained from the DOSY of PAMPTMA-*r*-BuMA (P8) was 4.87 nm **(Figure 2.20a)**, while that determined from the peak derived from PAMPTMA-*r*-BuMA in the DOPC/PAMPTMA-*r*-BuMA solution was 5.47

nm **(Figure 2.20b)**. The R_h value of the solution was higher than that obtained using the copolymer alone. I believe that the R_h value increased because of the interaction of P8 with the DOPC liposomes, which indicates their insertion into the liposomal membrane.

Similarly, R_h was calculated from the *D* values of the PAMPTMA homopolymer (P3) and was found to be 5.55 nm. The R_h value obtained from peak *D* derived from PAMPTMA alone and the PAMPTMA in the DOPC/PAMPTMA solution was almost the same. A possible explanation for this observation is that in the case of DOPC/PAMPTMA, some association was observed within the homopolymer and the DOPC **(Figure 2.21).** Consequently, some free PAMPTMA may remain in the solution. Therefore, the R_h value could not be correctly measured. Overall, an increase in the size of P8 with DOPC was due to the interaction of the hydrophobic group of the P8 with the DOPC membrane, which further confirms our hypothesis.

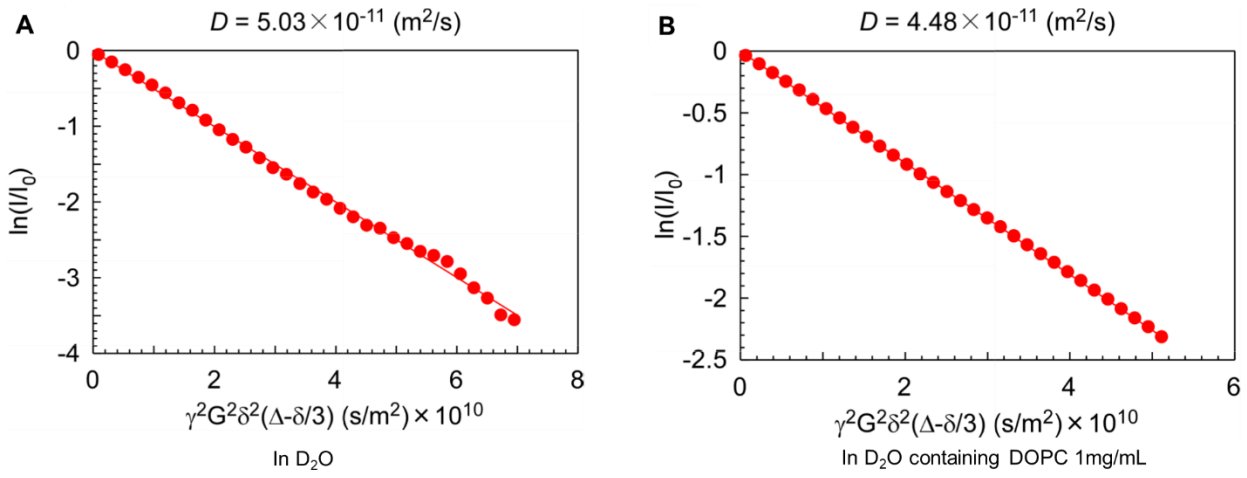

Figure 2.20: Diffusion peak intensity plots for pendant trimethylamine groups in the PAMPTMA unit for, a) PAMPTMA-*r*-BuMA (P8), and b) DOPC/PAMPTMA-*r*-BuMA (P8) in D_2O at 25 °C; the concentrations were 1 g/L.

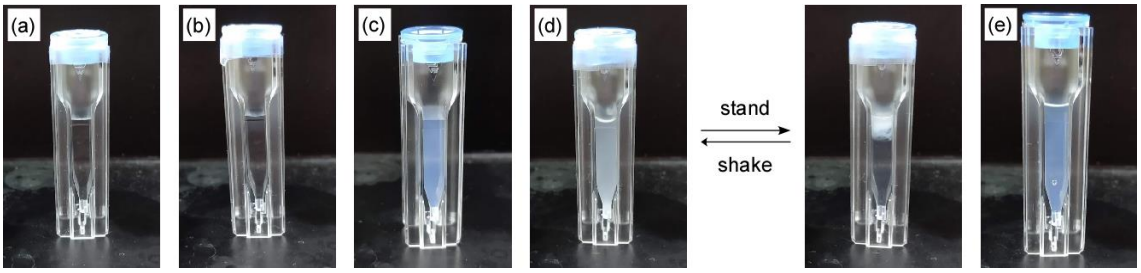

Figure 2.21: Photographs of (a) PAMPTMA (P3), (b) PAMPTMA-*r*-BuMA (P8), (c) DOPC, (d) mixture of DOPC/PAMPTMA, and (e) DOPC/PAMPTMA-*r*-BuMA in D_2O. Concentrations were fixed at 1 g/L.

2.3.6. DLS Measurement

PAMPTMA (P3) and PAMPTMA-*r*-BuMA (P8) were dissolved in heavy water at a concentration of 1 g/L and dynamic light scattering (DLS) was measured **(Figure 2.22)**. Both showed a bimodal particle size distribution with large R_h values (66–300 nm) **(Figure 2.22a & 2.22b)**. However, the light scattering intensity (LSI) is as low as 0.335–0.580 Mcps for both P3 and P8 (**Figures 2.22a & 2.22b**), forming low-density aggregates. This is considered to be caused by the formation of hydrogen bonds between the polymers owing to the presence of amide bonds in polymer side chains and association through hydrophobic interaction of dodecyl groups derived from the chain-transfer agent at the ends of polymer chains.

The DLS of DOPC/PAMPTMA (P3) and DOPC/PAMPTMAC-*r*-BuMA (P8) of a solution of DOPC and each polymer was measured. A unimodal peak at R_h = 76.5 nm was observed from the DOPC solution. Because the mixed solution of DOPC/PAMPTMA produced insoluble matter (**Figure 2.21**), many aggregates had R_h > 1000 nm and hence could not be measured. In contrast, DOPC/PAMPTMA-*r*-BuMA showed a unimodal peak at R_h = 90.3 nm and its LSI also increased after the mixing (**Figure 2.22e**). These results suggested an interaction between the BuMA of

PAMPTMA-*r*-BuMA (P8) and DOPC, thereby confirming our hypothesis that the hydrophobic group increases the interaction with the cell membrane.

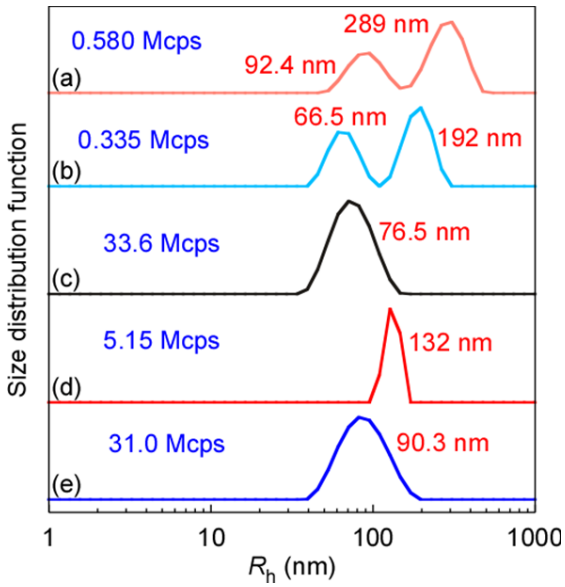

Figure 2.22: R_h distributions for (a) PAMPTMA (P3), (b) PAMPTMA-*r*-BuMA (P8), (c) DOPC, (d) mixture of DOPC/PAMPTMA, and (e) DOPC/PAMPTMA-*r*-BuMA in D_2O at 25 °C. Concentrations were fixed at 1 g/L.

2.3.7. Modelling and Molecular Dynamics Simulation

After confirming the effect of hydrophobic group on the cancer cell membrane. Finally, I elucidate how the PAMPTMA and PAMPTMA-*r*-BuMA polymers interact with the lipid cell membrane. To investigate their difference at the atomistic/molecular level, molecular dynamics (MD) simulations of the two polymer-membrane systems was performed. The outline of our approach to modelling and MD simulations can be found in the materials and method section. **Figure 2.23a** shows the time series of N_{count} values obtained from the NPT MD simulations for the two polymer-membrane systems, PAMPTMA-POPC and PAMPTMA-*r*-BuMA-POPC. Overall, PAMPTMA-*r*-BuMA-POPC is found to have larger N_{count} values than PAMPTMA-POPC: the total amount of

N_{count} values over 10 ns for PAMPTMA-*r*-BuMA-POPC is twice as large than that for PAMPTMA-POPC as shown **(Figure 2.23b)**. In other words, PAMPTMA-*r*-BuMA has more contact atoms with POPC than PAMPTMA. The more contact atoms imply the stronger interaction between the polymer and the membrane.

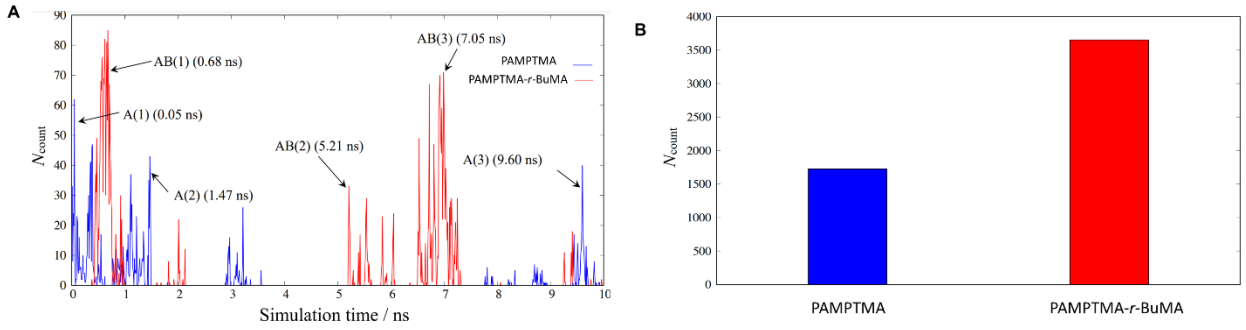

Figure 2.23: (a) Time series of N_{count} values from the NPT MD simulations for the two polymer-membrane systems, AMPTMA-POPC (blue) and PAPTMA-*r*-BuMA-POPC (red), where N_{count} is the number of contact atoms (one belonging to the polymer and the other to the membrane) within 4 Å. (b) The total amount of N_{count} over 10 ns for PAMPTMA-POPC (blue) and PAMPTMA-*r*-BuMA-POPC (red).

Next, the structural difference between PAMPTMA- and PAMPTMA-*r*-BuMA-POPC in order to see why PAMPTMA-*r*-BuMA has a stronger interaction with POPC than PAMPTMA was investigated. Here I focus on several structures with higher N_{count} values shown **(Figure 2.24a)**: shows snapshots of AMPTMA sampled at 0.05 ns (A(1)), understanding of why the AMPTMA-*r*-BuMA copolymer interacts with the POPC membrane more strongly than the PAMPTMA homopolymer. It can be seen from **figure 2.24a** that the main chain of the PAMPTMA polymer does not exhibit any specific molecular orientation to the membrane. On the other hand, the main chain of the PAMPTMA-*r*-BuMA polymer orients parallel to that of the 1.47 ns (A(2)), and 9.60

ns (A(3)), whereas **figure 2.24b** shows those of PAMPTMA-*r*-BuMA at 0.68 ns (AB(1)), 5.21 ns (AB(2)), and 7.05 ns (AB(3)). Note that the penetration of the polymer into the membrane was not observed in the present MD simulations for both the 15-mers. Their structural differences, however, shed light on the membrane, or equivalently the main chain is vertical to the membrane surface, as shown **(Figure 2.24b)**. The finding that the orientation of PAMPTMA-*r*-BuMA is vertical to the POPC surface implies that the PAMPTMA-*r*-BuMA polymer is more likely to rupture the POPC membrane and then penetrate into it than the APTAC polymer. The obtained results are in agreement with the previously reported literatures where the increase in hydrophobic alkyl chain has resulted in the increment of the anticancer properties of the AMPs and the ACPs.[50-52]

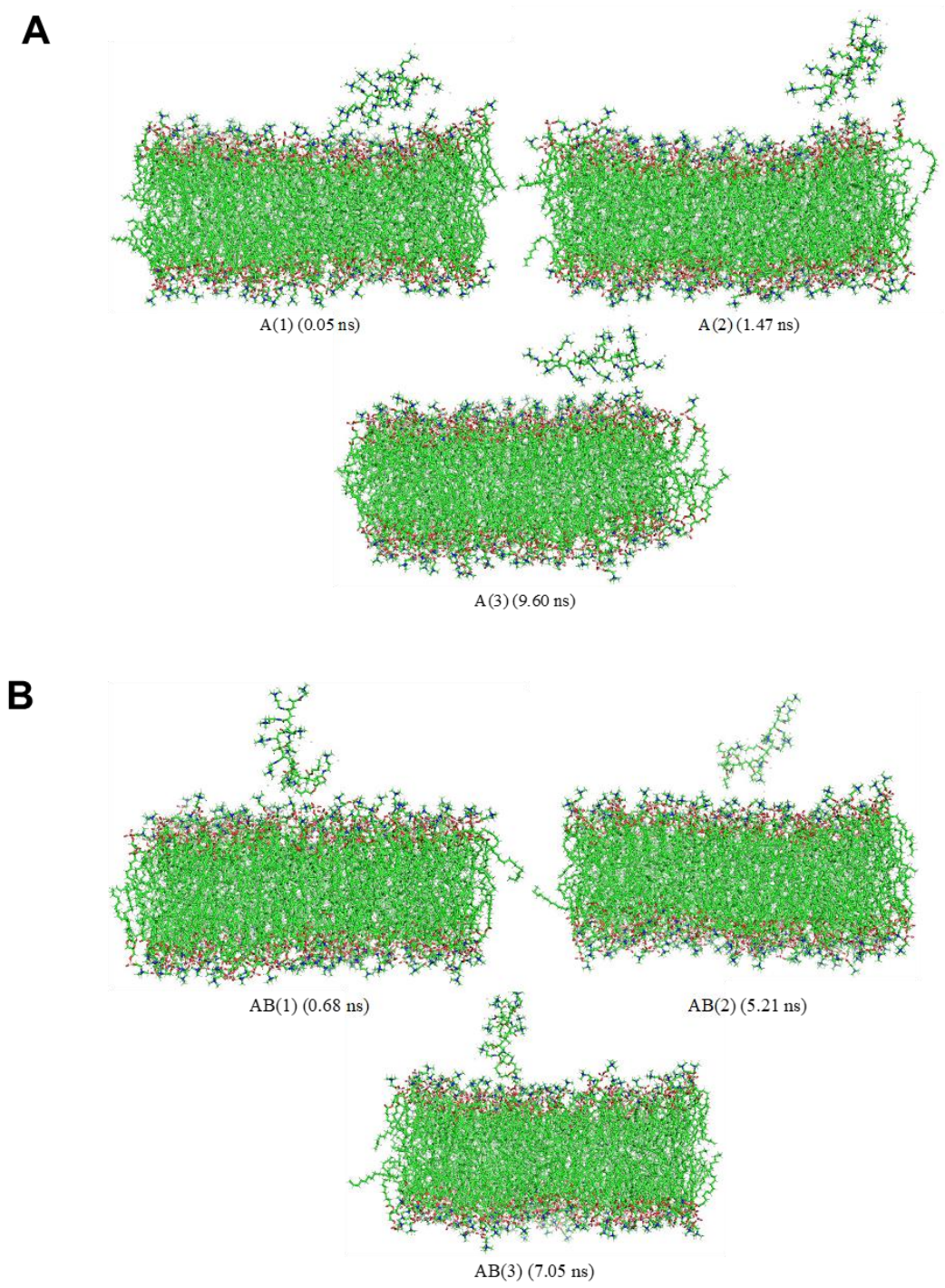

Figure 2.24: (a) PAMPTMA-POPC structures at 0.05 ns (A(1)), 1.47 ns (A(2)), and 9.60 ns (A(3)). (b) PAMPTMA-*r*-BuMA-POPC structures at 0.68 ns (AB(1)), 5.21 ns (AB(2)), and 7.05 ns (AB(3)).

2.4. Conclusion

Cationic copolymers containing hydrophobic groups such as BuMA (PAMPTMA-*r*-BuMA) exhibit superior anticancer activity with low IC_{50} (167 µg/mL for HepG2 cells) than that exhibited by the cationic homopolymer (PAMPTMA) itself, which is contrary to previous reports. Additionally, the effect of the size of the hydrophobic group was established. The copolymer (PAMPTMA-*r*-OctMA) demonstrated a higher anticancer efficacy (IC_{50} = 60 µg/mL) than that shown by copolymers with smaller hydrophobic groups (such as PAMPTMA-*r*-BuMA and PAMPTMA-*r*-HexMA). Therefore, I successfully demonstrated that the cationic charge or the cationic polymer alone is not sufficient for the anticancer activity and that hydrophobicity plays an important role in determining the anticancer activity. The cationic copolymer concentrates the cationic charge and attaches to the anionic cancer cell membrane, resulting in a high local concentration and the hydrophobic group cause a significant permeabilisation, leading to cell death. Hence, this study successfully demonstrates the anticancer activity of hydrophobic copolymers and their potential application in anticancer research. I am currently designing and developing similar systems comprising both a cationic charge and hydrophobic moieties with a focus on selectivity toward normal cells. I believe that the design principle for cationic anticancer polymers explained in this study will widen the cancer treatment research field, which may help in discovering new anticancer pharmaceuticals with a facile synthesis route and lower production cost, which may be useful in clinical medical trials for tumour treatment.

2.5. References

1. World Health Organisation, 2021, https://gco.iarc.fr/.

2. Kumar, N.; Fazal, S.; Miyako, E.; Matsumura, K.; Rajan, R., *Materials Today* **2021**, *51*, 317-349.

3. Desoize, B.; Jardillier, J.-C., *Critical Reviews in Oncology/Hematology* **2000**, *36*, (2), 193-207.

4. Yap, T. A.; Carden, C. P.; Kaye, S. B., *Nature Reviews Cancer* **2009**, *9*, (3), 167-181.

5. Ganoth, A.; Merimi, K. C.; Peer, D., *Expert Opinion on Drug Delivery* **2015**, *12*, (2), 223-238.

6. Mignani, S.; Bryszewska, M.; Klajnert-Maculewicz, B.; Zablocka, M.; Majoral, J.-P., *Biomacromolecules* **2015**, *16*, (1), 1-27.

7. Chabner, B. A.; Roberts, T. G., *Nature Reviews Cancer* **2005**, *5*, (1), 65-72.

8. Glassman, P. M.; Muzykantov, V. R., *Journal of Pharmacology and Experimental Therapeutics* **2019**, *370*, (3), 570.

9. Wang, H.; Evans, C. L., Chapter 11 - Coherent Raman Scattering Microscopy in Dermatological Imaging. In *Imaging in Dermatology*, Hamblin, M. R.; Avci, P.; Gupta, G. K., Eds. Academic Press: Boston, 2016; pp 103-117.

10. Ernsting, M. J.; Murakami, M.; Roy, A.; Li, S.-D., *Journal of Controlled Release* **2013**, *172*, (3), 782-794.

11. Nederberg, F.; Zhang, Y.; Tan, J. P. K.; Xu, K.; Wang, H.; Yang, C.; Gao, S.; Guo, X. D.; Fukushima, K.; Li, L.; Hedrick, J. L.; Yang, Y.-Y., *Nature Chemistry* **2011**, *3*, (5), 409-414.

12. Deslouches, B.; Peter Di, Y., *Oncotarget; Vol 8, No 28* **2017**.

13. Wei, G.; Nguyen, D.; Reghu, S.; Li, J.; Chua, C.; Ishida, Y.; Chan-Park, M. B., *ACS Applied Nano Materials* **2020**, *3*, (3), 2654-2664.

14. Utsugi, T.; Schroit, A. J.; Connor, J.; Bucana, C. D.; Fidler, I. J., *Cancer Research* **1991**, *51*, (11), 3062-3066.

15. Dobrzyńska, I.; Szachowicz-Petelska, B.; Sulkowski, S.; Figaszewski, Z., *Molecular and Cellular Biochemistry* **2005**, *276*, (1), 113-119.

16. Lee, H. S.; Park, C. B.; Kim, J. M.; Jang, S. A.; Park, I. Y.; Kim, M. S.; Cho, J. H.; Kim, S. C., *Cancer Letters* **2008**, *271*, (1), 47-55.

17. Kleeff, J.; Ishiwata, T.; Kumbasar, A.; Friess, H.; Büchler, M. W.; Lander, A. D.; Korc, M., *The Journal of Clinical Investigation* **1998**, *102*, (9), 1662-1673.

18. Haug, B. E.; Camilio, K. A.; Eliassen, L. T.; Stensen, W.; Svendsen, J. S.; Berg, K.; Mortensen, B.; Serin, G.; Mirjolet, J.-F.; Bichat, F.; Rekdal, Ø., *Journal of Medicinal Chemistry* **2016**, *59*, (7), 2918-2927.

19. Liu, X.; Cao, R.; Wang, S.; Jia, J.; Fei, H., *Journal of Medicinal Chemistry* **2016**, *59*, (11), 5238-5247.

20. Camilio, K. A.; Rekdal, Ø.; Sveinbjörnsson, B., *OncoImmunology* **2014**, *3*, (6), e29181.

21. Felício, M. R.; Silva, O. N.; Gonçalves, S.; Santos, N. C.; Franco, O. L., *Frontiers in Chemistry* **2017**, *5*.

22. Schweizer, F., *European Journal of Pharmacology* **2009**, *625*, (1), 190-194.

23. Oelkrug, C.; Hartke, M.; Schubert, A., *Anticancer Research* **2015**, *35*, (2), 635.

24. Park, N. H.; Cheng, W.; Lai, F.; Yang, C.; Florez de Sessions, P.; Periaswamy, B.; Wenhan Chu, C.; Bianco, S.; Liu, S.; Venkataraman, S.; Chen, Q.; Yang, Y. Y.; Hedrick, J. L., *Journal of the American Chemical Society* **2018**, *140*, (12), 4244-4252.

25. Zhong, G.; Yang, C.; Liu, S.; Zheng, Y.; Lou, W.; Teo, J. Y.; Bao, C.; Cheng, W.; Tan, J. P. K.; Gao, S.; Park, N.; Venkataraman, S.; Huang, Y.; Tan, M. H.; Wang, X.; Hedrick, J. L.; Fan, W.; Yang, Y. Y., *Biomaterials* **2019**, *199*, 76-87.

26. Takahashi, H.; Yumoto, K.; Yasuhara, K.; Nadres, E. T.; Kikuchi, Y.; Buttitta, L.; Taichman, R. S.; Kuroda, K., *Scientific Reports* **2019**, *9*, (1), 1096.

27. Gakhar, G.; Liu, H.; Shen, R.; Scherr, D.; Wu, D.; Nanus, D.; Chu, C.-C., *Anticancer Research* **2014**, *34*, (8), 3981.

28. Yong, C. W., *Philosophical Transactions of the Royal Society B: Biological Sciences* **2015**, *370*, (1661), 20140036.

29. Ding, H.-m.; Ma, Y.-q., *Small* **2015**, *11*, (9-10), 1055-1071.

30. Riedl, S.; Zweytick, D.; Lohner, K., *Chemistry and Physics of Lipids* **2011**, *164*, (8), 766-781.

31. BIOVIA, D. S. https://www.3ds.com/products-services/biovia/products/molecular-modeling-simulation/biovia-materials-studio/

32. Wang, J.; Cieplak, P.; Kollman, P. A., *Journal of Computational Chemistry* **2000**, *21*, (12), 1049-1074.

33. Becke, A. D., *The Journal of Chemical Physics* **1993**, *98*, (7), 5648-5652.

34. Lee, C.; Yang, W.; Parr, R. G., *Physical Review B* **1988**, *37*, (2), 785-789.

35. Ditchfield, R.; Hehre, W. J.; Pople, J. A., *The Journal of Chemical Physics* **1971**, *54*, (2), 724-728.

36. Frisch, M. J.; Trucks, G. W.; Schlegel, H. B.; Scuseria, G. E.; Robb, M. A.; Cheeseman, J. R.; Scalmani, G.; Barone, V.; Petersson, G. A.; Nakatsuji, H.; Li, X.; Caricato, M.; Marenich, A. V.; Bloino, J.; Janesko, B. G.; Gomperts, R.; Mennucci, B.; Hratchian, H. P.; Ortiz, J. V.; Izmaylov, A. F.; Sonnenberg, J. L.; Williams; Ding, F.; Lipparini, F.; Egidi, F.; Goings, J.; Peng, B.; Petrone, A.; Henderson, T.; Ranasinghe, D.; Zakrzewski, V. G.; Gao, J.; Rega, N.; Zheng, G.; Liang, W.; Hada, M.; Ehara, M.; Toyota, K.; Fukuda, R.; Hasegawa, J.; Ishida, M.; Nakajima, T.; Honda, Y.; Kitao, O.; Nakai, H.; Vreven, T.; Throssell, K.; Montgomery Jr., J. A.; Peralta, J. E.; Ogliaro, F.; Bearpark, M. J.; Heyd, J. J.; Brothers, E. N.; Kudin, K. N.; Staroverov, V. N.; Keith, T. A.; Kobayashi, R.; Normand, J.; Raghavachari, K.; Rendell, A. P.; Burant, J. C.; Iyengar, S. S.; Tomasi, J.; Cossi, M.; Millam, J. M.; Klene, M.; Adamo, C.; Cammi, R.; Ochterski, J. W.; Martin, R. L.; Morokuma, K.; Farkas, O.; Foresman, J. B.; Fox, D. J. *Gaussian 16 Rev. C.01*, Wallingford, CT, 2016.

37. Jo, S.; Kim, T.; Iyer, V. G.; Im, W., *Journal of Computational Chemistry* **2008**, *29*, (11), 1859-1865.

38. Wang, J.; Wang, W.; Kollman, P. A.; Case, D. A., *Journal of Molecular Graphics and Modelling* **2006**, *25*, (2), 247-260.

39. D.A. Case, H. M. A., K. Belfon, I.Y. Ben-Shalom, J.T. Berryman, S.R. Brozell, D.S. Cerutti, T.E. Cheatham, III, G.A. Cisneros, V.W.D. Cruzeiro, T.A. Darden, R.E. Duke, G. Giambasu, M.K. Gilson, H. Gohlke, A.W. Goetz, R. Harris, S. Izadi, S.A. Izmailov, K. Kasavajhala, M.C. Kaymak, E. King, A. Kovalenko, T. Kurtzman, T.S. Lee, S. LeGrand, P. Li, C. Lin, J. Liu, T. Luchko, R. Luo, M. Machado, V. Man, M. Manathunga, K.M. Merz, Y. Miao, O. Mikhailovskii, G. Monard, H. Nguyen, K.A. O'Hearn, A. Onufriev, F. Pan, S. Pantano, R. Qi, A. Rahnamoun, D.R. Roe, A. Roitberg, C. Sagui, S. Schott-Verdugo, A. Shajan, J. Shen, C.L. Simmerling, N.R. Skrynnikov, J. Smith, J. Swails, R.C. Walker, J. Wang, J. Wang, H. Wei, R.M. Wolf, X. Wu, Y. Xiong, Y. Xue, D.M. York, S. Zhao, and P.A. Kollman *Amber 2022*, University of California, San Francisco, 2022.

40. Wu, E. L.; Cheng, X.; Jo, S.; Rui, H.; Song, K. C.; Dávila-Contreras, E. M.; Qi, Y.; Lee, J.; Monje-Galvan, V.; Venable, R. M.; Klauda, J. B.; Im, W., *Journal of Computational Chemistry* **2014**, *35*, (27), 1997-2004.

41. Jo, S.; Lim Jb Fau - Klauda, J. B.; Klauda Jb Fau - Im, W.; Im, W., (1542-0086 (Electronic)).

42. Jo, S.; Kim T Fau - Im, W.; Im, W., (1932-6203 (Electronic)).

43. Lee, J.; Cheng, X.; Swails, J. M.; Yeom, M. S.; Eastman, P. K.; Lemkul, J. A.; Wei, S.; Buckner, J.; Jeong, J. C.; Qi, Y.; Jo, S.; Pande, V. S.; Case, D. A.; Brooks, C. L., III; MacKerell, A. D., Jr.; Klauda, J. B.; Im, W., *Journal of Chemical Theory and Computation* **2016**, *12*, (1), 405-413.

44. Brooks, B. R.; Brooks Iii, C. L.; Mackerell Jr, A. D.; Nilsson, L.; Petrella, R. J.; Roux, B.; Won, Y.; Archontis, G.; Bartels, C.; Boresch, S.; Caflisch, A.; Caves, L.; Cui, Q.; Dinner, A. R.; Feig, M.; Fischer, S.; Gao, J.; Hodoscek, M.; Im, W.; Kuczera, K.; Lazaridis, T.; Ma, J.; Ovchinnikov, V.; Paci, E.; Pastor, R. W.; Post, C. B.; Pu, J. Z.; Schaefer, M.; Tidor, B.; Venable, R. M.; Woodcock, H. L.; Wu, X.; Yang, W.; York, D. M.; Karplus, M., *Journal of Computational Chemistry* **2009**, *30*, (10), 1545-1614.

45. Chen, B.; Le, W.; Wang, Y.; Li, Z.; Wang, D.; Ren, L.; Lin, L.; Cui, S.; Hu, J. J.; Hu, Y.; Yang, P.; Ewing, R. C.; Shi, D.; Cui, Z., *Theranostics* **2016**, *6*, (11), 1887-1898.

46. Rajan, R.; Hayashi, F.; Nagashima, T.; Matsumura, K., *Biomacromolecules* **2016**, *17*, (5), 1882-1893.

47. Rajan, R.; Jain, M.; Matsumura, K., *Journal of Biomaterials Science, Polymer Edition* **2013**, *24*, (15), 1767-1780.

48. Sharker, K. K.; Shigeta, Y.; Ozoe, S.; Yusa, S.-i., *Chemistry Letters* **2020**, *49*, (12), 1443-1446.

49. Van Zee, N. J.; Peroutka, A. S.; Crabtree, A.; Hillmyer, M. A.; Lodge, T. P., *Biomacromolecules* **2022**, *23*, (3), 1433-1442.

50. Yang, Y.; Zhang, H.; Wanyan, Y.; Liu, K.; Lv, T.; Li, M.; Chen, Y., *ACS Omega* **2020**, *5*, (34), 21513-21523.

51. Huang, Y.-b.; Wang, X.-f.; Wang, H.-y.; Liu, Y.; Chen, Y., *Molecular Cancer Therapeutics* **2011**, *10*, (3), 416-426.

52. Ramamurthi, P.; Zhao, Z.; Burke, E.; Steinmetz, N. F.; Müllner, M., *Advanced Healthcare Materials* **2022**, *11*, (12), 2200163.

Chapter 3

Design of highly selective Zn-coordinated polyampholyte towards cancer treatment and inhibition of tumor metastasis

3.1. Introduction

With the advancement in technology and the treatment, mortality due to cancer has reduced over the few years but still, many cancer patients have ultimately lost their battle against it.[1, 2] It exerts tremendous financial, physical, and emotional strain on individual, family, as well as society. Chemotherapy has proved to be one of the most effective treatments, but the drugs used like doxorubicin (DOX) or paclitaxel (PTX) have their certain limitations. For the desired therapeutic application, a high dose is required thereby causing severe cytotoxicity, drug resistance development, and metastasis along with severe cardiotoxicity and congestive heart failure.[3, 4] Nevertheless, some of the nanomaterials-based drug delivery systems showed great promise than the conventional treatments with increased clinical trials and FDA approval[5] but suffers from the various bottlenecks like they rely on activity of drug, burst release, and off-target toxicity.[6, 7] Usage of anticancer peptides (ACPs) often leads to short circulation half-life, proteolytic cleavage and also the transition from the bench to the bed-side require more research and a understanding of cost to benefit ratio.[8, 9]

The noted limitations of these traditional treatments and materials have compelled the researchers to look for potentially effective systems that use cationic polymers as chemotherapeutic agents.[10] Cationic polymers have already proved to be promising in selective binding and lysis of bacterial cell membrane.[11] Similar to bacterial cell membrane, cancer cell membrane carries a net negative charge on its surface, resulting from overexpression of the phospholipids, phosphatidylserine sialylated gangliosides, and heparan sulfates then the normal cells which may results in potent selectivity.[12, 13] Currently, very few studies have been reported on the use of cationic polymers as anticancer therapeutics and in

treatment of drug resistant and the dormant cancer cells.[10, 14-16] The reported polymers showed good anticancer activity but showed limited selectivity. Also, the synthetic route to obtain these polymers consisted of many steps and complexities which may not be feasible to produce in large quantities. To this end, we aimed to design an appropriate biocompatible cationic polymer that can be easily prepared in scalable quantities with facile synthetic route, having potent anticancer activity with high selectivity. It is believed that the synthesised polymers would also show anticancer activity towards the MDR cells also due to their distinctive anticancer mechanism. The designed system is expected overcome the existing limitations of the previously reported ACPs, nanoparticle-based drug delivery systems (DDS) and standard chemotherapeutic agents.

To circumvent these obstacles and to enhance the selectivity and therapeutic performance of these cationic polymers coordinated self-assemblies of these polymers could be adopted. It has been reported these coordinated self-assembled structures results in a high surface-to-volume ratio resulting an impact on the biological surfaces.[17, 18] Also, this kind of formation will preserve most of the interacting functional groups away from nontargeted cell surfaces (normal cell membrane surface) by keeping them in the core of the structure during its administration. Therefore, the cationic moiety will not be exposed to the normal cell membrane and hence will not be toxic for the normal cells. Contemporaneously, collapsing of these bound polymers at the cancer cell membrane will allow it to selectively kill the cancer cell. For this purpose, the usage of metal ions especially the Zn metal ion has been successfully established for combating bacterial infection.[19, 20]

Hence, as a proof-of-concept, I designed new macromolecular anticancer chemotherapeutics with PLL as a cationic polymeric back bone.[21] This works as a highly tunable platform which offers an excellent handle (-NH_2) to introduce the necessary functional group to drive the nanoformulations as per the proposed mechanism. The -NH_2 groups were then modulated with

the NA (PLL-NA_m) which act as a ligand, followed by the subsequent modification with varying amount of the DDSA acting as the hydrophobic moiety. To minimize the cytotoxicity towards the normal cell the NA, was coordinated with the Zn^{2+} as the metal ion source. The anticancer activity of the Zn-bound and non-bound polymers were evaluated against the cancer cell lines along with the MDR cells and their selectivity was studied against the normal cell line The anticancer mechanism of the polymers was investigated by the lactate dehydrogenase (LDH) leakage assay, confocal microscopy, and the flow cytometry. Capability of the polymers to overcome the tumour metastasis was finally evaluated by the migration inhibition analysis.

3.2. Materials and methods

3.2.1. Materials

A 25% (w/w) aqueous ε-poly-L-lysine (PLL, MW 4000) solution was purchased from JNC Corp. (Tokyo, Japan). Nicotinic acid (NA) and dodecylsuccinic anhydride (DDSA) were purchased from the TCI Japan. 1-(3-dimethylaminopropyl)-3-ethylcarbodiimide Hydrochloride (EDC-HCl) and n-hydroxysuccinimide were purchased from the Wako chemicals Japan. Zinc nitrate hexahydrate ($ZnNO_3.6H_2O$) was purchased from the nacalai tesque. All materials were of reagent grade and were used without further purification.

3.2.2. Synthesis of PLL-NA polymer

For the synthesis of PLL-NA, initially NA (, 75mmol), EDC.HCl (, 75 mmol) and NHS (, 75 mmol) were dissolved in water and kept for stirring at room temperature (rt) for 6 h. To this, 25 % aqueous solution of PLL (48 mL, 12 g, 3 mmol) was added and kept for stirring at 25^oC rt for next 12 h. The obtained product was dialyzed against the distilled water for 4 days with 3500 MWCO dialysis membrane (Spectra/Por Dialysis membrane) followed by lyophilization. A similar synthetic procedure was carried out with increasing the amount of NA (14.77 g, 120 mmol) to obtain PLL with different amount of NA.

3.2.3. Insertion DDSA in PLL-NA

I synthesized the PLL-NA-DDSA polymer by varying the amount of DDSA from the previously obtained PLL-NA. For example, PLL-NA (2 g, 0.377 mmol) and DDSA (202.13 mg, 0.754 mmol) were dissolved in water and kept for stirring at 50 ˚C for 2 h. The obtained solution after 2 h was purified by dialysis against distilled water (4 days) with 3500 MWCO dialysis membrane (Spectra/Por Dialysis membrane) followed by lyophilization.

3.2.4. Coordination of Zn metal ion

The Zn coordinated polymers were obtained, the PLL-NA-DDSA (100 mg) and the $Zn.NO_3.6H_2O$ (50 mmol in water, 3ml) were dissolved in water and kept for stirring at 25ºC for 12 h. The resultant solution was purified by dialysis against distilled water (4 days) with 3500 MWCO dialysis membrane (Spectra/Por Dialysis membrane) followed by lyophilization.

3.2.5. Characterization of polymers

^{1}H-NMR of the obtained polymers were recorded on a Bruker Avance NEO 400 spectrometer (400 MHz). The chemical shifts were referenced based on the solvent peak (δ = 4.79 ppm for D_2O). Dynamic light scattering (DLS) and zeta-potential measurements were carried out on a Zetasizer Nano-ZS instrument (Malvern, UK) by using disposable folded capillary cells (DTS1070) with a scattering angle of 173°. The elemental analysis of the coordinated polymer was performed by X-ray photoelectron spectroscopy (XPS) spectroscopy using the AXIS ULTRA-DLD.

3.2.6. Cell culture

The cancer cells (HepG2, and Colon 26) were acquired from American Type Culture Collection (ATCC). Primary human dermal fibroblast (HDF) which is a normal cell line was purchased from the (CELL, applications, San diego). All these cell lines were cultured in

Dulbecco's modified Eagle's medium (DMEM, Sigma-Aldrich) supplemented with 10 % fetal bovine serum (FBS, Invitrogen, Singapore) at 37 °C in a CO_2 incubator in a humidified atmosphere. The multidrug- resistance (MDR) cell line (COR-L23/R) was purchased from the (ECACC) and was maintained in Roswell Park Memorial Institute-1640 (RPMI-1640) medium with 10 % FBS along with 0.2 µg/mL of the doxorubicin (DOX) in culture media to maintain the resistance phenotype but the medium was changed to DOX-free RPMI-1640 one week before the experiments. Cells were sub-cultured after the confluency using trypsin solution (0.25 % [w/v] trypsin containing 0.0 2% [w/v] ethylenediaminetetraacetic acid in PBS) to detach the cells.

3.2.7. *In vitro* cytotoxicity assay

The cytotoxicity of polymers against cancer cell lines and normal cell line was examined by 3-(4,5-dimethylthiazol-2-yl)-2,5-diphenyltetrazolium bromide (MTT) assay. The cells were seeded in a 96-well plate at a density of 3×10^3 cells per well in 100 µL of respective culture media for 24 h at 37 °C in a 5 % CO_2 incubator in a humidified atmosphere. After 24 h the culture medium was then replaced with fresh medium containing various concentrations of polymers ranging from 2 µg/mL to 1000 µg/mL or with DOX concentration from 0.5 µg/mL to 100 µg/mL and incubated for 48 h at 37 °C. MTT solution 100 µL (300 µg/mL in DMEM) was then added. Cells were incubated for 3 h and the medium containing MTT was replaced and replaced with 100 µL of DMSO. The absorbance was determined at 540 nm using a microplate reader (Infinite 200Pro, Infinite M Nano, Tecan). The experiment was independently repeated three times.

3.2.8. LDH leakage assay

The HepG2 cells were seeded at 3×10^3 cells per well in 96-well flat-bottom polystyrene cell culture plate for 24 h. Then the medium was replaced by a serial concentration of the polymer

(P3-P11, Table 1) for 48 h. After 48 h of treatment, 10 µL of the Lysis Buffer of Cytotoxicity LDH assay Kit-WST (Dojindo) was added to four wells (positive control indicating 100% lysis) and incubated for 30 min at 37 °C as per manufacturers instruction. Then, 100 µL of the Working Solution to all wells and incubated for 30 min at room temperature. To stop the reaction, 50 µL of the Stop Solution was added and absorbance at 490 nm was measured by Infinite 200Pro, Infinite M Nano, Tecan microplate reader). The percentage of LDH leakage was determined relative 100 % lysed cells. Each assay was independently repeated three times.

3.2.9. Cellular uptake analysis

HepG2 cells were seeded onto a four-well glass bottom dish (Matsunami), at the density of 3 × 10^4 cells per well and allowed to attach and grow for 24 h. The medium was then replaced with an equal volume of medium containing AlexaFluor 488 tagged polymer (at IC_{50} concentration). After 2 h and 24 h of incubation, the cells were rinsed 3 times with PBS for any free dye removal. The cells were fixed by 4 % formaldehyde for 15 min at 37 °C followed by washing in PBS for 3 times. The cells were subsequently stained with Image-IT™ Live Plasma Membrane and Nuclear Labeling Kit (Invitrogen, Singapore) according to the manufacturer's instructions and washed 3 times with PBS, cells were then observed under confocal laser scanning microscopy (Olympus FV1000D, oil immersed 60 × objective lens).

3.2.9.1. Tagging with AlexaFluor 488. A stock solution of the AlexaFluor 488 (NHS ester for amino group) is prepared by dissolving it in high quality of the DMSO. This stock solution was added dropwise to the polymer solution approximately 10 mmol of the polymer solution and the rection is kept for stirring for 4 h at 25 ºC with protection from the light. The unreacted dye was removed from the Sephadex G-25 gel filtration column. The solution was dried under vacuum and obtained powder was the AlexaFluor tagged polymer.

3.2.10. *In vitro* cancer cell migration

HepG2 cells were seeded in 24-well plates at a density of 1 x10^5 cells per well. After 24 h, the plate surface was scratched with a 1000 μL pipette tip to generate a gap with uniform width. The medium was replaced by fresh medium containing polymers or DOX at their respective IC_{50}. The cells were then incubated at 37 °C in the presence of 5 % CO_2. Images of the gaps were taken using a bright field microscope (Olympus, Japan) at 0 h and 24 h after scratching.

3.3. Result and Discussion

3.3.1. Polymer characterization

Poly-L-lysine (PLL) and nicotinic acid (NA) based polymers with varying amount of DDSA were synthesized according to **Scheme 3.1**. ε-PLL is an L-lysine homopolymer biosynthesized by *Streptomyces* species.[21, 22] It has cationic charge density due the presence of α-amino groups in its side chain and thus possesses antimicrobial activities.[23] NA which is also called niacin (vitamin B3) was introduced in the PLL as it is well-known that cancer patients are deficient in niacin and chemotherapy may further stress niacin status in patients .[24] Additionally, it contains tertiary nitrogen which can work as the Lewis base for binding with a metal ion. The substitution of NH_2 group by NA in PLL was confirmed by the appearance of the aromatic protons in the ^{1}H-NMR (δ = 6.5-8.0 ppm) (**Figure 3.1**). Further, the degree of substitution of NH_2 group by the NA was calculated by comparing the integral peak of γ-proton (δ = 1.38-1.55 ppm) to aromatic proton (δ = 7.39-7.54 ppm).

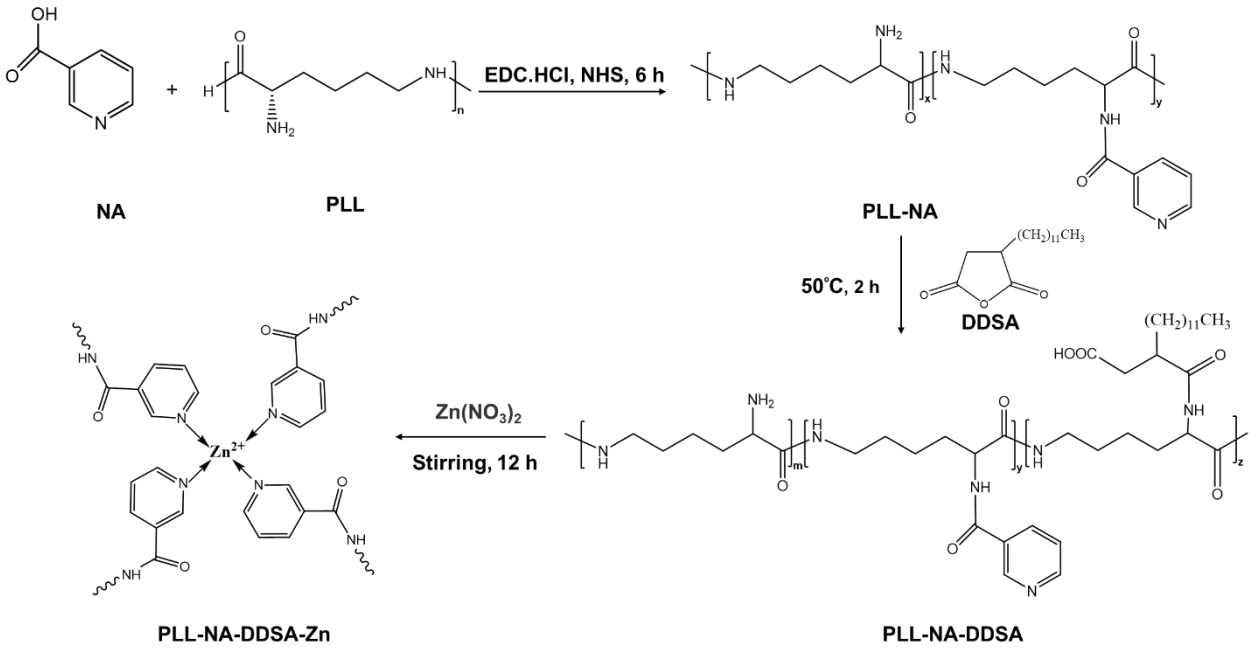

Scheme 3.1: Schematic representation of the reaction of PLL with NA and DDSA followed by its coordination with Zn metal ion.

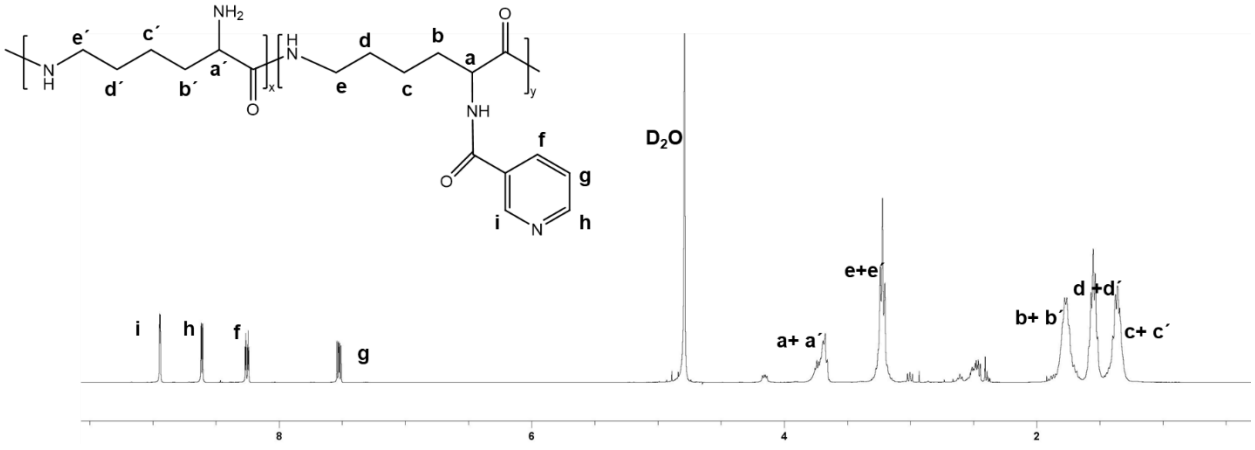

Figure 3.1: ^{1}H-NMR of the PLL-NA synthesized.

The dried PLL-NA obtained in first step was further used for incorporating the DDSA group in them. DDSA was introduced to control the cationic charge as well as to introduce some hydrophobicity in the polymer. The insertion of the DDSA was confirmed by the ^{1}H-NMR **(Figure 3.2)** and compared with the PLL-NA **(Figure 3.3a)**. The amount of DDSA incorporated in the PLL-NA was calculated by 1H-NMR by comparing the integral peak of

methyl protons of the DDSA (δ = 0.74 ppm) to the β-methylene peak of poly-L-lysine (δ = 1.5 to 1.8 ppm) found according to the addition (**Figure 3.3b**).[25]

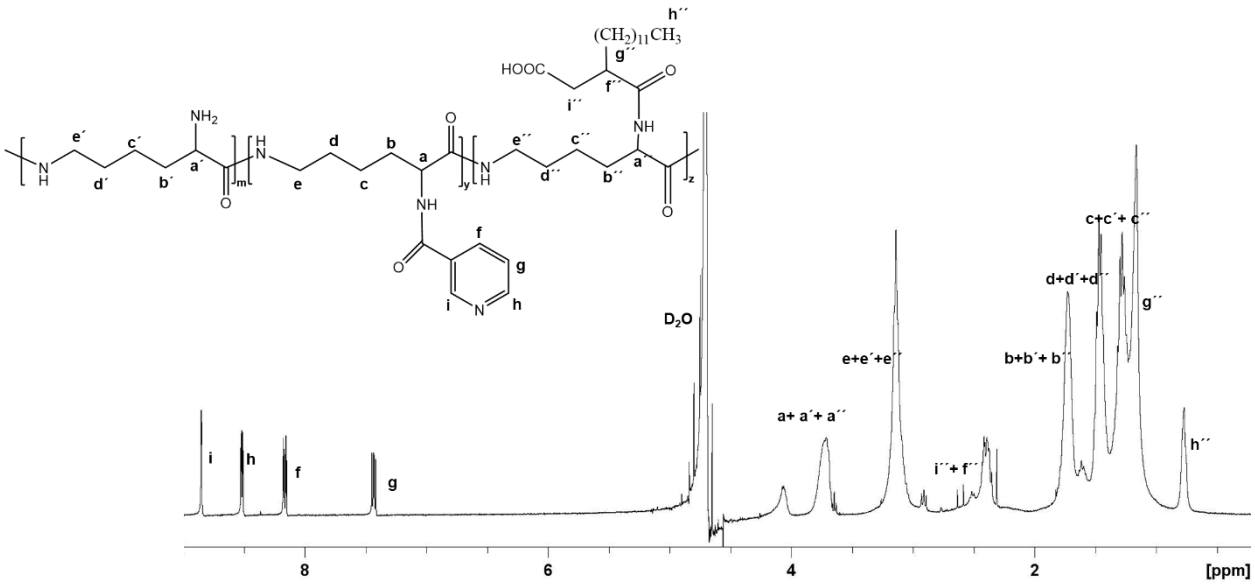

Figure 3.2: ^{1}H-NMR of the PLL-NA-DDSA synthesized.

The obtained polymer was further coordinated with Zn^{2+} ions by using the $ZnNO_3.6H_2O$ (zinc nitrate hexahydrate). The elemental analysis of the coordinated polymer was performed by X-ray photoelectron spectroscopy (XPS) spectroscopy. The pyridinium group in the NA functions as a Lewis base whereas Zn^{2+} ions act as the Lewis acid and thus can be coordinated with each other. The N 1s peak showed a significant shift from 399.2 eV (N-C) to 401.8 eV (Zn-N-C) **(Figure 3.3c).** Also, Zn 2p showed peaks at 1020.5 and 1043.6 eV ascribed to Zn $2P^{3/2}$ and Zn $2P^{1/2}$ respectively **(Figure 3.3d).**

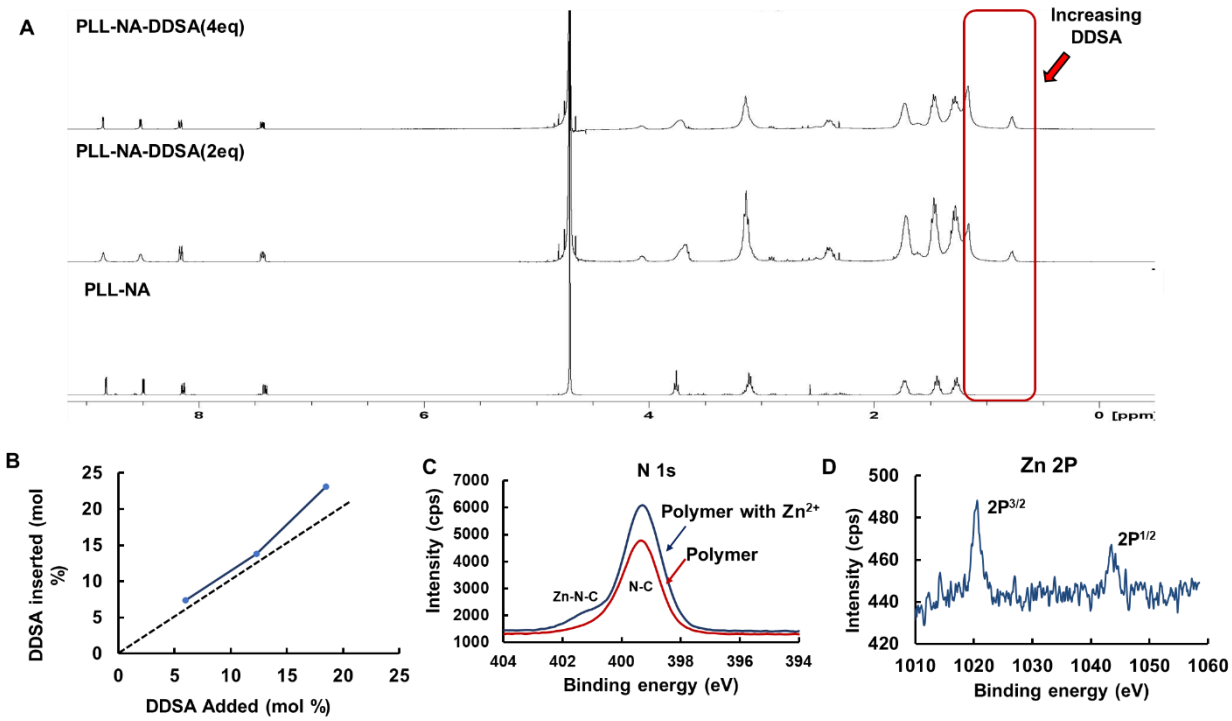

Figure 3.3: a.) ^{1}H-NMR spectra of the obtained PLL-NA polymers showing the increase in the amount of DDSA in the obtained polymers, b.) the graph shows amount of the DDSA introduced in the final polymers as per the amount added during the reaction, c.) XPS spectra of N1s of the Zn-bound and non-bound polymer, d.) Zn 2P spectra of the Zn-bound polymer.

3.3.2. *In vitro* cytotoxicity assay

The *in vitro* anticancer activity of the polymers (N1-N16) and their Zn coordinated complexes was evaluated against the cancer cell lines: HepG2 and Colon 26 and against the normal cell line HDF for the selectivity. All polymers showed potent anticancer activity with low IC_{50} values **(Table 3.1).** The polymer PLL (N1) and PLL-NA_{11} (N2) did not show any anticancer activity against all cell lines tested up to 1000 µg/mL **(Figure 3.4a & 3.4b)**. DDSA was introduced in the pure PLL (N3: 2 NH_2 group replaced, N4: 4 NH_2 groups replaced) and their anticancer activity was evaluated. With the introduction of the DDSA in pure PLL the anticancer activity was enhanced with lower IC_{50} value (IC_{50} = 60 µg/mL) for the polymer N3 **(Table 3.1)**. Also, with further increase in DDSA in N4, the anticancer activity was further

enhanced with IC_{50} = 47 µg/mL **(Figure 3.4c, Table 3.1)**. Although, the insertion of DDSA in N3 and N4 increased the cytotoxicity towards the cancer cells, however the cytotoxicity towards the normal cell line was also increased (IC_{50} = 88 and 68 µg/mL) and hence no selectivity **(Figure 3.4c, Table 3.1)**. This may be due to the enhancement of the hydrophobicity in these polymers which results in the undesired cytotoxicity towards all the cell lines tested. As in case of ACPs and AMPs it has been reported that they first selectively bind to the PS lipid-rich membrane of the cancer cell by electrostatic interactions, and then insert the hydrophobic domain of their helix into the cell membrane, resulting in the disruption of the cell membrane and subsequent lysis of the cell.[26] However, the insertion of DDSA in the polymer PLL-NA polymer enhanced the cytotoxicity with lower IC_{50} values **(Table 3.1)** as well as retains its selectivity towards the normal cell line. I believed that this enhancement in cytotoxicity towards the cancer cells was due to the hydrophobicity and the selectivity was due the of the cationic charge of the NA, means a synergistic effect of both is required.[27] So, I believe that a combination of both is required for better anticancer activity and the enhanced selectivity. It was observed that the cytotoxicity of the PLL-NA_{11}-DDSA (N5, N7) (IC_{50} = 365 and 223 µg/mL) was higher than the PLL-NA_{11} (N2) (IC_{50} = N.D.) which was in accordance with my hypothesis **(Table 3.1).**

Table 3.1. *In vitro* anticancer activity (IC_{50} values) of all the polymers synthesized.

S.No.	Polymer	Composition	Zeta potential (mV)[a]	IC_{50} HepG2 (µg/ml)	IC_{50} Colon 26 (µg/ml)	IC_{50} HDF (µg/ml)
1.	N1	PLL	2.11 ± 1.72	N.D.	N.D.	N.D.
2.	N2	PLL-NA_{11}	15.4 ± 2.02	N.D.	N.D.	N.D.
3.	N3	PLL-$DDSA_2$	4.17 ± 0.40	60	70	88
4.	N4	PLL-$DDSA_4$	9.86 ± 0.42	47	148	68
5.	N5	PLL-NA_{11}-$DDSA_2$	8.63 ± 0.59	365	413	N.D.
6.	N6	PLL-NA_{11}-$DDSA_2$-Zn[b]	9.58 ± 0.21	179	196	N.D.
7.	N7	PLL-NA_{11}-$DDSA_4$	5.57 ± 3.91	223	370	N.D.
8.	N8	PLL-NA_{11}-$DDSA_4$-Zn	5.98 ± 2.46	110	208	N.D.

2, 4-are the number of NH_2 groups replaced in PLL by DDSA, N.D.-not determined upto 1000µg/mL,

a: determined in PBS, b: 50 mM $Zn(NO_3)_2$

Although the introduction of the DDSA in PLL enhanced the cytotoxicity but it was much lower than the therapeutic values reported in the previous literatures.[14] In order to achieve that, Zn was introduced in the polymers where the pyridinium ring of NA will work as Lewis base and the metal ion as counter -Lewis acid **(Scheme 3.1).** Although the metal ions like Zn^{2+}, Cu^{2+} and the Fe^{3+} have the ability to coordinate with formed polymer, but zinc was selected due to its lower cytotoxicity and reported potent antimicrobial activity as well as its anticancer activity. [28]

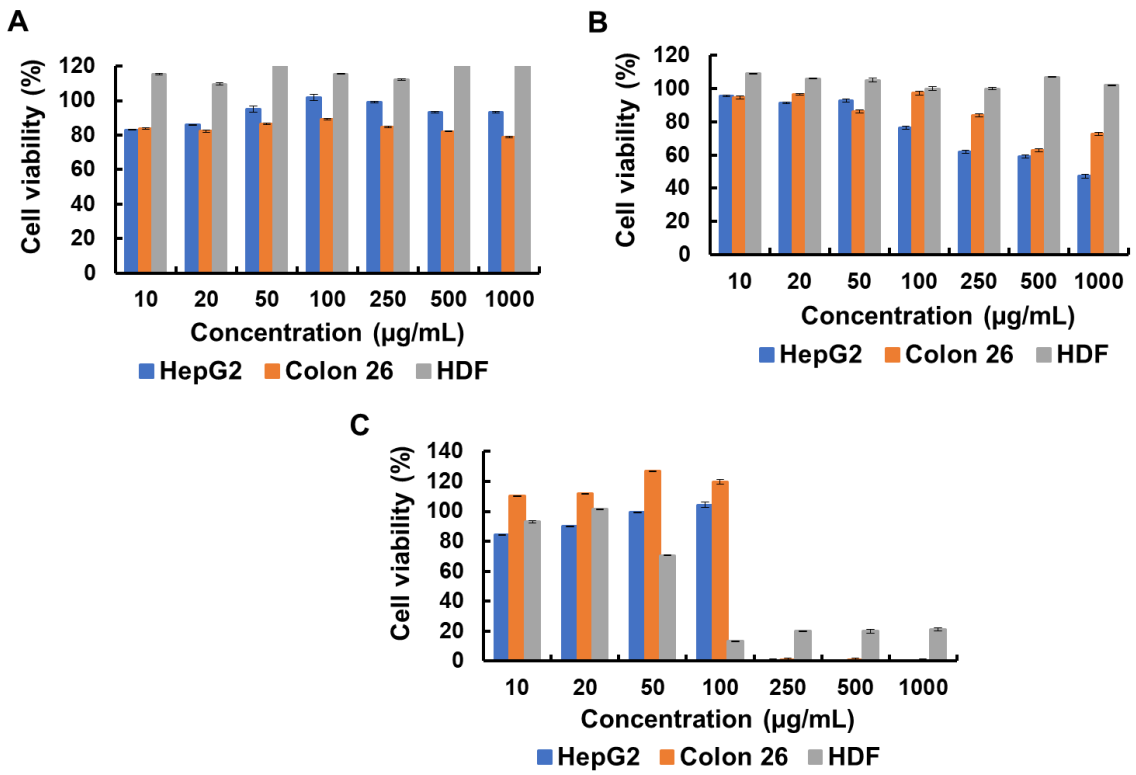

Figure 3.4: Cytotoxicity towards the cancer cell and the normal cell lines: a.) for the pure PLL, b.) for the PLL-NA_{11} c.) for the PLL-$DDSA_4$.

With the introduction of Zn^{2+} ions in polymer N5 (called N6) the cytotoxicity towards the cancer cell was increased. The IC_{50} values for the HepG2 was decreased from the 365 µg/mL to 179 µg/mL in N7 **(Figure 3.5a, Table 3.1).** Similar results were observed for Colon 26 cancer cell line **(Figure 3.5b, Table 3.1).** The coordination of the Zn^{2+} ions in N7 enhanced the cytotoxicity with lowering in IC_{50} values from 223µg/mL to 110 µg/mL for the HepG2 cancer cell line **(Figure 3.5d, Table 3.1)**. For the colon 26 cancer cells, a similar trend was observed in enhancement of cytotoxicity with the insertion of the Zn^{2+} ions **(Figure 3.5e, Table 3.1)**. Although the cytotoxicity towards the cancer cell lines were enhanced, interestingly both the polymers N6 and N8 showed significantly very high selectivity towards the normal cell line HDF with no IC_{50} up to 1000 µg/mL of the polymer concentration **(Figure 3.5f, Table 3.1).** I believed that the insertion of the Zn^{2+} ions make the coordinated self-assemblies with our

polymers by taking the cationic charge of the NA into its core structure. These structures selectively disrupt on the cancer cell membranes owing to its more negative charge in its surface and thus enables the free cationic PLL based polymers to interact with and spontaneously kill the cancer cells. Since there was no toxicity against HDF cell line, we believe that they remain intact against the normal cells. It is worth mentioning that Zn^{2+} ions have its own antimicrobial, anticancer activity. The electrostatic interaction between the Zn^{2+} ions and the cancer cell membrane along with the production of the reactive oxygen spices would be the two-underlying mechanism of killing the cancer cells thereby producing a synergistic effect with my synthesized polymers.[29]

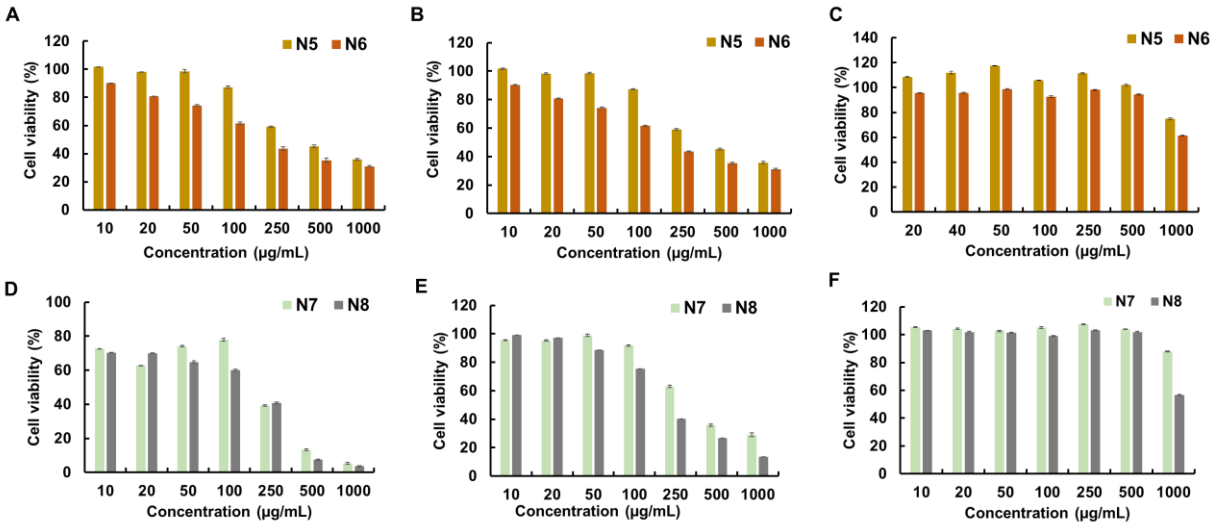

Figure 3.5: MTT cell viability assay of the polymers: a.) for N5 and N6 against the HepG2 cell ne, b.) N5 and N6 against the colon 26 cancer cell line, c) N5 and N6 against the normal HDF cell line, d) for N7 and N8 against the HepG2 cell line, e) N7 and N8 against the colon 26 cell line , f) N7 and N8 against the HDF cell line. .

Thereafter, the coordinated polymers were prepared by varying the amount of the Zn^{2+} ions and keeping the number of coordinating sites as constant. Hence, I prepared a series of three different coordinated polymers by using N7 as the basic polymer, as it showed better anticancer property. N9 to N11 were prepared by constantly lowering the amount of zinc with respect to

the number of the coordinating sites in N7. In N9 the Zn^{2+} ions were added ½ of the total coordinating sites present in the N7, similarly in N10 and N11 the Zn^{2+} ions were added ¼ and 1/8 of the coordinating sites respectively. Polymer N9 showed almost similar anticancer activity with lower IC_{50} (108 µg/mL) as compared to the N8 (IC_{50} = 110 µg/mL) on HepG2 cancer cell line **(Figure 3.6a, Table 3.2)**. However, as the Zn^{2+} was reduced in N10 the anticancer activity was enhanced with low IC_{50} = 89 µg/mL which was further enhanced in N11 (IC_{50} = 78 µg/mL) with reduced amount of Zn^{2+} then the N10 **(Figure 3.6a, Table 3.2)**. Similar results were obtained with the colon 26 cancer cell line **(Figure 3.6b, Table 3.2)**. However, a similar enhanced cytotoxic effect was observed with lowered amount of Zn^{2+} in case of the HDF as normal cell line **(Figure 3.6c, Table 3.2)**. I believed that with the lowered amount of the Zn^{2+} ions there were structural changes at the nanoscale level which results in the size dependent anticancer activities at the nanoscale level.

Table 3.2. The *in vitro* anticancer activity (IC_{50} values) of all the polymers with varying amount of Zn^{2+} ions.

S.No.	**Polymer**	**Composition**	**Zeta potential (mV)[a]**	**IC_{50} HepG2 (µg/mL)[b]**	**IC_{50} Colon 26 (µg/mL)[b]**	**IC_{50} HDF (µg/mL)[b]**
9.	N9	PLL-NA_{11}-$DDSA_4$-Zn_1	2.25±0.47	108	68	910
10.	N10	PLL-NA_{11}-$DDSA_4$-Zn_2	-1.82±0.38	89	94	N.D.
11.	N11	PLL-NA_{11}-$DDSA_4$-Zn_3	0.66±0.34	78	42	738

a: determined in PBS, b: determined by MTT assay, N.D.: not determined

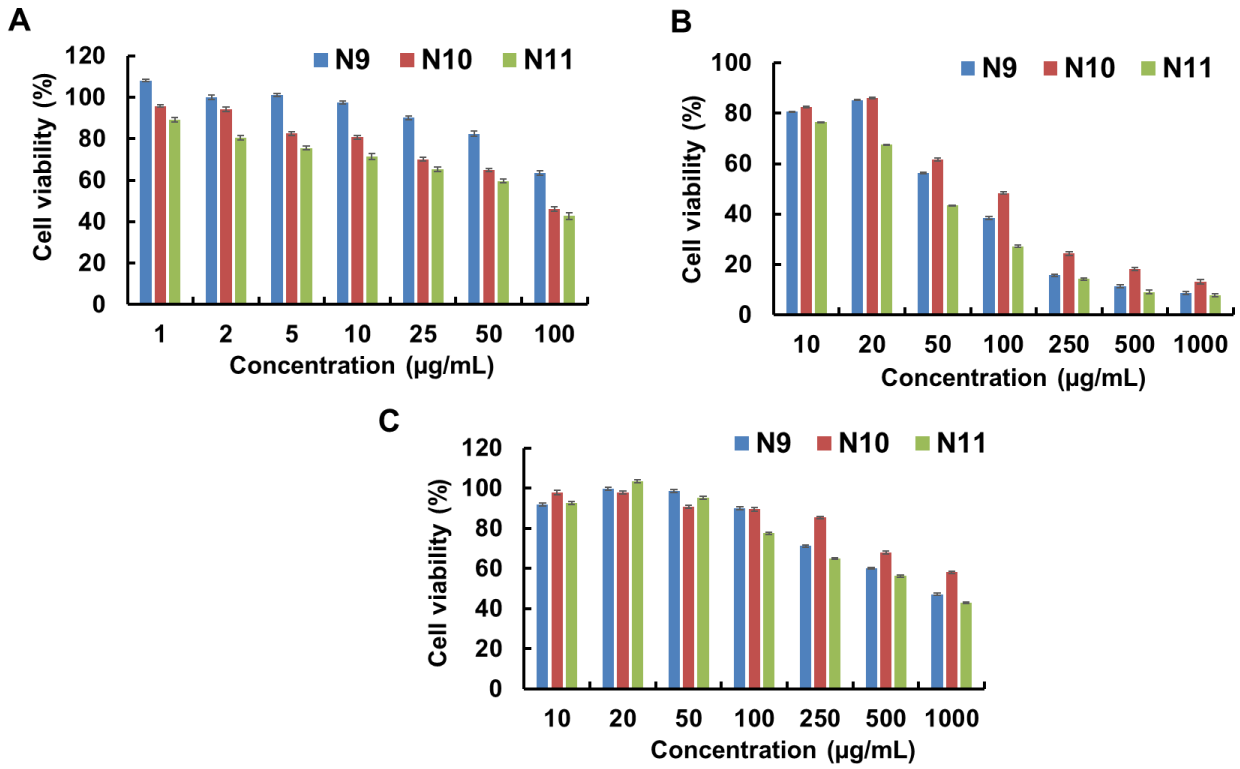

Figure 3.6: MTT cell viability assay of the polymers with different amount of Zn^{2+} ions: a.) against the HepG2 cell, b.) against the colon 26 cancer cell line, c) against the normal HDF cell line.

Further, to understand the effect of the NA in our polymers, next I synthesized the new PLL-NA with the more NA replaced with the NH_2 groups present in the pure PLL. The modification of the PLL with NA and its degree of substitution was confirmed by ^{1}H-NMR. The DDSA group was incorporated in the obtained PLL-NA_{16} and further coordinated with the Zn^{2+} ions as in previous sections. The *in vitro* anticancer activity of the polymers (N12-N16) and their Zn coordinated complexes was evaluated against the cancer cell lines: HepG2 and Colon 26 and against the normal cell line HDF for the selectivity **(Table 3.3)**. The polymer N12 (PLL-NA_{16}) did not show any anticancer activity against the all the cancer cell lines tested **(Figure 3.7)**. The introduction of the DDSA group in the PLL enhanced the cytotoxicity towards the cancer cells as well as the normal cell lines may be due enhanced hydrophobicity of the DDSA.

The insertion of the DDSA in N12 (IC_{50} = N.D.) by replacing the NH_2 groups as in N13 (2-NH_2 groups replaced) and N14 (4-NH_2 groups replaced) enhanced the cytotoxicity towards the cancer cell lines with lower IC_{50} of 201 µg/mL and 180 µg/mL respectively **(Table 3.3)**. The insertion of the Zn^{2+} ions as in N15 and N16 (from N12 and N13 respectively) further enhanced the cytotoxicity towards both cancer cell lines **(Table 3.3).** However, the enhancement of the NA group in the PLL enhanced the anticancer activity towards the cancer lines but the selectivity towards the normal cell was simultaneously reduced with lowering in IC_{50} values for N14 (197 µg/mL) and N15 (172 µg/mL) respectively **(Table 3.3).**

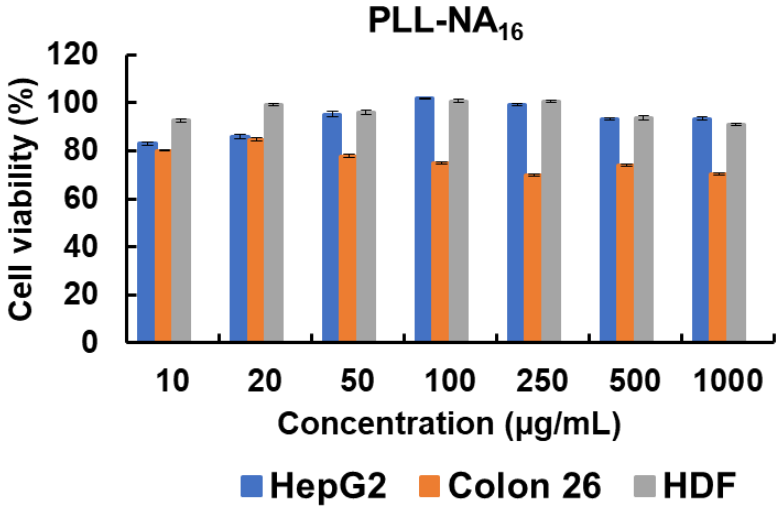

Figure 3.7: Cytotoxicity towards the cancer cell and the normal cell lines for the PLL-NA_{16}.

Table 3.3. The *in vitro* anticancer activity of the polymers obtained from the PLL-NA_{16} as a precursor polymer.

S.No.	Polymers	Composition	Zeta Potential (mV)[a]	IC_{50} HepG2 (µg/ml)[b]	IC_{50} Colon 26 (µg/ml)[b]	IC_{50} HDF (µg/ml)[b]
12.	N12	PLL-NA_{16}	3.17 ± 2.32	N.D.	N.D.	N.D.
13.	N13	PLL-NA_{16}-$DDSA_2$	8.63 ± 2.64	201	326	292
14.	N14	PLL-NA_{16}-$DDSA_4$	10.5 ± 1.04	180	172	195
15.	N15	PLL-NA_{16}-$DDSA_2$-Zn	3.87 ± 0.74	130	54	197
16.	N16	PLL-NA_{16}-$DDSA_4$-Zn	6.89 ± 1.04	42	143	172

a: determined in PBS, b: determined by MTT assay, N.D.: not determined

3.3.3. Mechanistic Investigations

3.3.3.1. LDH leakage: To investigate the mechanism of action of polymers, I examined the effect of polymer on the cancer cell membrane. To understand the membrane disruptive mechanism of the polymers, firstly we carried out lactate dehydrogenase (LDH) leakage assay with all the model polymers selected (N7, N8, and N10) because of their potent anticancer activity and the selectivity. To quantify the damage to the cell membrane by polymer, an extracellular leakage of the cytoplasmic enzyme LDH form HepG2 cells treated with polymers (N7, N8 and N10) for 48 hours was examined. All the polymers caused significantly higher LDH leakage at the higher polymer concentrations suggesting that the cell membrane was permeabilized **(Figure 3.8a)**. The introduction of the Zn in polymer N8 and N10 resulted in higher LDH leakage as compared to the non-bound polymer N7. N10 polymer containing the lower amount of Zn showed significant LDH leakage at higher concentration as well as at the lower concentration up to 250 µg/mL of the polymer concentration **(Figure 3.8a)**. The percentage of the LDH released was in agreement with the cell viability of the cells treated

with these polymers. The results suggest that the polymer induced cell death was due the cell membrane disruption.

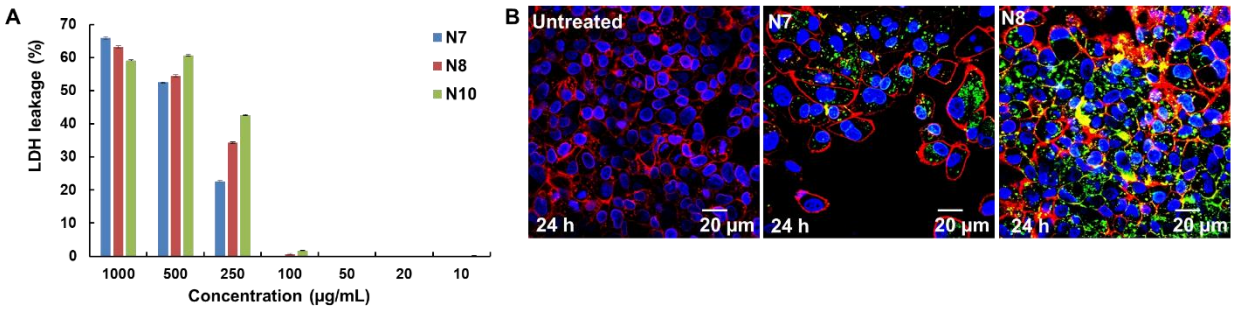

Figure 3.8: Mechanistic study on the selected polymers a.) LDH leakage assay on the HepG2 cell line, b.) HepG2 uptake of the polymers tagged with the AlexaFluor488 after the 24 hour of incubation time at their respective IC_{50} values. Hoechst (blue): nucleus; Red: cell membrane; Green: AlexaFluor488-labelled N7/N8.

3.3.3.2. Cellular uptake analysis: The anticancer mechanism was further explored by studying the cellular uptake of polymer N7 and N8 tagged with AlexaFluor 488 by HepG2 human liver cancer cells under a confocal microscope **(Figure 3.8b)**. Cells when incubated with medium only (untreated) no green coloration was observed, however on treatment with tagged polymers green color was observed. Interestingly, both N7 (without Zn) and N8 (Zn-bound) were taken up by the cells and can be seen in the cytosol region of the cells after the 24 h of treatment indicating the translocation activity of the polymer. However, the density of N8 tagged polymer in cancer cell was found to be much higher as compared to the N7 polymer. This suggests that the Zn-bound polymers were more strongly attracted and internalized by the cancer cell membrane as compared to the non-bound one and thus results in maximum cell damage.

3.3.4. Comparison with Doxorubicin

I further compared our best Zn-bound polymer (N10) and its non-bound counterpart with the commercially available well-known drug DOX. I carried out the MTT cytotoxicity assay with the HepG2 cancer cell line, and for selectivity the HDF as normal cell line was used **(Figure 3.9)**. N7 showed lowest cytotoxicity as no IC_{50} value was determined at a low polymer concentration below 100 µg/mL. However, N10 showed significantly better cytotoxicity than N7 with IC_{50} value of 89 µg/mL **(Figure 3.9a)**. Dox showed very high cytotoxicity with very low IC_{50} (1 µg/mL) when compared to both polymers. Although DOX showed the highest cytotoxicity in cancer cell lines but when I tested on normal cell lines the results were completely different. Cell viability of only 20-30 % was observed on normal cell line even at very low concentration of the drug used showing very high cytotoxicity and no selectivity **(Figure 3.9b)**. In contrast, both polymers N7 and N10 showed almost no cytotoxicity, with 85-90% cell viability even at the highest concentration tested (125 µg/mL). These results showed that, the synthesized polymers were highly selectivity towards the normal cell line. Overall, the synthesized polymers were found to be effective and selective when compared to the commercially available drug DOX.

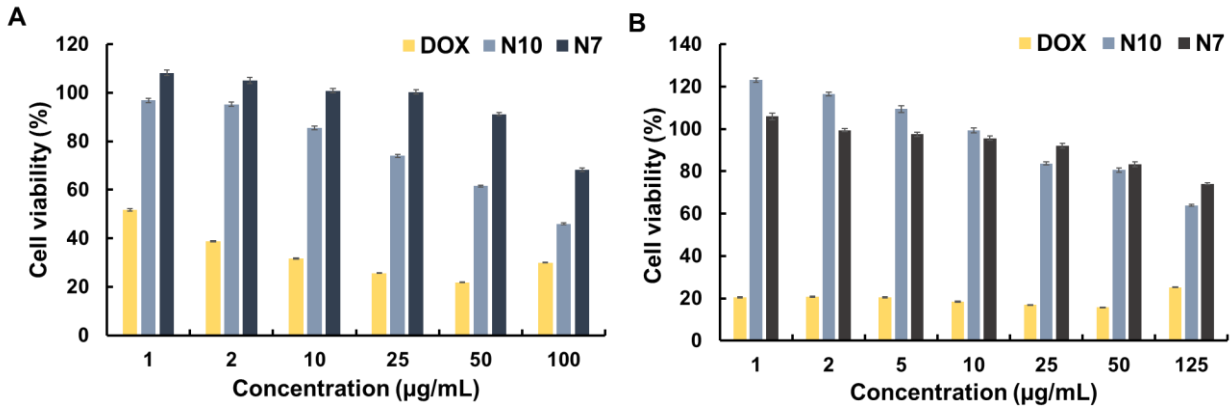

Figure 3.9: Comparison of the selected polymers along with the DOX a.) against the HepG2 cancer cell, b.) for selectivity comparison against the HDF normal cell line.

3.3.5. Evaluation against Drug-resistant cells

Based on my mechanistic investigations, the mode of action of synthesized polymers is to disrupt the cell membrane and then further lysis, ultimately leading to cell death. Due to this distinctive mode of action, we believed that the Zn-bound polymers would be able to treat the drug-resistance cancer cell line as well. To demonstrate this the N7 and N10 were further evaluated against the DOX resistance human caucasian lung large cell carcinoma (COR-L23/R) cancer cell line. The small molecule drug DOX was less effective against the COR-L23/R with increased IC_{50} value 66 µg/mL which was almost 65 to 66 times higher than the IC_{50} against the HepG2 cell line (1µg/mL) **(Figure 3.10)**. The N7 could not show any anticancer efficacy against the MDR cell line up to the 100 µg/mL of the polymer concentration. In contrast, N10 effectively inhibited the growth of drug resistance cell line with IC_{50} value (84 µg/mL) of almost the same order of magnitude **(Figure 3.10)**.

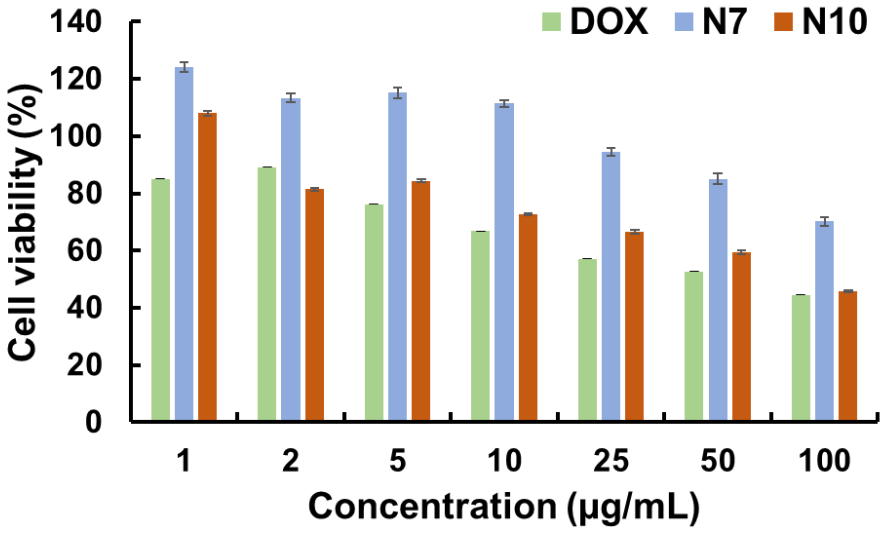

Figure 3.10: MTT cell viability assay of the selected polymers and the DOX against the MDR (COR-L23/R) dox-resistance cell line.

3.3.6. Migration Inhibition Analysis

To further investigate the anticancer properties of these polymers, migration inhibition analysis was carried out to examine their ability to prevent cancer cell migration. HepG2 cells were cultured in a 24 -well plate and a rift was scratched into the cell wells with 1000 µL tip. The cells were then treated with polymers or DOX at their respective IC_{50} concentrations (**Figure 3.11)**. For the PLL-NA, cells were treated with 500 µg/mL of the concentration as it does not show any IC_{50} value **(Table 3.1)**. Cell migration was observed over a period of 24 h after the treatment with the polymers. The untreated cells migrated across the rift after 24 h of the culture period. Cell migration was also observed in the polymer not bound to the Zn (N7). Also, cell migration was observed for DOX treated samples at their IC_{50} concertation. However, both the Zn-bound polymers (N8 and N10) effectively prevented the cell migration across the rift created. To further analysis we carried the same experiment for the 7 days of time. We found that the cell migration was prevented even up to the 7 days by the Zn-bound polymers. So, these results not only suggest the effective killing of the cancer cells but also prevention of their further metastasis and relapse.

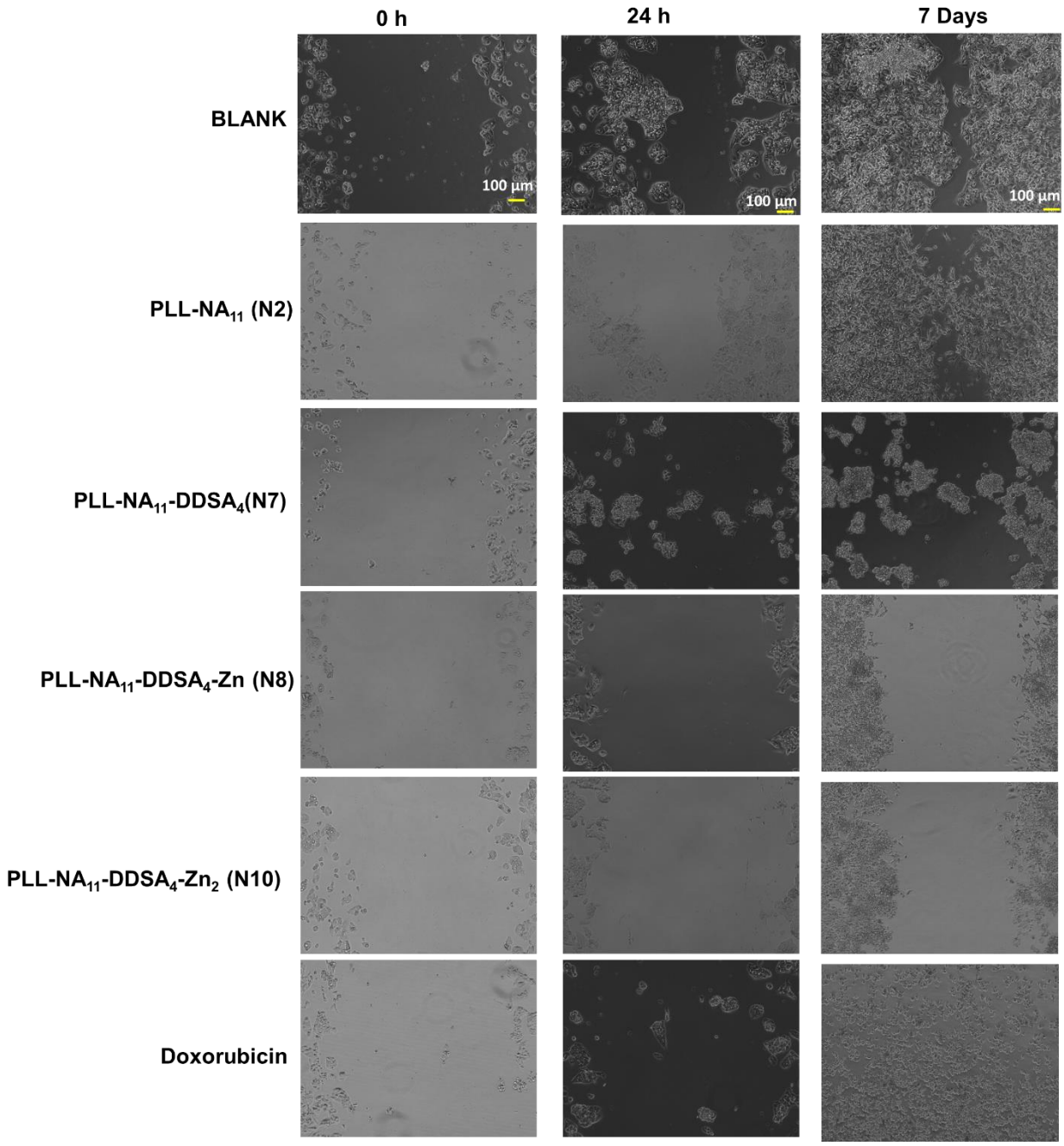

Figure 3.11: Effect Dox and the polymers on the cancer cell migration of HepG2 cell line.

3.4. Conclusion

In conclusion, I have successfully synthesized the biodegradable PLL-NA based polymers with varying amount of the DDSA in them. The synthesized polymers successfully coordinated with the Zn^{2+} ions which were reflected from the N1s peak shift from 399.2 eV (N-C) to 401.8 eV (Zn-N-C). The coordinated polymers showed potent anticancer activity which was revealed

from their lower IC_{50} Values (50-200 µg/mL) then the non-coordinated one. The polymers showed very high selectivity towards the normal cell line with no or significantly very low IC_{50} values. The polymers were effective in killing of the cancer cells with high selectivity when compared with DOX, as well as the drug-resistance cancer cells were also significantly killed by these polymers. Also, these polymers not only showed their potency in killing, but also in prevention of further migration of the cancer cells which making them effective for prevention of the tumor metastasis. Overall, all the NA-based zinc bound polymers showed excellent *in vitro* antitumor properties against both the cancer cell lines selectively. Considering the easy synthetic reaction scheme, availability and biodegradability of these polymers they could prove to be a promising approach towards cancer treatment. The Metal coordinated cationic polymers approach can open a new window in macromolecular chemotherapeutics and could be an attractive option in overcoming the limitations of cancer treatment.

3.5. References

1. Siegel, R. L.; Miller, K. D.; Jemal, A., *CA: A Cancer Journal for Clinicians* **2019**, *69*, (1), 7-34.
2. Kumar, N.; Fazal, S.; Miyako, E.; Matsumura, K.; Rajan, R., *Materials Today* **2021**, *51*, 317-349.
3. Erttmann, R.; Erb, N.; Steinhoff, A.; Landbeck, G., *Journal of Cancer Research and Clinical Oncology* **1988**, *114*, (5), 509-513.
4. Wang, S.; Konorev, E. A.; Kotamraju, S.; Joseph, J.; Kalivendi, S.; Kalyanaraman, B., *Journal of Biological Chemistry* **2004**, *279*, (24), 25535-25543.
5. Dawidczyk, C. M.; Kim, C.; Park, J. H.; Russell, L. M.; Lee, K. H.; Pomper, M. G.; Searson, P. C., *Journal of Controlled Release* **2014**, *187*, 133-144.
6. Heilman, B. J., *Photoactive nitric oxide delivery systems based on metal nitrosyl-biomaterial composites*, University of California, Santa Cruz, 2014.
7. Ganoth, A.; Merimi, K. C.; Peer, D., *Expert Opinion on Drug Delivery* **2015**, *12*, (2), 223-238.
8. Schweizer, F., *European Journal of Pharmacology* **2009**, *625*, (1), 190-194.

9. Oelkrug, C.; Hartke, M.; Schubert, A., *Anticancer Research* **2015**, *35*, (2), 635.

10. Park, N. H.; Cheng, W.; Lai, F.; Yang, C.; Florez de Sessions, P.; Periaswamy, B.; Wenhan Chu, C.; Bianco, S.; Liu, S.; Venkataraman, S.; Chen, Q.; Yang, Y. Y.; Hedrick, J. L., *Journal of the American Chemical Society* **2018**, *140*, (12), 4244-4252.

11. Nederberg, F.; Zhang, Y.; Tan, J. P. K.; Xu, K.; Wang, H.; Yang, C.; Gao, S.; Guo, X. D.; Fukushima, K.; Li, L.; Hedrick, J. L.; Yang, Y.-Y., *Nature Chemistry* **2011**, *3*, (5), 409-414.

12. Dobrzyńska, I.; Szachowicz-Petelska, B.; Sulkowski, S.; Figaszewski, Z., *Molecular and Cellular Biochemistry* **2005**, *276*, (1), 113-119.

13. Utsugi, T.; Schroit, A. J.; Connor, J.; Bucana, C. D.; Fidler, I. J., *Cancer Research* **1991**, *51*, (11), 3062-3066.

14. Zhong, G.; Yang, C.; Liu, S.; Zheng, Y.; Lou, W.; Teo, J. Y.; Bao, C.; Cheng, W.; Tan, J. P. K.; Gao, S.; Park, N.; Venkataraman, S.; Huang, Y.; Tan, M. H.; Wang, X.; Hedrick, J. L.; Fan, W.; Yang, Y. Y., *Biomaterials* **2019**, *199*, 76-87.

15. Gakhar, G.; Liu, H.; Shen, R.; Scherr, D.; Wu, D.; Nanus, D.; Chu, C.-C., *Anticancer Research* **2014**, *34*, (8), 3981.

16. Takahashi, H.; Yumoto, K.; Yasuhara, K.; Nadres, E. T.; Kikuchi, Y.; Buttitta, L.; Taichman, R. S.; Kuroda, K., *Scientific Reports* **2019**, *9*, (1), 1096.

17. Zheng, K.; Setyawati, M. I.; Lim, T.-P.; Leong, D. T.; Xie, J., *ACS Nano* **2016**, *10*, (8), 7934-7942.

18. Peng, B.; Zhang, X.; Aarts, D. G. A. L.; Dullens, R. P. A., *Nature Nanotechnology* **2018**, *13*, (6), 478-482.

19. Panja, S.; Bharti, R.; Dey, G.; Lynd, N. A.; Chattopadhyay, S., *ACS Applied Materials & Interfaces* **2019**, *11*, (37), 33599-33611.

20. Panja, S.; Dey, G.; Bharti, R.; Mandal, P.; Mandal, M.; Chattopadhyay, S., *Chemistry of Materials* **2016**, *28*, (23), 8598-8610.

21. Matsumura, K.; Hyon, S.-H., *Biomaterials* **2009**, *30*, (27), 4842-4849.

22. Yamanaka, K.; Maruyama, C.; Takagi, H.; Hamano, Y., *Nature Chemical Biology* **2008**, *4*, (12), 766-772.

23. Saimura, M.; Takehara, M.; Mizukami, S.; Kataoka, K.; Hirohara, H., *Biotechnology Letters* **2008**, *30*, (3), 377-385.

24. Kirkland, J. B., *Molecular Cancer Therapeutics* **2009**, *8*, (4), 725-732.

25. Ahmed, S.; Hayashi, F.; Nagashima, T.; Matsumura, K., *Biomaterials* **2014**, *35*, (24), 6508-6518.

26. Riedl, S.; Zweytick, D.; Lohner, K., *Chemistry and Physics of Lipids* **2011**, *164*, (8), 766-781.

27. Ilker, M. F.; Nüsslein, K.; Tew, G. N.; Coughlin, E. B., *Journal of the American Chemical Society* **2004**, *126*, (48), 15870-15875.

28. Pasquet, J.; Chevalier, Y.; Pelletier, J.; Couval, E.; Bouvier, D.; Bolzinger, M.-A., *Colloids and Surfaces A: Physicochemical and Engineering Aspects* **2014**, *457*, 263-274.

29. Xu, Q.; Zheng, Z.; Wang, B.; Mao, H.; Yan, F., *ACS Applied Materials & Interfaces* **2017**, *9*, (17), 14656-14664.

Chapter 4

Enhancement of anticancer activity of methyl jasmonate using cationic polymer

4.1. Introduction

Cancer is a severe threat to the humankind and is one of the major causes of death worldwide according to WHO.[1] The design and discovery of the molecules effective in cancer treatment always remains a challenge. Numerous treatments, such as radiation therapy, chemotherapy, and various drugs are currently in use, but their harmful side effects, aggressive drug resistance, low aqueous solubility, rapid clearance from body and off-target toxicity have caused major roadblocks in cancer treatment regimens.[2-6] There it is urgent need to develop effective cancer treatments and drugs having fewer side effects with low cost. The design of the drug must meet the condition that the molecular target must be distinctive from normal cells for selectivity.

Otto Warburg proved that cancer cells differ in their energy consumption as compared to normal cells. [7, 8] In terms of energy production, they followed high rate of glycolytic pathway rather than tricarboxylic acid (TCA) cycle even in abundant oxygen which results higher lactate production and thus local acidification in cancerous cell.[9] Phosphorylation of glucose to glucose-6-phosphate is the first step in glycolysis which is catalyzed by the hexokinase-II enzyme (HK-II), which is overexpressed in cancer cells then the normal cells.[10, 11] Therefore, the energy consumption of the cancer cell can be prevented by inhibiting the HK-II enzyme in glycolysis cycle and could be effective and attractive target for anticancer drug development.[12] Methyl jasmonate (MJ) is a well-known HK-II inhibitor and also the therapeutic potential of the MJ and its derivatives against cancer have been investigated both *in vivo* and *in vitro*.[13, 14] Also, in normal eukaryotic cells, phosphatidylethanolamine and phosphatidylserine are present in the inner leaflet of the cell membrane, whereas choline-containing phospholipids, sphingomyelin, and phosphatidylcholine are mainly present in the outer leaflet of the cell

membrane. In addition to phosphatidylserine, O-glycosylated mucins,[3,4] sialylated gangliosides,[5] and heparan sulfates[6] are also overexpressed in cancer cell membranes. The knowledge of the anionic nature of cancer cell may attribute to the high selectivity and potency to the chemotherapeutics.

Based on the above knowledge my proposed plan was the combination of these pharmacophoric moieties of bioactive substance like MJ with cationic macromolecule or to polymerise themselves to produce a new hybrid compound with improved affinity and efficacy when compared to the parent drug and it can be considered as a new trend in drug designing. Research on anticancer polymers is comparatively new and promising in cancer treatment. A very few literatures have been reported where polymer itself is used as anticancer drug. In this research work I used the polymer itself as drug not as drug carrier. Also, the polymerization of the MJ a bioactive compound is not reported anywhere and completely new in trend of drug designing.

In the light of these findings, I have designed and synthesized the novel modified MJ based monomers. The synthesized monomers were further copolymerized with the varying amount of the cationic monomer (3-acrylamidopropyl)trimethylammonium chloride (AMPTMA). The modification of the MJ based monomer and its copolymers were confirmed by the proton nuclear magnetic resonance (NMR) spectroscopy. The anticancer activity was further evaluated against the cancer cell lines (HepG2, Colon 26 and B16F10). For the selectivity, the obtained polymers were further tested on the normal cell line primary human dermal fibroblast (HDF).

4.2. Materials and methods

4.2.1. Materials

Methyl jasmonate, lithium hydroxide monohydrate ($LiOH.H_2O$), 2-(dodecylthiocarbonothioylthio)-2-methylpropionic acid (RAFT agent) and

azobisisobutyronitrile (AIBN; initiator) were purchased from Sigma-Aldrich (St. Louis, MO) and used as received. A 75% aqueous solution of the monomer (3-acrylamidopropyl)trimethylammonium chloride (AMPTMA), 2-hydroxethyl methacrylate (HEMA), and 4-dimethylaminopyridine (DMAP) were purchased from the TCI Japan. Coupling agent used, 1-(3-Dimethylaminopropyl)-3-ethylcarbodiimide hydrochloride (EDC.HCl) were purchased from Wako chemicals. All the solvents used were of reagent grade and used without further purification.

4.2.2. Monomer synthesis

4.2.2.1. Synthesis of jasmonic acid (JA)

For the conversion of the methyl jasmonate to jasmonic acid, methyl jasmonate (1 mmol) was dissolved in the mixture of THF and water (1:1), to this mixture $LiOH.H_2O$ (2 mmol) was then added and the reaction was kept for stirring for 1 h at 25^oC. After 1 h the reaction was diluted with 30 ml of water. To this further hexane was added (30 ml) and then acidified by 1N HCl and subjected to extraction with ethyl acetate. The EtOAc was dried over Na_2SO_4 and the solvent was evaporated to give light yellow oil as final product.

4.2.2.2. Synthesis of 1,2,4-oxadiazole MJ based monomer

For compound 1 (step b): To a mixture of JA (1 mmol) in acetone (10 ml), DCC (1.1 mmol) was added. The reaction mixture was stirred at 25^oC for the 30 min time interval and then the 3-pyridine carboxamide oxime (1 mmol) was added. The reaction mixture was kept for stirring for the next 12 h. After that, the acetone evaporated under the reduced pressure and the reaction mixture was further diluted with the 50 ml of water. The obtained solution was extracted with the ethyl acetate and dried over Na_2SO_4 and the solvent was evaporated. For compound 2 (step c): To the obtained compound 1 (1 mmol) in step b DMSO (10 ml) was added. To this reaction mixture KOH (1 mmol) was added and stirred at 25^oC for the next 20 min. It was then further

diluted with 30-40 ml of water and then extracted by using ethyl acetate. The obtained compound was purified by using column chromatography with 2:3 (EtOAc:Hxn) mixture.

4.2.2.3. Synthesis of ethylene diamine MJ based monomer

For compound 7 (step b). JA (1 mmol), EDC.HCl (1.1 mmol) and the NHS (1 mmol) were dissolved in DCM and were kept for stirring at 25^{o}C for 5 h. After that Boc-amine was added to it and kept for stirring for the next 12 h at 25^{o}C. After 12 h the compound was extracted by the ethyl acetate and finally dried under vacuum. For compound 8 (step c) to compound 7 the CF_3COOH was added, and the reaction was kept for stirring for 4 h and the product was obtained by work up procedure with ethyl acetate and then washing with the $NaHCO_3$. For compound 9 (step d), in 8 the methacrylic anhydride (1.1 mmol), TEA (1.1 mmol) in DCM was kept for stirring at 25^{o}C for 2 h. The obtained monomer was tested or the homopolymerization by using AIBN as an initiator and raft agent for 36 h at 70^{o}C.

4.2.2.4. Synthesis of 2-hydroxylethyl methacrylate (HEMA) MJ based monomer

For compound 11 (step b). To the JA (1 mmol) and EDC.HCl (1 mmol) was added to the precooled DCM (0-5^{o}C) and kept for stirring for 2 h at 25^{o}C. To this DMAP (1 mmol) and the 2-hydroxyethyl methacrylate (HEMA) (1 mmol) was added to this reaction mixture and was kept for stirring at 25 ^{o}C for another 12 h. The solution was diluted with the 1N HCl and the resultant mixture was extracted with EtOAc while washing with $NaHCO_3$, and brine solution. The compound was finally dried with Na_2SO_4 and finally dried under vacuum. The obtained compound was purified by column chromatography.

4.2.3. Copolymer synthesis of JA-HEMA and AMPTMA

I synthesized various copolymers (Scheme 4) by varying the proportion of AMPTMA as a co-monomer. As an example, JA-HEMA : AMPTMA (1:2) copolymer was synthesized by adding JA-HEMA (1 g, 3.1 mmol), AMPTMA (1.28 g, 6.202 mmol), a RAFT agent (22.62 mg, 0.062 mmol), and AIBN (2.71 mg, 0.012 mmol) to the round-bottomed flask, followed by adding 25

mL of DMF. The resulting solution was then purged with nitrogen gas for 30 min and stirred at 70 °C for 24 h. The obtained random copolymer was purified by dialysis using distilled water (4 days) with a 3500 MWCO dialysis membrane (Spectra/Por Dialysis membrane), followed by lyophilization.

4.2.4. PEG based copolymers of JA-HEMA and AMPTMA

4.2.4.1. PEG-macro raft agent (PEG-CTA): For the synthesis of the PEG-CTA, the 2-(dodecylthiocarbonothioylthio)-2-methylpropionic (raft agent, 5 mmol), oxalyl chloride (20 mmol) were added in a round bottom flask. To this the dry CH_2Cl_2 (20 mL) was added as the reaction solvent. The resultant mixture was stirred at 25ºC for 2-3 h until the evolution of the gas was stopped. The excess solvent was removed under vacuum, and the obtained residue was redissolved in 80 mL of the dry CH_2Cl_2 and then polyethylene glycol (1mmol, Mn = 4000g/mol) was added to it and kept for stirring at 25ºC for 24 h. After 24 h the mixture was concentrated under vacuum and then precipitated in cold diethyl ether. The obtained yellow powder was filtered by Whatman filter paper and then further dried under vacuum.

4.2.4.2. PEG based copolymer: I synthesized various copolymers by varying the proportion of JA-HEMA and AMPTMA as a co-monomer. For example, for the synthesis of (1:1) copolymer JA-HEMA (0.931 mmol), PEG-CTA (raft agent, 0.0931), AMPTMA (0.931 mmol) and AIBN (initiator, 0.0186 mmol) were dissolved in the DMF (25 mL) in a round bottom flask. The resulting solution was then purged with nitrogen gas for 30 min and stirred at 70 °C for 24 h. The obtained random copolymer was purified by dialysis using distilled water (4 days) with a 3500 MWCO dialysis membrane (Spectra/Por Dialysis membrane), followed by lyophilization.

2.5. Polymer characterization

^{1}H-NMR and ^{13}C-NMR spectra of the obtained polymers were recorded on a Bruker Avance NEO 400 spectrometer (400 MHz). The chemical shifts were referenced based on the solvent peak (δ = 4.79 ppm for D_2O). The molecular weight and distribution (polydispersity index, PDI) of the polymers were determined by gel-permeation chromatography (GPC, Waters e2695) using the Ultrahydrogel 250 column and 2414 refractive index detector at 50 °C. A 10% methanol–PBS solution (pH 7.4) was used as the mobile phase (flow rate: 1 mL min^{-1}) and a Shodex standard was used as the standard. Zeta-potential measurements were carried out on a Zetasizer Nano-ZS instrument (Malvern, UK) by using disposable folded capillary cells (DTS1070) with a scattering angle of 173°.

4.3. Results and Discussion

4.3.1. Synthetic chemistry-synthesis of monomer and reaction optimization

Initially the ester group of MJ was modified by installing the oxadiazole moieties which would work as druggable handle. Therefore, I started with the conversion of the MJ to JA which worked as an initial building block for further modification. The formation of the JA was confirmed by the ^{1}H-NMR. In order to obtain the 1,2,4-oxadiazole moiety in our compound (2) the DCC coupling strategy was used with pyridine carboxamide oxime followed by the basic condensation. Pyridinium functional moiety was used as it proved to be a heterocycle having various biological activities, mainly anticancer activities.[15, 16] Also, it will be used to modify as the quaternary nitrogen in order to obtain the cationic polymers. Formation of both the compounds 1 and 2 were confirmed by the ^{1}H-NMR after their purification through the column chromatography. The obtained compound (2) was further reduced by using the $NaBH_4$ to modify the ketonic carbonyl carbon to the hydroxyl group so that further steps towards the formation of the MJ based cationic polymer could be carried out **(Scheme 4.1)**. However, the conversion of this ketonic group to the hydroxyl group was not confirmed by the ^{13}C-NMR,

also the slight reduction in the double bond present in alkyl side chain of MJ was observed in ^{1}H-NMR.

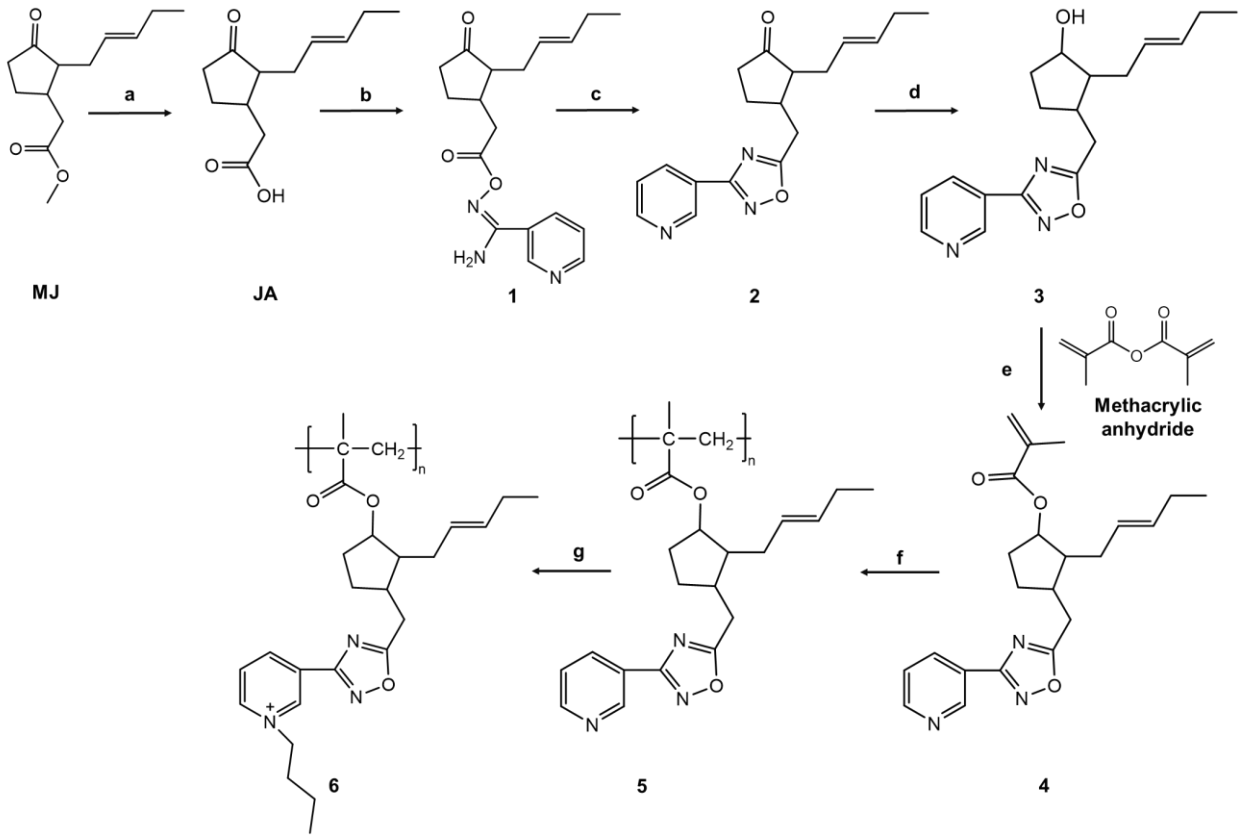

Scheme 4.1: Synthesis of Methyl Jasmonate modified monomer 1-4[a] and its subsequent polymerization and generation on cationic charge in the polymer 4-6. [a]Reagents and conditions: (a) for JA: MJ (1 mmol), LiOH. H_2O (2 mmol), THF-Water (1:1) solvents, stir 1 h, rt. (b) for 1: i. DCC (1.1 mmol), acetone solvent, stir 30 min, rt, ii. Pyridine carboxamide oxime (1 mmol), stir 12 h, rt. (c) for 2: DMSO, KOH (1mmol), stir 30 min, rt. (d) for 3: $NaBH_4$ (1.5 mmol), methanol, stir 3 h, 0^{o}C.

After obtaining the negative results from the previous reaction scheme and involvement of seven complex reaction steps I thought to make reaction scheme much easier with lesser reaction steps. Next, I tried to modify the JA through the introduction of the ethylene diamine which was further reacted with the methacrylic anhydride followed by its subsequent polymerization **(Scheme 4.2)**.

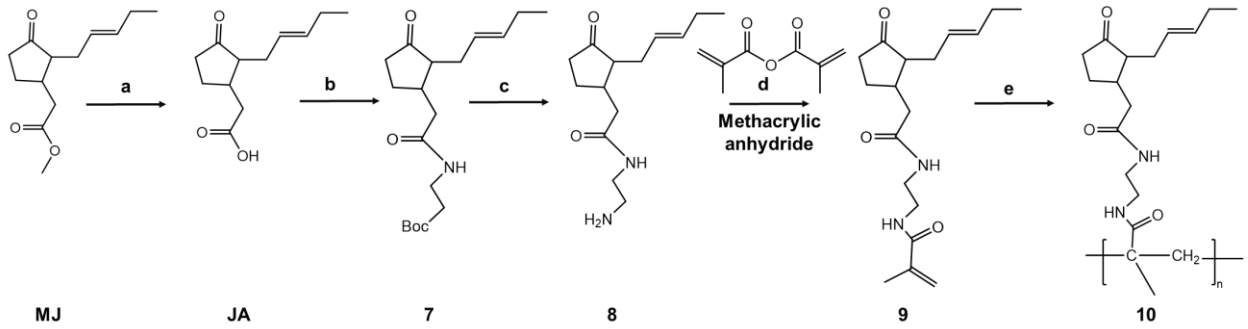

Scheme 4.2. Synthesis of Methyl Jasmonate modified monomer 7-10[a] and its subsequent polymerization. [a]Reagents and conditions: (a) for JA: MJ (1 mmol), LiOH. H_2O (2 mmol), THF-Water (1:1) solvent, stir 1 h, rt. (b-c) for 7-8: EDC.HCl (1.1 mmol), NHS (1.1 mmol), Boc-ethylene diamine (1.1 mmol), DCM solvent, 24 h, rt and CF_3COOH, rt (d) for 9: methacrylic anhydride (1.1 mmol), TEA (1.1 mmol), DCM, stir 2 h, rt. (e) for 10: AIBN, ethanol, DCM, 24-36 h, 70^{o}C.

The JA was successfully modified to compounds 7 and 8 which was confirmed by the ^{1}H-NMR. The compound 9 was then further modified with the methacrylic anhydride in order to obtain the MJ based monomer. The formation of monomer was confirmed by the ^{1}H-NMR after the purification by column chromatography. Compound 9 was then subjected to raft polymerization to obtain the polymer 10. However, this reaction was carried out up to the 36 h and the NMR was checked at different time interval and I found that the peak of the acrylic double bond was not completely disappeared and hence suggesting that the reaction was not completed under those conditions.

The above two approaches could not lead to the desired result, so I planned for another approach to obtain the MJ based monomers and their subsequent polymers **(Scheme 4.3)**. In this approach, after the conversion of the MJ to JA, the carboxylic acid group of JA was coupled with the hydroxy group of the HEMA as shown in reaction scheme. In this approach the MJ was first converted to the JA, then the carboxylic acid group of JA was coupled with the hydroxy group of HEMA as shown below in scheme.

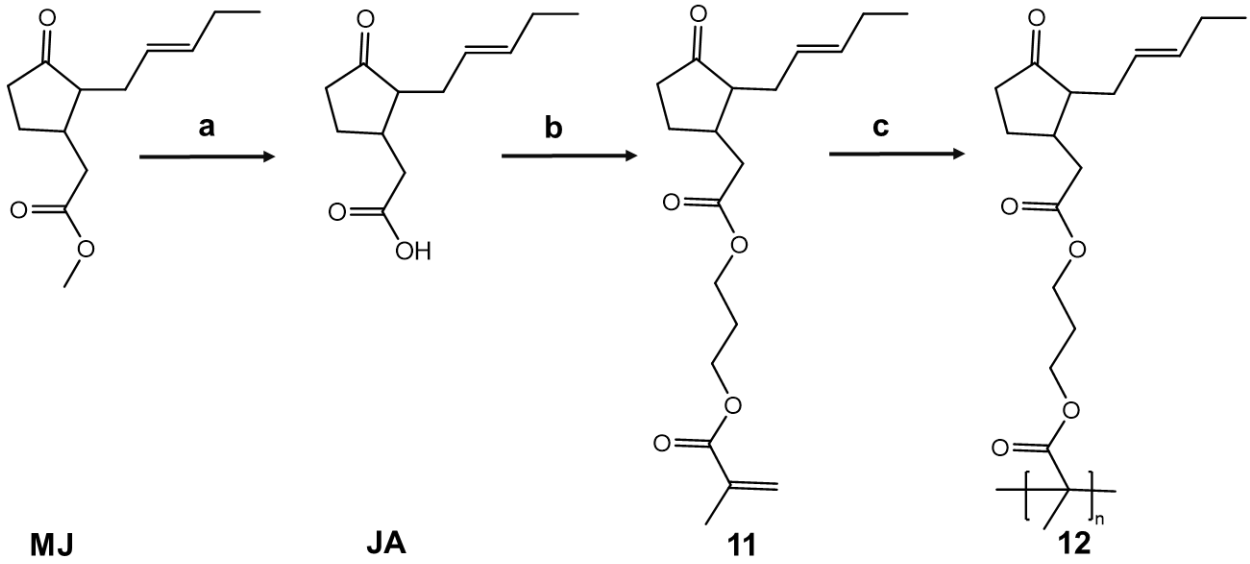

Scheme 4.3. Synthesis of Methyl Jasmonate modified monomer 11[a] and its subsequent polymerization 12[a]. [a]Reagents and conditions: (a) for JA: MJ (1 mmol), LiOH. H_2O (2 mmol), THF-Water (1:1) solvent, stir 1 h, rt. (b) for 11: HEMA, DCC (1.1eq), DMAP (1.1eq), dry DCM, stir 2 h, rt. (c) Raft agent, AIBN, ethanol (1.1eq), DCM, stir overnight, 70°C **.**

In this approach the number of steps were further reduced to make the reaction synthesis easier. The formation of the JA was confirmed by the ^{1}H-NMR **(Figure 4.1)**. The obtained JA was then subjected to esterification with the hydroxyl group of HEMA and then purified by the column chromatography. The formation of compound 11 (JA-HEMA) was confirmed by the ^{1}H-NMR **(Figure 4.2)**. Monomer 11 was further polymerized and this time the reaction was successfully confirmed by the disappearance of the methacrylic double bonds in ^{1}H-NMR, however the polymer formed was insoluble in water so the JA-HEMA monomer was copolymerized with the cationic monomer (3-Acrylamidopropyl)trimethylammonium chloride (AMPTMA).

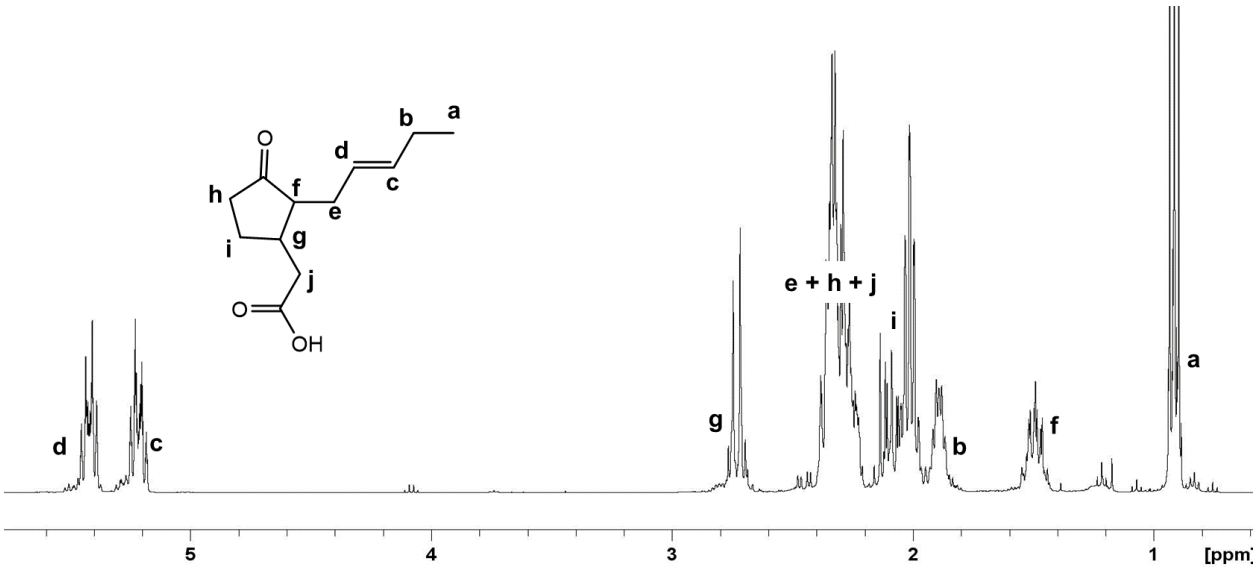

Figure 4.1: Confirmation of the formation of the JA through ^{1}H-NMR.

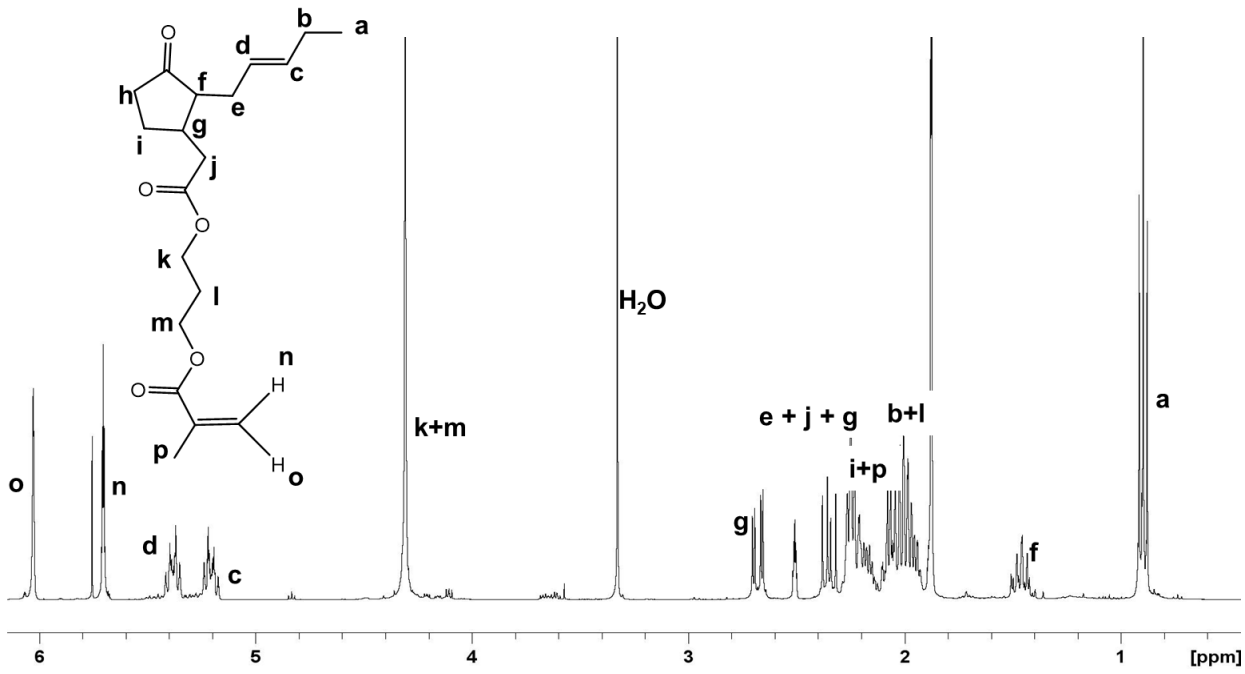

Figure 4.2: Confirmation of formation of monomer JA-HEMA (11) by ^{1}H-NMR.

4.3.2. Copolymerization with cationic monomer AMPTMA

After successful formation of the monomer JA-HEMA and its polymerization, the monomer was further copolymerized with the cationic monomer AMPTMA. The cationic monomer was introduced to balance the solubility of the homopolymer of JA-HEMA as well as the

introduction of cationic monomer could lead characteristic macromolecular therapeutic effect along with the selectivity towards the cancer cells.

A series of random copolymers P-[(JA-HEMA)-r-(AMPTMA)] were synthesized by varying the amount of AMPTMA from 1:1 mol % to 1:3 mol % **(Scheme 4.4)**. Their formation was confirmed by the disappearance of the double bond peaks (δ = 5.4–4.2 ppm) related to the acrylate protons of the JA-HEMA and the AMPTMA **(Figure 4.3)**. The amount of JA-HEMA and AMPTMA added and inserted in each copolymer was calculated by comparing the integral value of the methyl proton in JA-HEMA (δ = 0.8 ppm) and methylene peak of AMPTMA (δ = 3.0–3.5 ppm) in ^{1}H-NMR **(Figures 4.4, Table 4.1)**. Figure 4.5 shows the comparison of the homopolymer and the copolymer containing different mol % of AMPTMA. The incorporation of AMPTMA was easily controlled by changing the initial feed amount. Based on the GPC results, I calculated the number-average molecular weight (M_n) and weight-average molecular weight (M_w) values. The polydispersity index (PDI) values were found to be in good range **(1.1–1.5; Table 4.1)**.

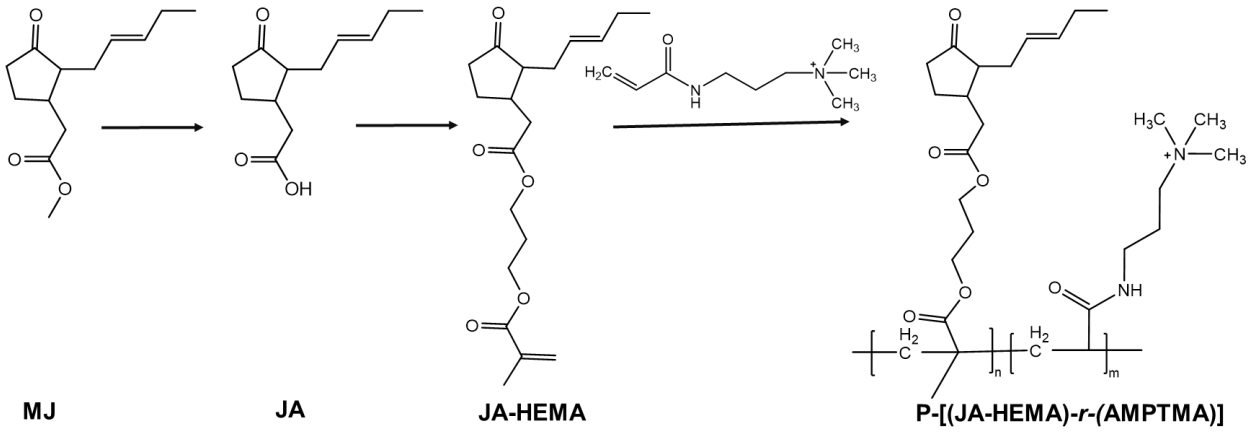

Scheme 4.4. Synthesis of copolymers of JA-HEMA and the AMPTMA.

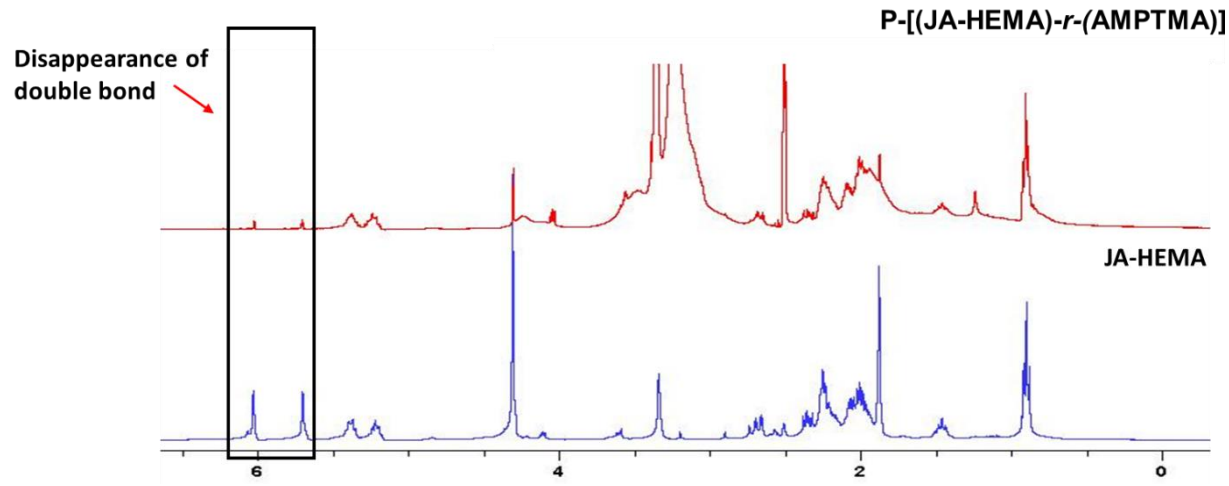

Figure 4.3: Comparison of the ^{1}H-NMR of the monomer JA-HEMA and its subsequent copolymer P-[(JA-HEMA)-r-(AMPTMA)].

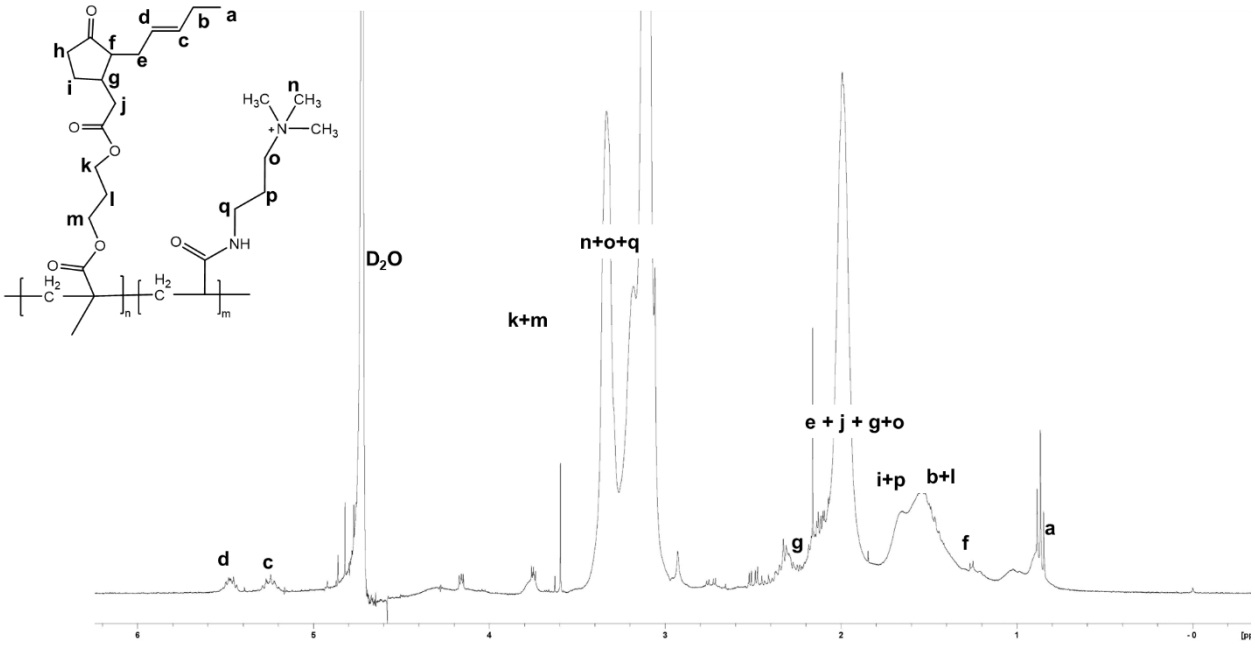

Figure 4.4: ^{1}H-NMR of copolymer P-[(JA-HEMA)-r-(AMPTMA)].

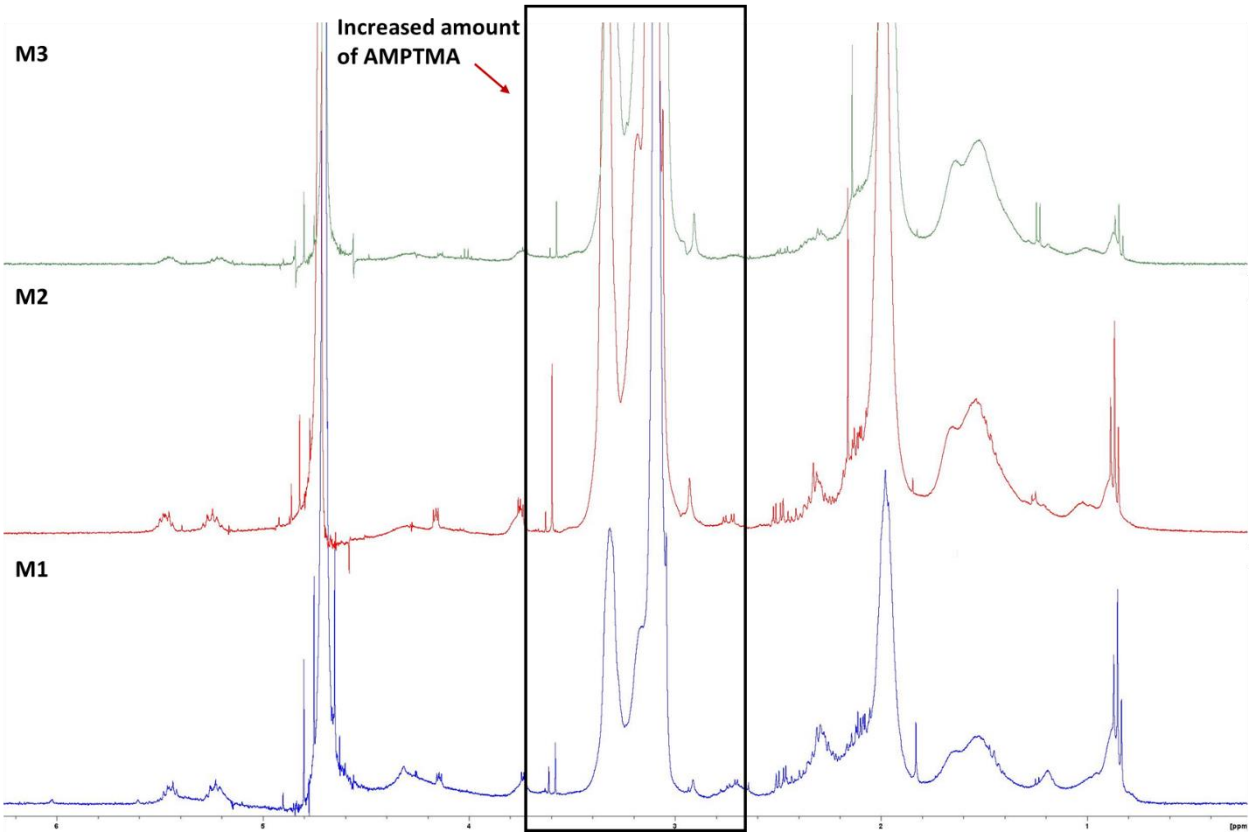

Figure 4.5: Comparison of the copolymers formed P-[(JA-HEMA)-r-(AMPTMA)].

4.3.3. *In vitro* cytotoxicity determination

The anticancer activity of the polymers was evaluated against cancer cell line—HepG2, using the MTT assay. Cancer cells have more negative charges than those of the normal cells because of the overexpression of phospholipids on the surface of cancer cells.[17] Initially, the cytotoxicity of cationic homopolymer of AMPTMA (M0) was determined. M0 did not show any anticancer activity against HepG2 cancer cell line (IC_{50} = N.D.) or very less activity against colon 26 cell line (IC_{50} = 402 µg/mL) **(Table 4.1)**. However, the insertion of the JA-HEMA in the copolymers enhances the anticancer activity with lower IC_{50} values. The MJ showed low anticancer activity with high IC_{50} value (IC_{50} = 313 µg/mL) against the HepG2 cell line and the colon 26 (IC_{50} = 300 µg/mL). The JA also showed very low cytotoxicity towards both the cancer cell lines **(Table 4.1)**. However, the modification of the MJ to its polymer and subsequently formation of its copolymers with cationic monomer enhances the anticancer

activity. The copolymers with the varying amount of the of AMPTMA monomer were synthesised and their formation was confirmed by the ^{1}H-NMR **(Figure 4.5, Table 4.1)**. The M1 copolymer having the 2 equivalents of AMPTMA as compared to the JA-HEMA showed good anticancer activity with lower IC_{50} (IC_{50} = 65 µg/mL) against the HepG2 cancer cell line. As the amount of the AMPTMA was increased in the copolymers from the polymer M1 to M3 **(Table 4.1)** the anticancer activity was reduced. I believe the reduction the cytotoxicity is due to the reduced amount of JA-HEMA inserted in the copolymer. With the reduction of JA-HEMA in the polymer could lead to the decreased inhibition of the HK-II enzyme which may leads to the further reduction in the anticancer activity.[18]

To evaluate the selectivity of the polymers towards the normal cell line, the cytotoxicity of the polymers (M0-M3) was tested against the primary human dermal fibroblasts (HDF) cell line **(Table 4.1).** All the polymers synthesised showed very high cytotoxicity towards the HDF cell line with very low IC_{50} values. I believed that the undesired cytotoxicity was acquired due the high cationic charge due to the larger chain length of AMPTMA as well as the large chain length of the JA-HEMA. Next, I synthesized a new polymer with reduced chain length of both the JA-HEMA as well as the AMPTMA in order to control the cationic chain length and the amount of JA-HEMA in copolymer (M4). The formed polymer M4 showed higher cytotoxicity against the HepG2 cancer cell line (IC_{50} = 68 µg/mL) however still the selectivity was missing in the normal cell line. Then I again synthesised the polymer M5 with lesser number of chain length however the cytotoxicity was reduced towards the cancer cell line, however the selectivity towards the HDF was still missing **(Table 4.1)**.

Table 4.1. Summary of the copolymers of JA-HEMA:AMPTMA synthesized and their anticancer activity.

S.No	Polymer		Zeta Potential (mV)[a]	Added (JA-HEMA:AMPTM)	Obtained (JA-HEMA:AMPTMA)[b]	$M_n \times 10^{3,c}$	M_w/M_n	IC_{50} for HepG2[d] (µg/mL)	IC_{50} for HDF (µg/mL)
1.	MJ	Methyl jasmonate	-	-	-	-	-	313	498
2.	JA	Jasmonic acid	-	-	-	-	-	300	267
3.	M0	$PAMPTMA_{100}$	20.2 ± 0.47	100	100	9.5	1.15	N.D.	187
4.	M1	P-[$(JA\text{-}HEMA)_{50}$-*r*-$(AMPTMA)_{100}$]	21.6 ± 1.07	1:2	1:5	14.1	1.19	65	14
5.	M2	P-[$(JA\text{-}HEMA)_{50}$-*r*-$(AMPTMA)_{150}$]	20.4 ± 0.17	1:3	1:8	23.0	1.56	84	11
4	M3	P-[$(JA\text{-}HEMA)_{50}$-*r*-$(AMPTMA)_{200}$]	9.54 ± 0.86	1:4	1:25	21.5	1.59	219	20
5	M4	P-[$(JA\text{-}HEMA)_{25}$-*r*-$(AMPTMA)_{50}$]	18.6 ± 1.96	1:2	1:22	21.3	2.03	68	13
6	M5	P-[$(JA\text{-}HEMA)_{15}$-*r*-$(AMPTMA)_{50}$]	12.8 ± 0.85	1:3.3	1:6	13.7	1.45	N.D.	37

a: determined in PBS, b: by NMR, c: by GPC, d: by MTT assay, N.D.: not determined

4.3.4. PEG based copolymers

Since the selectivity was missing in the AMPTMA based random polymers, next I synthesized the PEG based polymers, as PEG was known for its biocompatibility.[19] Also, it has been reported for hydrophilicity and it can prolong the blood circulation time as well.[20-22] To this end I synthesized the PEG based JA-HEMA and AMPTMA copolymers with varying amount of the JA-HEMA and the AMPTMA as per the reaction **scheme 4.5**. Copolymer M6 to M8 were synthesized by keeping the amount of AMPTMA monomer constant (DP-10) and increasing the JA-HEMA monomer gradually from chain length 10-30 respectively (theoretical DP). Also, copolymers were synthesized by keeping the amount of JA-HEMA constant (DP-10) and then gradually increasing the amount of AMPTMA monomer gradually **(Table 4.2)**. At first the PEG-CTA that worked as the macro raft agent was synthesized **(step a)**, and its formation was confirmed by the ^{1}H-NMR **(Figure 4.6)**. After its successful formation,

copolymers were synthesized by varying the amount of the AMPTMA and JA-HEMA both (step b) **(Table 4.2)** and their formation was confirmed by the ^{1}H-NMR **(Figure 4.7)**. The methyl proton of JA-HEMA (δ = 0.8 ppm) and of olefinic double bond (δ = 5.2-5.4 ppm) confirms the presence of JA-HEMA in synthesized polymer. Also, the characteristic peak of quaternary methyl protons of AMPTMA (δ = 3.2-3.4 ppm) showed the presence of AMPTMA **(Figure 4.7)**. Overall, the copolymers containing all three parts (PEG, JA-HEMA and AMPTMA) were successfully synthesized. The number-average molecular weight (M_n) and weight-average molecular weight (M_w) values were determined by the GPC. The polydispersity index (PDI) values were found to be in the good range **(1.1–1.3; Table 4.2)**. After their successful formation, in vitro cytotoxicity experiments were performed.

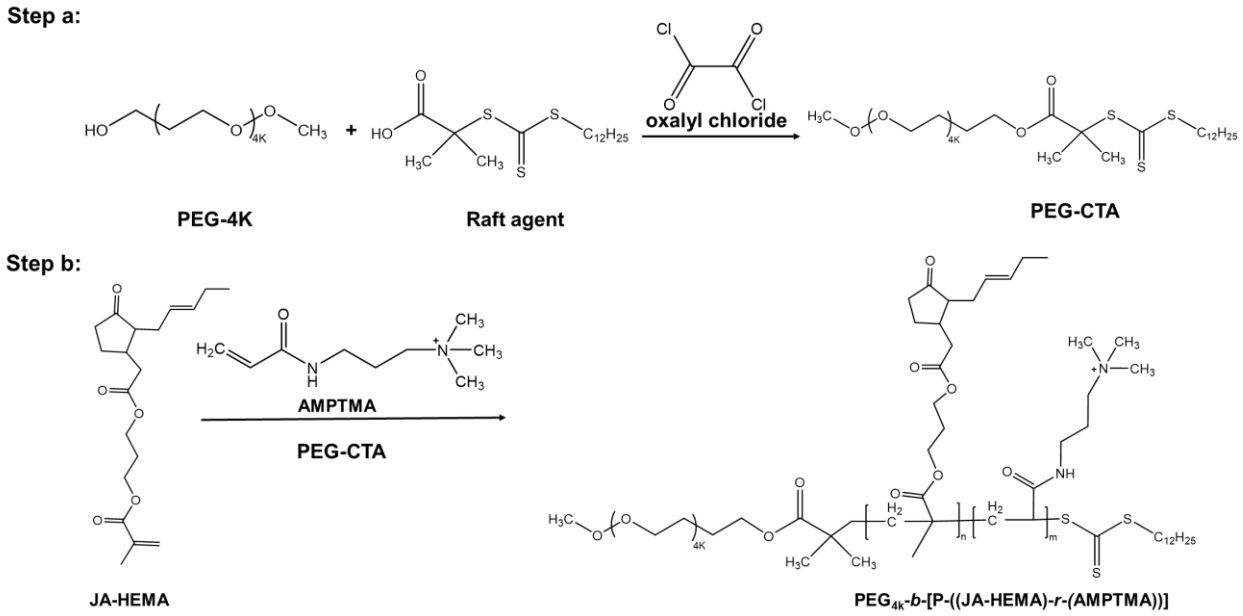

Scheme 4.5: Synthesis of PEG-CTA based copolymers of JA-HEMA and AMPTMA.

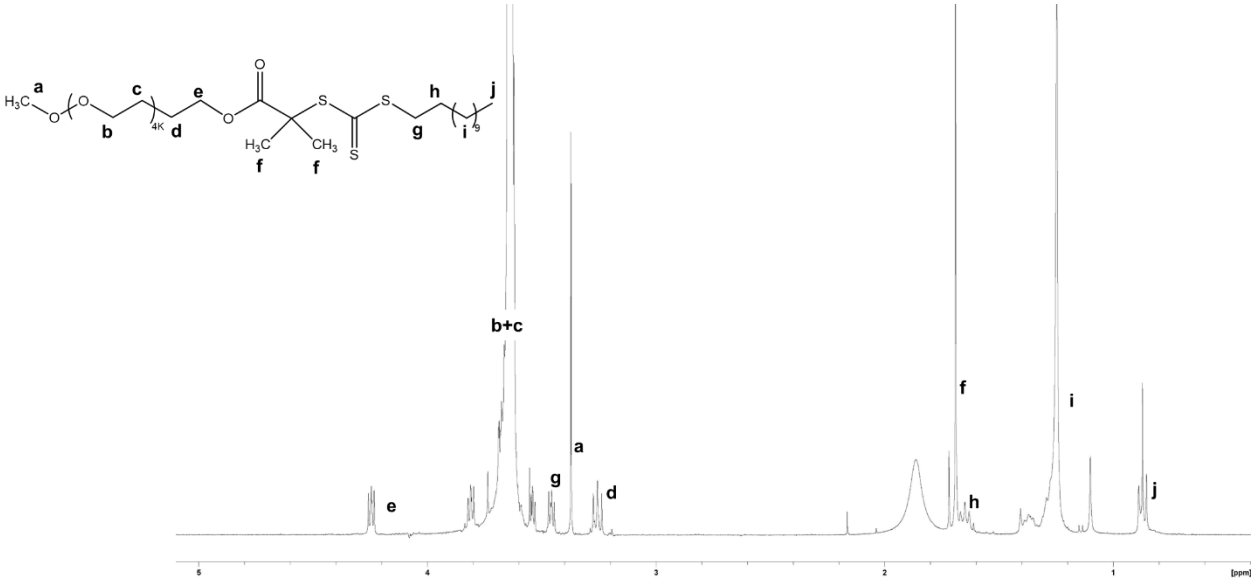

Figure 4.6: ^{1}H-NMR of the PEG-CTA (macro raft agent).

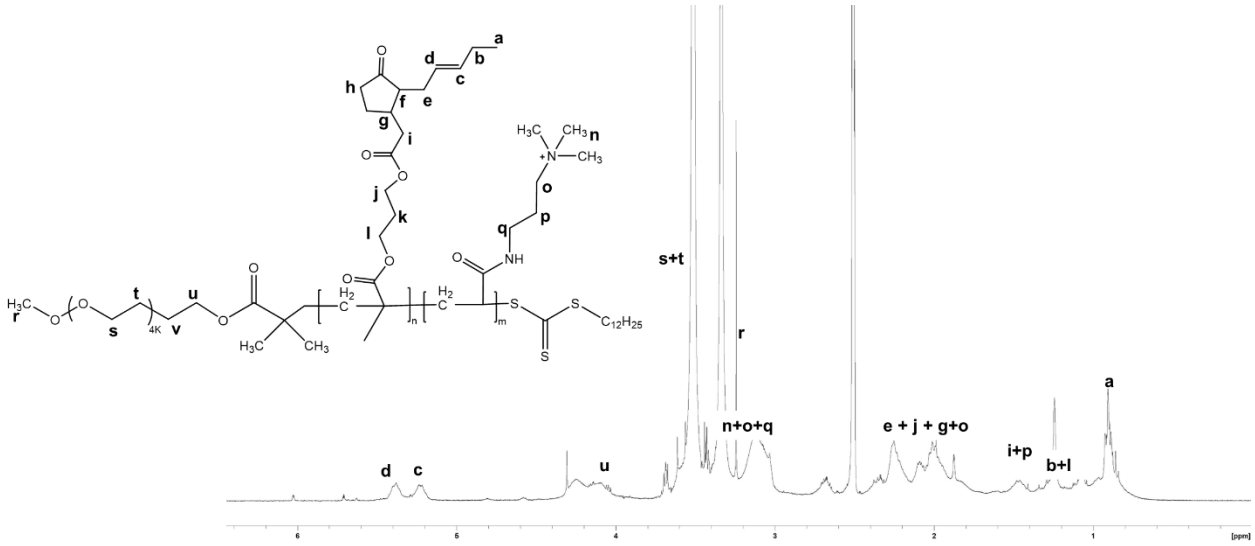

Figure 4.7: ^{1}H-NMR of the PEG-based copolymers of JA-HEMA and AMPTMA.

4.3.5. *In vitro* cytotoxicity determination of PEG based copolymers

The in vitro anticancer activity of the synthesized PEG-based copolymers was determined against the cancer cell lines-HepG2, Colon 26 and B16F10. M6 copolymer showed better anticancer activity against HepG2 (IC_{50}=641 µg/mL) **(Figure 4.8a)** which was further enhanced in colon 26 **(Figure 4.8b)** and B16F10 **(Figure 4.8c)** cancer cells with IC_{50} as 201 µg/mL and 62 µg/mL respectively, which was lower than then the MJ and JA. Enhancement

in the cytotoxicity results demonstrated the synergistic effect of both the small molecule MJ and the cationic polymer. With the further enhancement of the JA-HEMA monomer in M7 and P8 further enhanced the anticancer activity in case of B16F10 cancer cell line (IC_{50} = 28 µg/mL and 9 µg/mL) respectively. However, contrasting results were obtained in the case of the HepG2 and the colon 26 cancer cell lines. The activity towards these cell lines was reduced with the increasing JA-HEMA **(Table 4.2).**

However, when these copolymers were tested on the normal cell line (HDF), all the polymers showed very high selectivity. P6 polymer showed high selectivity with low IC_{50} (859 µg/mL) then the MJ and JA **(Figure 4.8d, Table 4.2)**. Similarly, the enhancement in selectivity was observed in M7 and M8, we believed that this enhanced selectivity was due to the over expression of HK-II enzyme in the cancer cell rather than the normal cells.[18]

Table 4.2. Summary of all the PEG-based copolymers and their *in vitro* cytotoxicity.

S. No	Polymer		Zeta Potential (mV)[a]	$M_n \times 10^{3,b}$	$M_n \times 10^{3,b}$	IC_{50} for HepG2[c] (µg/mL)	IC_{50} for colon26 (µg/mL)	IC_{50} B16F10[c] (µg/mL)	IC_{50} for HDF[c] (µg/mL)
1.	MJ	Methyl jasmonate	-	-	-	313	390	373	498
2.	JA	Jasmonic acid	-	-	-	300	639	663	267
1.	M6	PEG_{4k}-b-[P-$((JA\text{-}HEMA)_{10}$-*r*-$(AMPTMA)_{10})$]	-2.69 ± 0.22	7.10	1.01	641	201	62	859
2.	M7	PEG_{4k}-b-[P-$((JA\text{-}HEMA)_{20}$-r-$(AMPTMA)_{10})$]	-1.32 ± 0.45	7.34	1.02	N.D.	N.D.	28	N.D.
3.	M8	PEG_{4k}-b-[P-$((JA\text{-}HEMA)_{30}$-*r*-$(AMPTMA)_{10})$]	-1.86 ± 0.61	7.18	1.01	503	N.D.	9	N.D.
4.	M9	PEG_{4k}-b-[P-$((JA\text{-}HEMA)_{10}$-*r*-$(AMPTMA)_{20})$]	0.91 ± 0.26	8.31	1.06	N.D.	191	35	1000
5.	M10	PEG_{4k}-b-[P-$((JA\text{-}HEMA)_{10}$-*r*-$(AMPTMA)_{30})$]	2.35 ± 0.42	9.33	1.11	N.D.	425	32	894

a: determined in PBS, b: by GPC, c: by MTT assay, N.D.: not determined

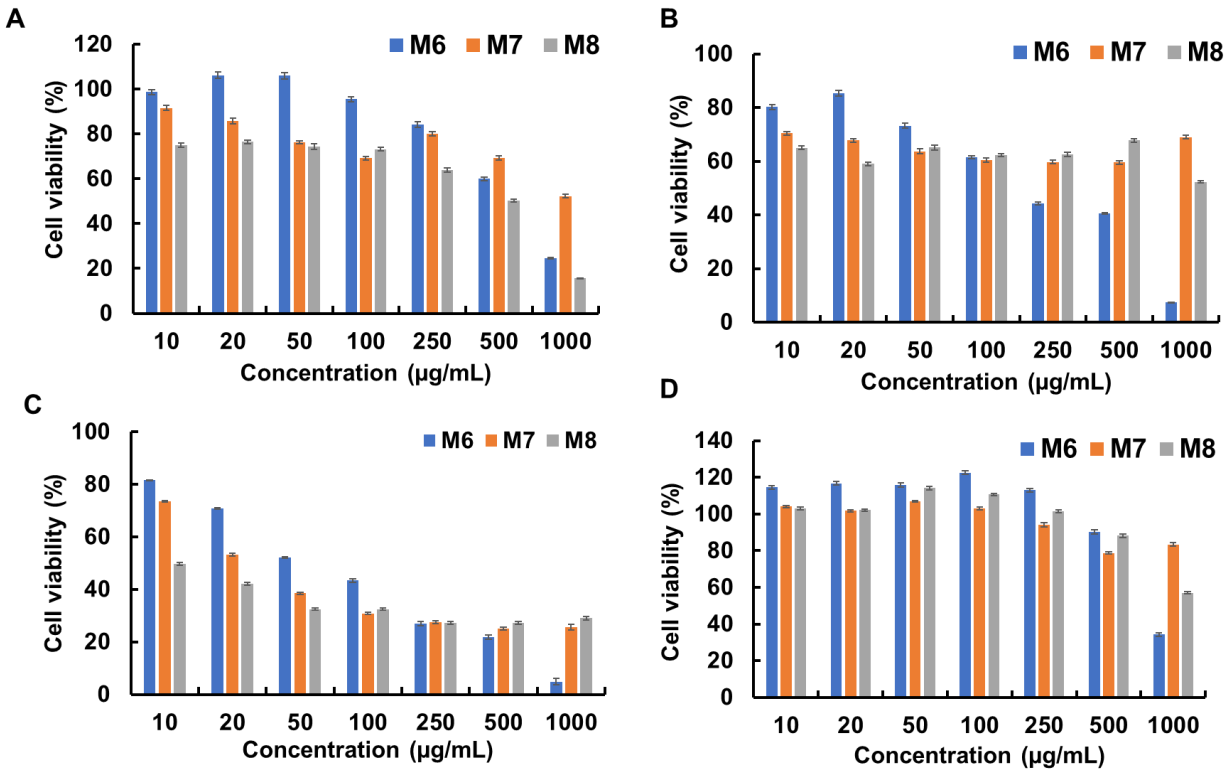

Figure 4.8: In vitro cytotoxicity of the PEG-based copolymers with varied amount of JA-HEMA; a.) for the HepG2 cell line, b.) for the colon 26 cells, c.) for the B16F10 cancer cells, d.) for HDF as normal cells.

Also, I synthesized the PEG-based copolymer by keeping the JA-HEMA constant and constantly increasing the amount of the AMPTMA from M9 to M10. The in vitro anticancer activity was evaluated of these polymers, and they were found to be effective against the cancer cells **(Table 4.2)**. Both M9 and M10 did not showed its anticancer activity up to 1000 µg/mL of the polymer concentration in HepG2 cancer cells **(Figure 4.9a)**. However, when both were tested upon colon 26 **(Figure 4.9b)** and the B16F10 (**Figure 4.9c)** cancer cell lines they showed very good anticancer activity with lower IC_{50} values **(Table 4.2)**. Polymer M9 showed good selectivity against the HDF cell line with IC_{50} of almost 1000 µg/mL. On the other hand, the selectivity towards the HDF cells were slightly reduced (IC_{50}=894 µg/mL) this may be due to the increase in the cationic chain length **(Figure 4.9d)**.

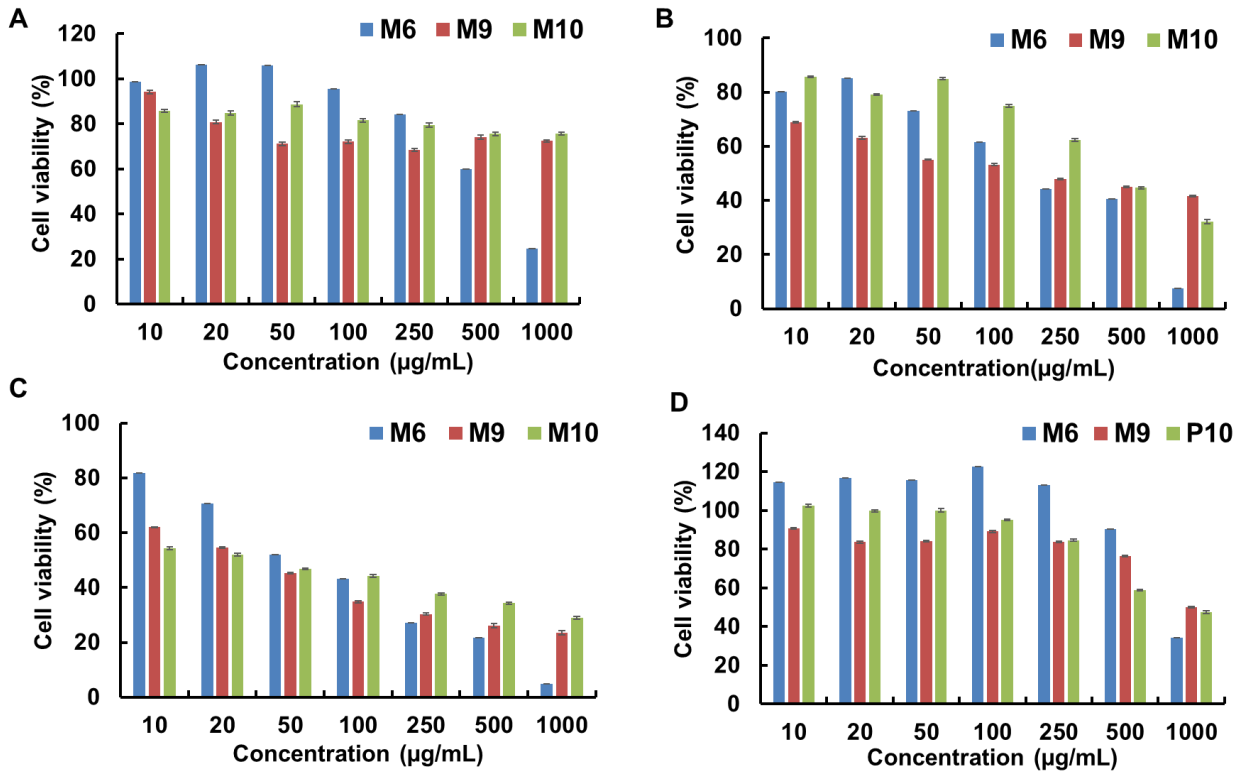

Figure 4.9: In vitro cytotoxicity of the PEG-based copolymers with varied amount of AMPTMA; a.) for the HepG2 cell line, b.) for the colon 26 cells, c.) for the B16F10 cancer cells, d.) for HDF as normal cells.

Overall, the PEG-based copolymers although reduced the cytotoxicity towards the cancer cells when compared to the P-[(JA-HEMA)-r-(AMPTMA)] copolymers, but the enhancement in selectivity towards the normal cells was observed which may be due to the enhanced biocompatibility due to the insertion of the PEG. Although these polymers were not that effective against the HepG2 cancer cell, but they were found to be the most effective against the colon 26 and the B16F10 which were the more malignant cancer cells. So, the polymers were effective and selective against the malignant cancer cells.

4.4. Conclusion

In this study I successfully synthesized the methyl jasmonate monomer and then further copolymerized it with the cationic comonomer. The obtained copolymers showed the enhanced solubility and the cytotoxicity almost 10 times towards the cancer cells (IC_{50}=65 µg/mL). These

novel polymerised MJ based polymers motivated me to synthesis the PEG-based copolymers of JA-HEMA (MJ analogue) and the AMPTMA. The synthesised polymers were found to be very effective against the cancer cells with very low IC_{50} even up to the 9 µg/mL. All the PEG-based copolymers showed enhanced selectivity towards the normal cell line and they were found to selective against the normal cells as well. Also, homopolymer PAMPTMA has no cytotoxicity towards the cancer cell line, so MJ has its effect on the cytotoxicity. Overall, the polymerization of the MJ a bioactive compound is not reported anywhere and completely new in trend of drug designing and the cytotoxicity of the MJ analogues was significantly increased by almost 10-12 folds as compared to the novel MJ molecule with further enhancement of the selectivity.

4.5. References

1. Kumar, N.; Fazal, S.; Miyako, E.; Matsumura, K.; Rajan, R., *Materials Today* **2021**, *51*, 317-349.

2. Ganoth, A.; Merimi, K. C.; Peer, D., *Expert Opinion on Drug Delivery* **2015**, *12*, (2), 223-238.

3. Mignani, S.; Bryszewska, M.; Klajnert-Maculewicz, B.; Zablocka, M.; Majoral, J.-P., *Biomacromolecules* **2015**, *16*, (1), 1-27.

4. Chabner, B. A.; Roberts, T. G., *Nature Reviews Cancer* **2005**, *5*, (1), 65-72.

5. Livney, Y. D.; Assaraf, Y. G., *Advanced Drug Delivery Reviews* **2013**, *65*, (13), 1716-1730.

6. Rowinsky, E. K.; Eisenhauer, E. A.; Chaudhry, V.; Arbuck, S. G.; Donehower, R. C., *Semin Oncol* **1993**, *20*, (4 Suppl 3), 1-15.

7. Bhardwaj, V.; Rizvi, N.; Lai, M. B.; Lai, J. C. K.; Bhushan, A., *Anticancer Research* **2010**, *30*, (3), 743-749.

8. Liberti, M. V.; Locasale, J. W., (0968-0004 (Print)).

9. Otto, A. M., *Cancer & Metabolism* **2016**, *4*, (1), 5.

10. Bao, F.; Yang, K.; Wu, C.; Gao, S.; Wang, P.; Chen, L.; Li, H., *Fitoterapia* **2018**, *125*, 123-129.

11. Chen, Z.; Zhang, H.; Lu, W.; Huang, P., *Biochimica et Biophysica Acta - Bioenergetics* **2009**, *1787*, (5), 553-560.

12. Lin, H.; Zeng, J.; Xie, R.; Schulz, M. J.; Tedesco, R.; Qu, J.; Erhard, K. F.; Mack, J. F.; Raha, K.; Rendina, A. R.; Szewczuk, L. M.; Kratz, P. M.; Jurewicz, A. J.; Cecconie, T.; Martens, S.; McDevitt, P. J.; Martin, J. D.; Chen, S. B.; Jiang, Y.; Nickels, L.; Schwartz, B. J.; Smallwood, A.; Zhao, B.; Campobasso, N.; Qian, Y.; Briand, J.; Rominger, C. M.; Oleykowski, C.; Hardwicke, M. A.; Luengo, J. I., *ACS Medicinal Chemistry Letters* **2016**, *7*, (3), 217-222.

13. Dang, H. T.; Lee, H. J.; Yoo, E. S.; Hong, J.; Bao, B.; Choi, J. S.; Jung, J. H., *Bioorganic and Medicinal Chemistry* **2008**, *16*, (24), 10228-10235.

14. Liu, S.; Wang, W. H.; Dang, Y. L.; Fu, Y.; Sang, R., *Tetrahedron Letters* **2012**, *53*, (32), 4235-4239.

15. Mohamed, E. A.; Ismail, N. S. M.; Hagras, M.; Refaat, H., *Future Journal of Pharmaceutical Sciences* **2021**, *7*, (1), 24.

16. Albratty, M.; Alhazmi, H. A., *Arabian Journal of Chemistry* **2022**, *15*, (6), 103846.

17. Dobrzyńska, I.; Szachowicz-Petelska, B.; Sulkowski, S.; Figaszewski, Z., *Molecular and Cellular Biochemistry* **2005**, *276*, (1), 113-119.

18. Sucu, B. O.; Ipek, O. S.; Kurtulus, S. O.; Yazici, B. E.; Karakas, N.; Guzel, M., *Bioorganic Chemistry* **2019**, *91*, 103146.

19. Gref, R.; Minamitake, Y.; Peracchia, M. T.; Trubetskoy, V.; Torchilin, V.; Langer, R., *Science* **1994**, *263*, (5153), 1600-1603.

20. Pasut, G.; Veronese, F. M., *Advanced Drug Delivery Reviews* **2009**, *61*, (13), 1177-1188.

21. Gref, R.; Lück, M.; Quellec, P.; Marchand, M.; Dellacherie, E.; Harnisch, S.; Blunk, T.; Müller, R. H., *Colloids and Surfaces B: Biointerfaces* **2000**, *18*, (3), 301-313.

22. Chen, S.; Yang, K.; Tuguntaev, R. G.; Mozhi, A.; Zhang, J.; Wang, P. C.; Liang, X.-J., *Nanomedicine: Nanotechnology, Biology and Medicine* **2016**, *12*, (2), 269-286.

Chapter 5

SUMMARY AND OUTLOOK

5.1. Conclusion

This thesis addresses the feasibility of cationic polymers in cancer treatment. The polymers were synthesized using the RAFT polymerization through which the molecular weight and the polydispersity index of these polymers were controlled in an easy manner. The obtained polymers showed good anticancer activity and enhanced selectivity.

In Chapter 2: The cationic copolymers containing hydrophobic groups such as BuMA (PAMPTMA-*r*-BuMA) were synthesized which exhibit superior anticancer activity with low IC_{50} than that exhibited by the cationic homopolymer (PAMPTMA) itself, which is contrary to previous reports. Additionally, the effect of the size of the hydrophobic group was established. The copolymer (PAMPTMA-*r*-OctMA) demonstrated a higher anticancer efficacy than that shown by copolymers with smaller hydrophobic groups (such as PAMPTMA-*r*-BuMA and PAMPTMA-*r*-HexMA). Therefore, it was successfully demonstrated that the cationic charge or the cationic polymer alone is not sufficient for the anticancer activity and that hydrophobicity plays an important role in determining the anticancer activity. The cationic copolymer concentrates the cationic charge and attaches to the anionic cancer cell membrane, resulting in a high local concentration and the hydrophobic group cause a significant permeabilization, leading to cell death. Hence, this study successfully demonstrates the anticancer activity of hydrophobic copolymers and their potential application in anticancer research. Although the literature has reported the use of cationic polymers, their adsorption behavior and the role of hydrophobicity on the cancer cell membrane have not been reported yet.

In Chapter 3: In chapter 2 the role of hydrophobic moiety and their interaction towards the cancer cell membranes was successfully established so in this chapter, I intended to synthesize new cationic polymers with selectivity towards the normal cells. The biodegradable PLL-NA based polymers with varying amount of the DDSA in them were synthesized . The synthesized polymers successfully coordinated with the Zn^{2+} ions. The coordinated polymers showed potent anticancer activity which was revealed from their lower IC_{50} values than the non-coordinated one. The polymers showed very high selectivity towards the normal cell line with no or significantly very low IC_{50} values. The polymers were effective in killing of the cancer cells with high selectivity when compared with DOX, as well as the drug-resistance cancer cells were also significantly killed by these polymers. Also, these polymers not only showed their potency in killing, but also in prevention of further migration of the cancer cells which makes them effective for prevention of the tumor metastasis. Overall, all the NA-based zinc bound polymers showed excellent *in vitro* antitumor properties against both the cancer cell lines selectively.

In Chapter 4: My intent was to convert the simple methyl jasmonate a bioactive compound to cationic polymer or to synthesize its copolymers in order to enhance its cytotoxicity towards the cancer cells and as well as enhancement of selectivity towards the normal cells. So, in this study the methyl jasmonate monomer were successfully synthesized and then further copolymerized it with the cationic comonomer. The obtained copolymers showed enhanced solubility and cytotoxicity almost 10 times towards the cancer cells. These novel polymerised MJ based polymers motivated me to synthesis the PEG-based copolymers of JA-HEMA (MJ analogue) and the AMPTMA. The synthesised polymers were found to be very effective against the cancer cells with very low IC_{50}. All the PEG-based copolymers showed enhanced selectivity towards the normal cell line. Also, homopolymer PAMPTMA has no cytotoxicity towards the cancer cell line, so MJ has its effect on the cytotoxicity. Overall, the polymerization

of the MJ a bioactive compound is not reported anywhere and completely new in trend of drug designing and the cytotoxicity of the MJ analogues was significantly increased by almost 10-12 folds as compared to the novel MJ molecule with further enhancement of the selectivity.

5.2. Outlook and scope

The potential of the cationic polymers towards the cancer treatment was successfully proved while overcoming the limitations of the previously used treatments. The RAFT polymerization used in this study was simpler and easier with the controlled molecular weight as compared to the previously reported literature.

In chapter 2 the role of hydrophobicity in the cationic polymers and their mechanistic investigations of interaction towards the cancer cell was established. I believe that the design principle for cationic anticancer polymers explained in this study will widen the cancer treatment research field, which may help in discovering new anticancer pharmaceuticals with a facile synthesis route and lower production cost, which may be useful in clinical medical trials for tumour treatment.

In chapter 3 the selectivity by masking the cationic charge with the usage of the Zn metal ion was obtained and that metal coordinated cationic polymers approach can open a new window in macromolecular chemotherapeutics which could be an attractive option in overcoming the limitations of cancer treatment research. Also, it would be very interesting if in future one could use the different metal ions like the Fe, Cu and others for the enhancement of cytotoxicity towards the cancer cells along with the enhanced selectivity. Considering the easy synthetic reaction scheme, availability and biodegradability of these polymers they could prove to be a promising approach towards cancer treatment in future.

In chapter 4 as I modified the simple novel molecule MJ to its cationic copolymers, it would be interesting to use other simpler molecules with more selective mode of action towards the

cancer cells. Polymerization could improve its selectivity and therefore easier tuning of the physiological properties.

Although these cationic polymers have a broad range of applications towards cancer treatment and they were deemed effective and selective against various cancer cell lines, including multidrug-resistant cancer cells, inhibiting tumor metastasis, and suppressing tumor growth *in vitro*, but these are model systems only. It is a fundamental study which describes the different methodologies to develop cationic polymers for their application towards cancer treatment. However, in order to use them for clinical applications, *in-vivo* study needs to be carried out. Also, a detailed mechanistic study towards the interaction of these polymers and their mode of action on the cancer cells would be beneficial which is one of the limitations of this study. I believe my study has broadened the basic understanding of the cationic polymers and their working. Overall, synthetic cationic polymers provide a simple but novel platform that allows the tuning of the physiological properties and the consequent improvement of cytotoxicity and selectivity towards cancer cells. Polymer architectures and morphologies (e.g., polymer micelles) can also be obtained, and chemical modifications, including the inclusion of cancer-homing ligand groups or prodrug moieties can be performed, which will ultimately lead to the development of clinically potent selective compounds. Although further targeted research is required, I believe that these cationic platforms will allow for the rational design and screening of functional degradable polymers. Lastly this research has covered some pit-holes in the research field. I expect my study will assist in the development of better systems in the future

ACHIEVEMENTS

Main Publications:

1. **Nishant Kumar**, Sajid Fazal, Eijiro Miyako, Kazuaki Matsumura, Robin Rajan. Avengers Against Cancer: New Era of Nano- and Polymer Material-Based Therapeutics. ***Materials Today***. 2021, 51, 317-349 https://doi.org/10.1016/j.mattod.2021.09.020. (Selected as **inner cover page**)

2. **Nishant Kumar**, Kengo Takagi, Shin-ichi Yusa, Robin Rajan, Kazuaki Matsumura. Enhancement of cytotoxicity against cancer cells by incorporating the hydrophobic moiety into cationic polymers. **Journal of material chemistry B**. (In peer review)

Other Publications:

3. Robin Rajan, **Nishant Kumar**, Kazuaki Matsumura. Design of an Ice Recrystallization-Inhibiting Polyampholyte-Containing Graft Polymer for Inhibition of Protein Aggregation. **Biomacromolecules**. 2022, 23, 2, 487–496, https://doi.org/10.1021/acs.biomac.1c01126. (Selected as **supplementary cover**)

4. Robin Rajan, Sana Ahmed, Neha Sharma, **Nishant Kumar**, Alisha Debas and Kazuaki Matsumura. Review of the current state of protein aggregation inhibition from a materials chemistry perspective: special focus on polymeric materials. ***Materials Advances***, 2021, 2, 4, 1139-1176, http://dx.doi.org/10.1039/D0MA00760A. (Selected as **back cover**)

Patent

5. **Nishant Kumar**, Robin Rajan, Kazuaki Matsumura, 抗がん性高分子化合物 (anitcancer polymeric compound), In application

In preparation

1. **Nishant Kumar**, Robin Rajan, Kazuaki Matsumura. Design of highly selective Zn-coordinated polyampholyte for cancer treatment and inhibition of tumor metastasis.

2. **Nishant Kumar**, Robin Rajan, Kazuaki Matsumura. Enhancement of anticancer activity of methyljasmonate by cationic polymerization.

3. Robin Rajan, **Nishant Kumar**, Kazuaki Matsumura. Hydrogel preparation for Inhibition of Protein Aggregation and its delivery .

4. **Nishant Kumar,** Arouba Ifthkar, Robin Rajan**,** Kazuaki Matsumura. Gold nanostructures in cancer immunotherapy (Book chapter)

ACKNOWLEDGEMENT

I would like to express my sincere gratitude to my advisor, **Prof. Dr. Kazuaki Matsumura** for his kind guidance, valuable suggestions, and the wholehearted encouragement throughout this project. I really appreciate all his contributions of time, opinion, funding to make my Ph.D. experience productive and stimulating. I am very thankful to him for his patience, motivation, and immense knowledge.

I would also like to thank **Assist. Prof. Dr. Robin Rajan**, for guidance and encouragement at the professional and the personal level. His problem-solving skill, valuable discussion, cooperation, and immense knowledge in the field fueled my Ph.D. work to another level.

My lab mates have been my biggest support system and from them I have learned a lot. I would like to extend my love and regards to all the members of Matsumura lab for being the best colleagues and very helpful friends.

Besides my supervisor, I would also like to thank my sub supervisor Prof. Dr. Takahiro Hohsaka for his support during my doctoral study. I also express my sincere and deep sense of gratitude to Associate Prof. Dr. Eijiro Miyako, School of Materials Science, JAIST, who was my minor research supervisor, for not only providing me with the necessary laboratory facilities for my work but for also constantly encouraging and guiding me. I would also like to thank my review committee Prof. Dr. Tatsuo Kaneko, Prof. Dr. Motoichi Kurisawa, Associate Prof. Dr. Eijiro Miyako, and Prof. Dr. Satoshi Fujita who spent their valuable time reading my thesis and giving valuable comments.

I would also like thank my friends and seniors who always keep me motivated with their valuable input, cooperation, and stimulating discussions throughout my time in JAIST.

I would like to take this opportunity to thank the Mitani Foundation for their constant financial support through their scholarship.

Finally, I would like to thank my mother Kusum Lata father Mr. Bijender Kumar, brother, sisters and brother-in-law for the constant support, encouragement and love given throughout my research career. Without this and their prayer it would have been impossible. I dedicate this thesis to my parents as a tribute to their constant hard work, support and love towards me.

Nishant Kumar